AD_____

Award Number: DAMD17-98-1-8614

TITLE: Mechanisms of Virus-induced Neural Cell Death

PRINCIPAL INVESTIGATOR: Kenneth L. Tyler, M.D.

CONTRACTING ORGANIZATION: University of Colorado Health Sciences Center
Denver, Colorado 80262

REPORT DATE: September 2000

TYPE OF REPORT: Annual

PREPARED FOR: U.S. Army Medical Research and Materiel Command
Fort Detrick, Maryland 21702-5012

REPORT DOCUMENTATION PAGE

Form Approved
OMB No. 074-0188

1. AGENCY USE ONLY (Leave blank)	2. REPORT DATE	3. REPORT TYPE AND DATES COVERED
	September 2000	Annual (15 Aug 99 – 14 Aug 00)

4. TITLE AND SUBTITLE
Mechanisms of Virus-induced Neural Cell Death

5. FUNDING NUMBERS
DAMD17-98-1-8614

6. AUTHOR(S)
Kenneth L. Tyler, M.D.

7. PERFORMING ORGANIZATION NAME(S) AND ADDRESS(ES)
University of Colorado Health Sciences Center
Denver, Colorado 80262

E-MAIL:
ken.tyler@uchsc.edu

8. PERFORMING ORGANIZATION REPORT NUMBER

9. SPONSORING / MONITORING AGENCY NAME(S) AND ADDRESS(ES)
U.S. Army Medical Research and Materiel Command
Fort Detrick, Maryland 21702-5012

10. SPONSORING / MONITORING AGENCY REPORT NUMBER

11. SUPPLEMENTARY NOTES

12a. DISTRIBUTION / AVAILABILITY STATEMENT
Approved for public release; Distribution unlimited

12b. DISTRIBUTION CODE

13. ABSTRACT *(Maximum 200 Words)*

We are using post-mortem and brain-biopsy derived material from patients with herpes simplex and varicella zoster virus encephalitis to identify the presence of apoptotic cells in the CNS and their correlation with viral infection and tissue injury. We are also using reovirus infection as a model to study cellular mechanisms of virus-induced cell death. Reovirus infection is associated with the activation of the nuclear transcription factor NF-κB, and inhibition of this activation inhibits apoptosis. There is increased expression of the apoptosis inducing ligand TRAIL in reovirus-infected cells. Inhibition of TRAIL binding to its cell surface death receptors, DR4 and DR5, inhibits reovirus-induced apoptosis. mRNA levels of TRAIL and DR4 are increased in reovirus-infected cells, as are levels of mature DR5 protein. Reovirus infection is associated with activation of apoptosis-associated proteases including calpain and caspases. Caspase activation involves the death-receptor associated (caspase-8) and the mitochondrial-associated (caspase 9) apoptotic pathways. Inhibition of either calpain or caspase activation inhibits reovirus-induced apoptosis in vitro. In a murine model of reovirus-induced myocarditis, inhibition of calpain activation prevents apoptotic myocardial injury. This suggests that inhibition of apoptosis may be a novel strategy for anti-viral therapy. Reovirus-induced apoptosis and cell cycle dysregulation are both determined by the viral S1 gene. Reoviruses induce a G2M cell cycle arrest. The S1-encoded σ1s protein is necessary for this process, but is not essential for apoptosis. Reovirus-induced apoptosis can be inhibited without preventing G2M cell cycle arrest, indicating that apoptosis-associated DNA damage does not cause reovirus-induced cell cycle arrest.

14. SUBJECT TERMS
Neurotoxin , apoptosis, NF-kB, caspases, calpain, cell cycle, reovirus

15. NUMBER OF PAGES
112

16. PRICE CODE

17. SECURITY CLASSIFICATION OF REPORT	18. SECURITY CLASSIFICATION OF THIS PAGE	19. SECURITY CLASSIFICATION OF ABSTRACT	20. LIMITATION OF ABSTRACT
Unclassified	Unclassified	Unclassified	Unlimited

TABLE OF CONTENTS

4. INTRODUCTION (Subject, Purpose, Scope of the Research):

The clinical manifestations of viral injury result from the capacity of viruses to damage or kill cells in different organs (19). Two distinct patterns of cell death, necrosis and apoptosis, have been recognized and can be distinguished based on a variety of morphological criteria. Apoptotic cell death is characterized by diminution in cell size, membrane blebbing, and compaction, margination and fragmentation of nuclear DNA (4). DNA fragmentation occurs predominantly at internucleosomal regions resulting in the generation of pathognomonic DNA 'ladders' when DNA from apoptotic cells is subjected to agarose gel electrophoresis (6). The subject and purpose of this research project is to study the cellular mechanisms by which viruses induce apoptotic cell death.

This represents the second annual progress report on this research project. Since submission of our first annual progress report (reporting period 8-15-98 to 8-14-99) we have had four additional papers published or accepted for publication by the Journal of Virology and one additional paper currently undergoing review (see Reportable Outcomes). In accordance with the format requirements for preparing this progress report, we have included all these publications in an appendix, have briefly summarized their key points in the text (see Research Accomplishments) with detailed references to particular figures in individual papers. Accomplishments are reviewed below and keyed to the specific aims as outlined in the original research application.

5. RESEARCH ACCOMPLISHMENTS

(Keyed to individual specific aims in the original Statement of Work)

Specific Aim 1: Is apoptosis a general feature of human viral encephalitis?

In an initial survey of over 3000 autopsies performed at the University of Colorado Health Sciences Center (UCHSC) and affiliated institutions we identified thirteen cases of cytomegalovirus encephalitis (predominantly in HIV-infected individuals), six cases of varicella zoster virus encephalitis (VZVE), six cases of progressive multifocal leukoencephalopathy, six cases of viral encephalitis without an identified etiologic agent, four cases of herpes simplex virus encephalitis (HSVE), and individual cases of Epstein-Barr virus and parainfluenza virus encephalitis. As suggested by the reviewers in their annual report review (11-30-99) following submission of our first annual progress report, we have "limited the number of samples to be examined" and restricted the scope of this aim to, "focus initially on a single disease entity." We are in the process of examining the subset of our cases with herpes simplex encephalitis. We have performed preliminary TUNEL staining on tissue blocks from this subset of cases. Given the reviewers feeling that this aim represented the "weakest area of the initial submission," we have continued the shift in priority and emphasis towards aims 2 and 3 (as outlined in our initial progress report and supported by the reviewers).

Specific Aim 2: Is the ceramide-sphingomyelin pathway involved in reovirus-induced apoptosis? We have made substantial progress in accomplishing the goals of this specific aim. Since our last annual report, three additional papers have been published or are in press in the Journal of Virology (Connolly et al., 2000; Clarke et al.,

2000; DeBiasi et al., 2000) with a fourth paper (referred to as Kominsky et al., 2000) currently undergoing review (copies of all published, in press, and submitted papers are included in the appendix). Unless otherwise noted, figures referred to in the text are from these papers. We have shown that reovirus infection of HeLa cells (and a variety of other cell types) is associated with a dramatic increase in NF-κB activity in infected cells as measured both with luciferase reporter assays and using electrophoretic mobility shift assays (EMSAs)(Connolly et al., 2000, Fig.2 and Fig.3). This activity reaches a maximum at 12 hrs post-infection (Connolly et al., 2000, Fig.2) in EMSAs, and at 18 hrs post-infection (Connolly et al., 2000, Fig.3).

The inactive form of NF-κB is complexed in the cytoplasm with its inhibitor IκB (see (2) for review). Phosphorylation of IκB on two N-terminal serine residues marks the protein for ubiquitination and subsequent degradation in proteosomes. Degradation of IκB unmasks a nuclear localization signal (NLS) on NFκB, which subsequently translocates to the nucleus where it interacts to activate transcription of genes containing specific NFκB-responsive promoter elements.

We have generated HeLa cells over-expressing a dominant-negative form of IκB (in which the first 36 N-terminal amino acids, encompassing the two serine phosphorylation sites have been deleted)(IκBα-ΔN2 cells). NFκB is not activated in these cells in response to reovirus infection and apoptosis is markedly inhibited (Connolly et al., 2000, Fig. 5A). Similar results have been obtained in both HEK293 and MDCK cells over-expressing a dominant negative form of IκB in which the N-terminal serine phosphorylation sites have been mutated to alanines (data not shown). The results obtained using the luciferase-reporter assay have been confirmed by EMSAs (data not

shown). As additional evidence for the importance of NF-κB activation in reovirus-induced apoptosis, we have also shown that treatment of HeLa cells with a synthetic inhibitor of proteosome function (Z-L_3VS), and of NF-κB activation, also inhibits reovirus-induced apoptosis (Connolly et al., 2000, Fig. 4). Reovirus infection induces apoptosis in wild-type mouse embryo fibroblasts (MEFs), but this is virtually eliminated in immortalized MEFs derived from mice with knockout mutations involving either the p50 (p50 -/-) or p65 (p65 -/-) subunits of the NF-κB complex (Connolly et al., 2000, Fig. 6,7). Thus, reovirus-induced apoptosis requires the activation of NFκB and can be blocked by inhibition of NFκB.

Having shown that reovirus apoptosis required NFκB activation, we next wished to identify which apoptosis-associated genes were involved in this process. Preliminary studies utilizing ribonuclease protection assays (RPAs) indicated that reovirus infection was associated with a selective increase in the level of mRNAs encoding the cell death receptor DR4 and its apoptosis-inducing ligand TRAIL (TNF-related apoptosis inducing ligand) (see (1) for general review of death receptors, and (8,9,12,21) for specific review of DR4, DR5, and TRAIL). mRNAS of other TNF receptor superfamily death receptors were not increased in infected cells. mRNA levels for another TRAIL-related death receptor, DR5, were found to be constitutively expressed in reovirus-infected cells, but immunoblots showed a clear increase in the amount of mature DR5 protein in infected cells (Clarke et al., 2000, Fig. 3).

In order to determine whether the DR4/DR5/TRAIL system was involved in reovirus-induced apoptosis we examined the effects of treating cells with polyclonal anti-TRAIL antibodies. Anti-TRAIL antibodies, but not antibodies directed against other TNF-

receptor superfamily ligands (e.g. TNF, FasL) inhibited apoptosis in reovirus-infected HEK293 cells and mouse L929 fibroblasts (Clarke et al., 2000, Fig. 1). In order to confirm these results, cells were also pre-treated with soluble forms of the DR4 and DR5 receptor. These soluble receptors bind TRAIL, and inhibit its binding to functional cell-surface receptors. Pre-treatment of cells with soluble DR4 and DR5 receptors, but not with soluble TNF-receptor, inhibited reovirus apoptosis in a dose-dependent manner (Clarke et al., 2000, Fig.1).

Interaction of an activating ligand with a death receptor results in oligomerization of receptors. This allows cytoplasmic death domains (DDs) of these receptors to interact (1). Apposition of these DDs is followed by their interaction with adapter proteins (exemplified by TNF Receptor associated death domain protein, TRADD and Fas associated death domain protein, FADD)(see (3,13) for role of FADD in TRAIL-mediated apoptosis). These proteins contain death effector domain (DED) sequences that interact with initiator caspases (e.g. caspase-8). Initiator caspases in turn interact with other caspases in an ordered cascade that leads ultimately to the activation of effector caspases (e.g. caspase 3) and apoptosis (see (18) for review). Additional proteases, including the calcium-activated neutral protease, calpain, may also be involved in this process (15-17).

We have begun to characterize the pathway leading from death domain receptor activation to apoptosis. Reovirus-induced apoptosis requires a FADD-like adapter protein, and can be inhibited by over-expression of a dominant-negative form of FADD (Clarke et al., 2000, Fig. 5). The caspase cascade for death-receptor triggered apoptosis is initiated by the activation of caspase-8, following its interaction with FADD. We have

also shown that a cell permeable peptide inhibitor of caspase-8 (z-IETD-FMK) inhibits reovirus-induced apoptosis (Clarke et al., 2000, Fig. 5).

We have recently begun a detailed evaluation of the caspase cascades activated following reovirus infection. A paper describing this work is currently under review by the Journal of Virology (referred to subsequently as Kominsky et al., 2000, copy in appendix). We have shown using fluorigenic substrate assays, Western immunoblots, and caspase-3 specific substrate cleavage assays that reovirus-infection is associated with activation of caspase-3 (Kominsky et al., 2000, Fig. 1, 2). Caspase-3 is an effector caspase that forms part of the "final common pathway" following activation of caspase cascades by a variety of mechanisms. Having shown that caspase-3 was activated we then proceeded to exam the death-receptor initiated pathway of caspase activation (see above). We had previously shown (Clarke et al, 2000, Fig. 5) that pre-treatment of cells with a cell-permeable specific inhibitor of caspase-8 (z-IETD-FMK) inhibited reovirus-induced apoptosis. We extended these observations by showing that caspase-8 was activated in infected cells as documented by immunoblots showing the activity-associated disappearance of the caspase-8 zymogen band (Kominsky et al., 2000. Fig. 3). Inhibition of caspase-8 activation by pre-treatment of cells with the cell permeable caspase-8 inhibitor z-IETD-FMK, resulted in inhibition of activation of caspase-3 (Kominsky et al., 2000, Fig. 4). This indicated that caspase-8 activation was upstream of caspase-3 activation.

We have previously shown that over-expression of the anti-apoptotic protein Bcl-2 in MDCK cells inhibits reovirus-induced apoptosis (10). Although Bcl-2 may exert its anti-apoptotic actions through a variety of mechanisms, one of the best established of

these involves its capacity to inhibit release of cytochrome c into the cytoplasm from mitochondria. Cytoplasmic cytochrome c can interact with the protein Apaf-1 and ATP to form a complex that activates caspase cascades beginning with the initiator caspase, caspase-9. In order to determine whether mitochondrial apoptosis pathways were activated following reovirus infection, we performed immunoblots using cytochrome c specific antisera on cytoplasmic fractions from reovirus-infected cells. Reovirus-infection is associated with cytochrome c release as early as 6 hrs post-infection (Kominsky et al., 2000, Fig. 5). Cytochrome c oxidase (subunit II) was not detected in cytoplasmic fractions containing cytochrome c. (Cytochrome c oxidase is present in mitochondria, but unlike cytochrome c is not released into cytoplasm, and can therefore be used to detect inadvertent contamination of cytoplasmic fractions with mitochondrial proteins.). Following release of cytochrome c into the cytoplasm in reovirus-infected cells, the initiator caspase, caspase 9 is activated. This activation can be detected by immunoblots showing cleavage of the ~46 kD caspase-9 proenzyme into its ~37 kD active form (Kominsky et al., 2000, Fig. 6). Pre-treatment of reovirus-infected cells with a cell permeable specific peptide inhibitor of caspase-9 (z-LEHD-FMK) resulted in inhibition of caspase-3 activation (Kominsky et al., 2000, Fig. 7). This result indicates that caspase-9, like caspase-8, is involved in the activation of the effector caspase, caspase-3. These studies provide clear evidence that both death receptor-initiated and mitochondrially-initiated pathways of apoptosis are active in reovirus-infected cells. Experiments are currently underway to determine the inter-relationships between these two pathways. Recent studies suggest that a third pathway of caspase activation (distinct from both the death receptor and mitochondrially activated pathways) may also exist. In this pathway,

"stress" induced by either the accumulation of proteins or the presence of malfolded proteins in the Golgi and endoplasmic reticulum (ER) may trigger the activation of caspase cascades initiated by the activation of caspases 2, and 12. We are currently investigating whether markers of Golgi/ER stress can be detected in reovirus-infected cells

In previously published work, supported by this grant, we have shown that calpain is activated following reovirus infection and that inhibition of this activation with either active site or calcium-binding site inhibitors of calpain will inhibit reovirus apoptosis in vitro (5). We have extended these studies by testing calpain inhibitors for their capacity to inhibit reovirus-induced apoptosis in a murine model (DeBiasi et al., 2000). We have shown that myocarditis induced in mice following intramuscular injection of reovirus strain 8B is due to apoptosis. Hearts from reovirus-infected mice showed morphological changes consistent with apoptosis, TUNEL+ staining of myocardiocytes, and a laddering pattern of fragmentation of DNA (extracted from whole hearts) (DeBiasi et al, 2000, Fig. 1, 2). Treatment of mice with CTX295, a calpain inhibitor, resulted in dramatic reduction in morphological evidence of cardiac pathology, reduction in serum levels of cardiac-specific enzymes (a marker of the severity of cardiac injury), and marked inhibition in apoptosis (as demonstrated by reduction in TUNEL staining) (DeBiasi et al., Fig. 5,6,7). Similar results were also seen in primary myocardiocyte cultures.

Specific Aim 3: Is reovirus apoptosis associated with aberrant regulation of cell cycle progression and does this dysregulation occur in post-mitotic neurons?

In the original statement of work we anticipated that the major work on this aim would not occur until years 3 and 4 of the grant. We have continued to make earlier than anticipated progress in this area. A paper describing this work is in press in the Journal of Virology (Poggioli et al., 2000) (attached), and a second manuscript is being prepared for submission.

Reovirus infection is associated with an inhibition of cellular proliferation (7,11,14,20), and different strains of virus differ in this capacity (14,20) (Poggioli et al., 2000, Fig. 1). We have used flow cytometry to analyze DNA content in infected cells permeabilized and stained with propidium iodine. These studies indicate that reovirus strains that inhibit cellular proliferation cause a progressive accumulation of cells in the G2M phase of the cell cycle (Poggioli et al., 2000, Fig. 2), and that this occurs in a dose-dependent manner (Poggioli et al., 2000, Fig. 3). Mixing experiments involving co-infection of cells with G2M arrest inducing and non-inducing reovirus strains indicate that the arrest phenotype is dominant (Poggioli et al., 2000 Fig. 5). Studies using reassortant viruses containing different combinations of genes derived from the G2M arrest-inducing T3D and non-inducing T1L viral strains indicate that the viral S1 gene is the primary determinant of this process (Poggioli et al., 2000, Table 1).

The S1 gene is bicistronic, encoding two non-homologous viral proteins (σ1, σ1s) from over-lapping but out-of-sequence open reading frames (ORFs). We have tested the capacity of a mutant virus (T3C84-MA) that contains σ1, but lacks σ1s, to induce G2M arrest. T3C84-MA contains a mutation that introduces a premature stop codon in the σ1s ORF, but still encodes a full-length σ1 protein. This virus, although still able to grow in infected cells and induce apoptosis as well as its wild-type (σ1s+) parent (T3C84), fails to

induce G2M arrest (Poggioli et al., 2000, Fig. 6). This suggests that the σ1s protein is necessary for reovirus-induced G2M arrest, and provides the first evidence for a biological function for this viral protein. C127 cells expressing σ1s under the control of a cadmium inducible promoter, show an increased accumulation of cells in G2M phase of the cell cycle following cadmium treatment when compared to either non-induced cells or to cadmium treated C127 cells containing a control plasmid lacking σ1s (Poggioli et al., 2000, Fig. 7).

We have previously shown that the capacity of reoviruses to inhibit cellular proliferation and to induce apoptosis are closely associated (20). This suggested three possible models: (1) apoptosis and G2M arrest are triggered by the same events during viral infection, but represent parallel rather than sequential pathways, (2) apoptosis, with the associated disruption in DNA integrity and structure, results in G2M arrest, (3) aberrant cell cycle regulatory signals result in induction of apoptosis. We have now tested the capacity of several inhibitors of reovirus-induced apoptosis to also inhibit reovirus-induced G2M arrest. Inhibition of calpain activation, blockade of caspase-3 activation, inhibition of TRAIL binding to DR4/DR5, and inhibition of NF-κB activation all inhibit reovirus-induced apoptosis, yet none of these interventions prevents virus-induced G2M arrest in susceptible cells (Poggioli et al., 2000, Fig. 8). These results clearly indicate that reovirus-induced perturbation of cell cycle regulation is not simply the result of DNA damage occurring during apoptosis. We are currently trying to distinguish between the two remaining hypotheses (parallel rather than sequential pathways, and cell cycle perturbation resulting in induction of apoptosis).

KEY RESEARCH ACCOMPLISHMENTS

*Reovirus infection is associated with activation of the nuclear transcriptional activation factor, NFκB. NF-κB is translocated to the nucleus in infected cells, and is capable of inducing expression of genes containing NF-κB responsive promoter elements.

*Reovirus-induced apoptosis is inhibited in cells in which reovirus-induced NFκB activation is inhibited or prevented: (1) by over-expression of dominant negative forms of its cytoplasmic inhibitor IκB, (2) by treatment of cells with proteosome inhibitors or, (3) in cells lacking the p50 or p65 NF-κB subunits as a result of gene knockouts.

*Reovirus-induced NFκB activation results in selective up-regulation of mRNA levels of the TNF superfamily death receptor DR4 and enhanced expression of mature DR5 protein.

*Reovirus-induced apoptosis is specifically inhibited by antibodies directed against TRAIL, the ligand for death receptors DR4 and DR5, but not by antibodies against TNF or FasL. Apoptosis is also specifically inhibited by soluble DR4 or DR5 receptor, but not by soluble TNF-receptor.

*Reovirus infection is associated with activation of caspase cascades in infected cells. This activation involves both cell death receptor associated and mitochondrial pathways of cell death. Both caspase-8, the initiator caspase for death-receptor mediated caspase cascades, and caspase-9, the initiator caspase for mitochondrially initiated caspase cascades, are activated in reovirus-infected cells. Inhibition of activation of either caspase-8 or caspase-9 inhibits reovirus-induced apoptosis. Caspase-3 is also activated in reovirus-infected cells, and appears to act as a key effector caspase for both the death-receptor and mitochondrial pathways.

*Reovirus induces apoptosis in the heart following infection of mice with strain 8B. This is associated with activation of calpain in the heart, and can be inhibited by in vivo treatment of infected mice with calpain inhibitor.

*Reovirus-induced inhibition of cellular proliferation is associated with arrest of cells in the G2M phase of the cell cycle.

*The reovirus S1 gene is the primary determinant of differences in the capacity of reovirus strains to induce G2M arrest.

* The reovirus σ1s protein, which is encoded by the S1 gene, is necessary for reovirus-induced G2M arrest, and over-expression of this protein in susceptible cells results in increased accumulation of cells in the G2M phase of the cell cycle.

*Although the capacity of reovirus strains to induce apoptosis and G2M are closely associated, apoptosis can be inhibited without preventing the capacity of reoviruses to induce G2M arrest, indicating that G2M arrest is not simply the result of apoptosis-associated cellular DNA damage.

REPORTABLE OUTCOMES (Since last report only)

Manuscripts:

Clarke P, Meintzer SM, Gibson S, Widmann C, Garrington TP, Johnson GL, Tyler KL. Reovirus-induced apoptosis is mediated by TRAIL. J. Virol. 74:8135-8139, 2000.

Connolly JL, Rodgers SE, Clarke P, Ballard DW, Kerr LD, Tyler KL, Dermody TS. Reovirus-induced apoptosis requires activation of transcription factor NF-κB. J. Virol. 74:2981-2989, 2000.

DeBiasi RL, Edelstein CL, Sherry B, Tyler KL. Calpain inhibition protects against virus-induced apoptotic myocardial injury. J. Virol. (JVI#961-00, in press), 2000.

Kominsky DJ, Bickel RJ, Meintzer SM, Clarke P, Tyler KL. Reovirus-induced apoptosis involves both death receptor- and mitochondrial-mediated caspase-dependent pathways of cell death. J. Virol. (submitted), 2000.

Poggioli GJ, Keefer C, Connolly JL, Dermody TS, Tyler KL. Reovirus-induced G2M arrest requires σ1s and occurs in the absence of apoptosis. J. Virol. 74: (in press), 2000.

Abstracts (All presented at platform sessions of the indicated meetings):

Clarke P, Meintzer S, Johnson GL, Tyler KL. MEKK1 and NIK contribute to the activation of NF-κB in reovirus-infected cells via IKK. 19th Annual Meeting of the American Society for Virology, Fort Collins, CO, July 8-12, 2000.

Kominsky D, Clarke P, Tyler KL. Reovirus induces apoptosis through a caspase-9 dependent pathway. 19th Annual Meeting of the American Society for Virology, Fort Collins, CO, July 8-12, 2000.

Turner B, Clarke P, Johnson GL, Tyler KL. TRAIL mediates reovirus-induced apoptosis in cancer cell lines. 19th Annual Meeting of the American Society for Virology, Fort Collins, CO, July 8-12, 2000.

Tyler KL, Clarke P, Gibson SB, Widmann C, Johnson GL. NFκB-regulated expression of cell death receptors DR4, DR5 and their ligand TRAIL mediates viral apoptosis. 52nd Annual Meeting of the American Academy of Neurology, San Diego, CA, April 29-May 6, 2000.

Selected Invited Presentations (Kenneth L. Tyler, M.D.)

Department of Virology, Institut Pasteur, Paris, France

Mechanisms of virus-induced apoptosis in vitro and in vivo: insights from the reovirus system. (June, 2000)

4th semi-annual Federation of American Societies for Experimental Biology (FASEB) Conference on Microbial Pathogenesis. Snowmass, CO. Mechanisms of reovirus-induced apoptosis (August, 2000).

3rd International Symposium on Neurovirology. San Francisco, CA. Cellular mechanisms of virus-induced apoptosis: Role of the TRAIL/DR4/DR5 death receptor system (September, 2000).

CONCLUSIONS

The work completed during the first two years of this research project has lead to the identification of the linkage between reovirus induced apoptosis and activation of the nuclear transcription factor, NFκB. Reovirus-induced apoptosis has also been shown to involve the TNF receptor superfamily of cell surface death receptors, specifically death

receptors 4 and 5 and their ligand, TRAIL. Reovirus infection induces the activation of caspase cascades, including initiator caspases associated with both the mitochondrial (e.g. caspase-9) and death-receptor mediated (e.g. caspase-8) pathways of cell death. Inhibition of the activation of NF-κB, blocking the interaction of TRAIL with its cell surface receptors, or inhibiting the subsequent activation of caspase cascades have all been shown to inhibit reovirus-induced apoptosis in vitro. In an effort to demonstrate the feasibility of anti-apoptotic strategies for the treatment of virus-induced disease in vivo, we have shown, in a murine model of reovirus-induced myocarditis, that inhibition of virus-induced calpain activation can prevent virus-induced apoptotic tissue injury in the heart. This suggests that inhibition of apoptosis may provide a novel strategy for the treatment of certain viral diseases.

We have identified the phase in the cell cycle (G2M) at which reoviruses induce inhibition of cellular proliferation in susceptible cells, and have shown that this process is not simply the result of apoptosis-induced damage to cellular DNA. We have shown that the reovirus S1 gene is the major determinant both of differences in the capacity of reovirus strains to induce apoptosis and their capacity to induce G2M cell cycle arrest. However, two distinct, non-homologous, S1-encoded proteins are involved in these two events. The reovirus σ1s protein is not required for virus-induced apoptosis, but is necessary for virus-induced G2M cell cycle arrest.

REFERENCES

1. Ashkenazi A, Dixit VM. Death receptors: signaling and modulation. Science 1998;281:1305-8.

2. Baeurle PA, Baltimore D. NF-(kappa)B: Ten years after. Cell 1996;87:13-20.

3. Chaudhary PM, Eby M, Jasmin A, Bookwalter A, Murray J, Hood L. Death receptor 5, a new member of the TNFR family, and DR4 induce FADD-dependent apoptosis and activate the NF-κB pathway. Immunity 1997;7:821-30.

4. Cohen JJ. Apoptosis. Immunol Today 1993;14:126-30.

5. Debiasi RL, Squier MKT, Pike B, Wynes M, Dermody TS, Cohen JJ, Tyler KL. Reovirus-induced apoptosis is preceded by increased cellular calpain activity and is blocked by calpain inhibitors. J Virol 1998;73:695-701.

6. Duke RC, Cohen JJ. Morphological and biochemical assays of apoptosis. In: Coligan JE, editors. Current protocols in immunology. NY: Wiley; 1992; p. 3.17.1-3.17.16

7. Gaulton GN, Greene MI. Inhibition of cellular DNA synthesis by reovirus occurs through a receptor-linked signaling pathway that is mimicked by antiidiotypic, antireceptor antibody. J Exp Med 1989;169:197-211.

8. Pan G, Ni J, Wei Y-F, Yu G-L, Gentz R, Dixit VM. An antagonist decoy receptor and a death domain-containing receptor for TRAIL. Science 1997;277:815821

9. Pan G, O'Rourke K, Chinnaiyan AM, Geintz R, Ebner R, Ni J, Dixit VM. The receptor for the cytotoxic ligand TRAIL. Science 1997;276:111-3.

10. Rodgers SE, Barton ES, Oberhaus SM, Pike B, Gibson CA, Tyler KL, Dermody TS. Reovirus-induced apoptosis of MDCK cells is not linked to viral yield and is blocked by Bcl-2. J Virol 1997;71:2540-6.

11. Saragovi HU, Bhandoola A, Lemercier MM, Akbar GKM, Greene MI. A receptor that subserves reovirus binding can inhibit lymphocyte proliferation triggered by mitotic signals. DNA Cell Biol 1995;14:653-64.

12. Schneider P, Bodmer J-L, Thome M, Hofmann K, Holler N, Tschopp J. Characterization of two receptors for TRAIL. FEBS Letters 1997;416:329-34.

13. Schneider P, Thome M, Burns K, Bodmer J-L, Hofmann K, Kataoka T, Holler N, Tschopp J. TRAIL receptors 1 (DR4) and 2 (DR5) signal FADD-dependent apoptosis and activate NFκB. Immunity 1997;7:831-6.

14. Sharpe AH, Fields BN. Reovirus inhibition of cellular DNA synthesis: role of the S1 gene. J Virol 1981;38:389-92.

15. Squier MKT, Cohen JJ. Calpain and cell death. Death and Differentiation 1996;3:275-83.

16. Squier MKT, Cohen JJ. Calpain, an upstream regulator of thymocyte apoptosis. J Immunol 1997;158:3690-7.

17. Squier MKT, Miller ACK, Malkinson AM, Cohen JJ. Calpain activation in apoptosis. J Cell Physiol 1994;159:229-37.

18. Thornberry NA, Lazebnik Y. Caspases: enemies within. Science 1998;281:1312-6.

19. Tyler KL, Nathanson N. Pathogenesis of viral infections. In: Knipe DM, Howley PM, editors. Fields Virology. 4th ed. Philadelphia: Lippincott-Raven; 1999;

20.Tyler KL, Squier MKT, Brown AL, Pike B, Willis D, Oberhaus SM, Dermody TS, Cohen JJ. Linkage between reovirus-induced apoptosis and inhibition of cellular DNA synthesis: Role of the S1 and M2 genes. J Virol 1996;70:7984-7991.

21. Walczak H, Degli-Esposti MA, Johnson RS, Smolak P, Waugh J, Boiani N, Timour MS, Gerhart MJ, Schooley KA, Smith CA, et al. TRAIL-R2: a novel apoptosis-mediating receptor for TRAIL. EMBO J 1997;16:5386-97.

JOURNAL OF VIROLOGY, Apr. 2000, p. 2981–2989
0022-538X/00/$04.00+0

Vol. 74, No. 7

Reovirus-Induced Apoptosis Requires Activation of Transcription Factor NF-κB

JODI L. CONNOLLY,[1,2] STEVEN E. RODGERS,[1,2] PENNY CLARKE,[3] DEAN W. BALLARD,[1] LAWRENCE D. KERR,[1,4] KENNETH L. TYLER,[3,5,6,7,8] AND TERENCE S. DERMODY[1,2,9]*

Departments of Microbiology and Immunology,[1] Cell Biology,[4] and Pediatrics[9] and Elizabeth B. Lamb Center for Pediatric Research,[2] Vanderbilt University School of Medicine, Nashville, Tennessee 37232, and Departments of Neurology,[3] Medicine,[5] Microbiology,[6] and Immunology,[7] University of Colorado Health Sciences Center, and Neurology Service, Denver Veterans Affairs Medical Center,[8] Denver, Colorado 80220

Received 5 October 1999/Accepted 29 December 1999

Reovirus infection induces apoptosis in cultured cells and in vivo. To identify host cell factors that mediate this response, we investigated whether reovirus infection alters the activation state of the transcription factor nuclear factor kappa B (NF-κB). As determined in electrophoretic mobility shift assays, reovirus infection of HeLa cells leads to nuclear translocation of NF-κB complexes containing Rel family members p50 and p65. Reovirus-induced activation of NF-κB DNA-binding activity correlated with the onset of NF-κB-directed transcription in reporter gene assays. Three independent lines of evidence indicate that this functional form of NF-κB is required for reovirus-induced apoptosis. First, treatment of reovirus-infected HeLa cells with a proteasome inhibitor prevents NF-κB activation following infection and substantially diminishes reovirus-induced apoptosis. Second, transient expression of a dominant-negative form of IκB that constitutively represses NF-κB activation significantly reduces levels of apoptosis triggered by reovirus infection. Third, mutant cell lines deficient for either the p50 or p65 subunits of NF-κB are resistant to reovirus-induced apoptosis compared with cells expressing an intact NF-κB signaling pathway. These findings indicate that NF-κB plays a significant role in the mechanism by which reovirus induces apoptosis in susceptible host cells.

Many viruses are capable of inducing programmed cell death, which results in apoptosis of infected cells (43, 45, 52, 60). Apoptotic cell death is characterized by cell shrinkage, membrane blebbing, condensation of nuclear chromatin, and activation of endogenous endonucleases. These changes occur according to developmental programs or in response to certain environmental stimuli (2, 43, 52, 71). In some cases, apoptosis triggered by virus infection appears to serve as a host defense mechanism to limit viral replication or spread. This defense mechanism is mediated either directly by self-destruction of the host cell prior to completion of viral replication or indirectly through recognition of the infected cell by cytotoxic T lymphocytes (43, 52). In other cases, induction of apoptosis may enhance viral infection by facilitating virus spread or allowing the virus to evade host inflammatory or immune responses (20, 43, 60). For some viruses, cellular factors operant during apoptosis may function to increase the production of viral progeny (45, 52).

Mammalian reoviruses have served as useful models for studies of viral pathogenesis. Reoviruses are nonenveloped icosahedral viruses with a genome consisting of 10 double-stranded RNA gene segments (reviewed in reference 41). After infection of newborn mice, reoviruses are highly virulent, inducing injury to a variety of host organs including the central nervous system, heart, and liver (reviewed in reference 62). In both cultured cells (46, 63) and the murine central nervous system (42) and heart (R. DeBiasi, B. Sherry, and K. Tyler, Abstr. Am. Soc. Virol. 18th Annu. Meet., abstr. 52-1, p. 152, 1999), reoviruses induce the morphological and biochemical features of apoptosis.

* Corresponding author. Mailing address: Lamb Center for Pediatric Research, D7235 MCN, Vanderbilt University School of Medicine, Nashville, TN 37232. Phone: (615) 343-9943. Fax: (615) 343-9723. E-mail: terry.dermody@mcmail.vanderbilt.edu.

Insight into the mechanisms by which reoviruses trigger apoptosis has emerged from studies of viral prototype strains that vary in their capacity to elicit this cellular response. Reovirus strains type 3 Abney and type 3 Dearing (T3D) induce apoptosis in cultured cells to a substantially greater extent than does strain type 1 Lang (46, 63). Differences in the capacity of these strains to induce apoptosis are determined by the viral S1 gene (46, 63), which encodes two proteins, attachment protein σ1 and nonstructural protein σ1s (25, 31, 50). Reovirus σ1s-null mutant T3C84-MA induces apoptosis with an efficiency equivalent to its σ1s-expressing parental strain, T3C84 (47), which indicates that the σ1 protein is the S1 gene product responsible for mediating differences in the efficiency with which reovirus strains induce apoptosis. Therefore, these studies suggest that apoptosis induced by reovirus is triggered by a signaling pathway initiated by early steps in the virus replication cycle.

The nuclear factor kappa B (NF-κB) family of transcription factors plays a key role in the regulation of cell growth and survival. The prototypical form of NF-κB exists as a heterodimer of proteins p50 and p65 (RelA) (4, 27). In quiescent cells, NF-κB is sequestered in the cytoplasm by the IκB family of inhibitory proteins (3, 66). Following exposure of cells to a variety of stimuli (including tumor necrosis factor alpha [TNF-α], interleukin-1, and lipopolysaccharide), activation of NF-κB is accomplished by a mechanism involving site-specific phosphorylation, ubiquitination, and proteasomal degradation of IκB (11, 12, 17, 61). Release of IκB reveals a nuclear localization signal on NF-κB, which allows NF-κB to translocate to the nucleus (7), where it serves as a transcriptional regulator (reviewed in references 38 and 66). In systems in which NF-κB is activated during induction of apoptosis, NF-κB can either prevent (6, 35, 65, 69) or potentiate (1, 29, 32, 34) apoptosis.

We conducted experiments to investigate the role of NF-κB in reovirus-induced apoptosis. We show that NF-κB complexes

are activated in HeLa cells in response to reovirus infection and that these complexes contain both p50 and p65. Using two independent methods to block NF-κB activation following reovirus infection, we demonstrate that reovirus-induced apoptosis requires NF-κB. Furthermore, reovirus-induced apoptosis is inhibited in cells deficient in expression of either p50 or p65. These results provide strong evidence that reovirus activates NF-κB and that NF-κB activation is required for apoptosis induced by reovirus infection.

MATERIALS AND METHODS

Cells and viruses. Murine L929 (L) cells were maintained as previously described (47). p50+/+, p50−/−, p65+/+, and p65−/− immortalized fibroblasts were obtained from David Baltimore, California Institute of Technology, Pasadena, Calif. HeLa, p50+/+, p50−/−, p65+/+, and p65−/− cells were grown in Dulbecco's modified Eagle's medium (Gibco BRL, Gaithersburg, Md.) supplemented to contain 10% fetal bovine serum (Intergen, Purchase, N.Y.), 2 mM L-glutamine, 100 U of penicillin per ml, 100 μg of streptomycin per ml (Sigma Chemical Co., St. Louis, Mo.), and 0.25 μg of amphotericin B per ml (Irvine Scientific, Santa Ana, Calif.).

Reovirus strain T3D is a laboratory stock. Purified virion preparations were made as previously described using second-passage L-cell lysate stocks of twice-plaque-purified reovirus (26). Concentrations of virions in purified preparations were determined from the equivalence 1 optical density at 260 nm unit = 2.1×10^{12} virions per ml (54).

Quantitation of reovirus growth. Cells grown in 24-well tissue culture plates (Costar, Cambridge, Mass.) were infected with T3D at a multiplicity of infection (MOI) of 1 PFU per cell. After viral adsorption for 1 h, the inoculum was removed, 1.0 ml of fresh medium was added, and the cells were incubated at 37°C for various intervals. After incubation, cells and culture medium were frozen (−70°C) and thawed twice, and viral titers in cell lysates were determined by plaque assay using L-cell monolayers (67).

Quantitation of apoptosis by acridine orange staining. Cells grown in 24-well tissue culture plates were treated with 20 ng of human recombinant TNF-α (Sigma) per ml or infected with T3D at an MOI of 100 PFU per cell. This MOI was chosen to produce a synchronous infection and to ensure maximum levels of apoptosis. The percentage of apoptotic cells was determined using acridine orange staining as previously described (23, 46, 63). The cell culture medium was removed, and the cells were incubated with trypsin-EDTA (Irvine Scientific). The cell culture medium and trypsinized cells were combined and centrifuged. The cell pellet was resuspended in 200 μl of phosphate-buffered saline and stained using 10 μl of a solution containing 100 μg of acridine orange (Sigma) per ml and 100 μg of ethidium bromide (Sigma) per ml. For each experiment, 200 to 300 cells were counted and the percentage of cells exhibiting condensed chromatin was determined by epi-illumination fluorescence microscopy using a fluorescein filter set (Photomicroscope III; Zeiss, Oberköchen, Germany).

EMSA. Cells grown in 75-cm^2 tissue culture flasks (Costar) were either treated with 20 ng of TNF-α per ml or adsorbed with T3D at an MOI of 100 PFU per cell. After incubation at 37°C for various intervals, nuclear extracts were prepared by washing cells in phosphate-buffered saline and incubating them in hypotonic lysis buffer (10 mM HEPES [pH 7.9], 10 mM KCl, 1.5 mM $MgCl_2$, 0.5 mM dithiothreitol, 0.5 mM phenylmethylsulfonyl fluoride, protease inhibitor cocktail [Boehringer Mannheim, Indianapolis, Ind.]) at 4°C for 15 min. Then 1/20 volume of 10% Nonidet P-40 was added to the cell lysate, and the sample was vortexed for 10 s and centrifuged at 10,000 × *g* for 5 min. The nuclear pellet was washed once in hypotonic buffer, resuspended in high-salt buffer (25% glycerol, 20 mM HEPES [pH 7.9], 0.42 M NaCl, 1.5 mM $MgCl_2$, 0.2 mM EDTA, 0.5 mM dithiothreitol, 0.5 mM phenylmethylsulfonyl fluoride, protease inhibitor cocktail), and incubated at 4°C for 2 to 3 h. Samples were centrifuged at 10,000 × *g* for 10 min, and the supernatant was used as the nuclear extract.

Nuclear extracts were assayed for NF-κB activation by an electrophoretic mobility shift assay (EMSA) using a ^{32}P-labeled oligonucleotide consisting of the NF-κB consensus binding sequence (Santa Cruz Biotechnology, Santa Cruz, Calif.). Nuclear extracts (5 to 10 μg of total protein) were incubated at 4°C for 20 min with a binding-reaction buffer containing 2 μg of poly(dI-dC) (Sigma) in 20 mM HEPES (pH 7.9)–60 mM KCl–1 mM EDTA–1 mM dithiothreitol–5% glycerol. Radiolabeled NF-κB consensus oligonucleotide (0.1 to 1.0 ng) was added, and the mixture was incubated at room temperature for 20 min. For competition experiments, a 10-fold excess of unlabeled consensus oligonucleotide or of an oligonucleotide containing a point mutation in the NF-κB consensus site (Santa Cruz Biotechnology) was added to reaction mixtures. For supershift experiments, 1 μl of rabbit polyclonal antiserum raised against either human p50 or p65 (Santa Cruz Biotechnology) or a control antibody raised against reovirus nonstructural protein σ1s (47) was added to binding-reaction mixtures and incubated at 4°C for 30 min prior to the addition of radiolabeled oligonucleotide. Nucleoprotein complexes were subjected to electrophoresis on native 5% polyacrylamide gels at 180 V, dried under vacuum, and exposed to Biomax MR film (Kodak, Rochester, N.Y.).

Luciferase gene reporter assay. The NF-κB-dependent luciferase reporter construct was a gift from Lucy Ghoda. The construct is composed of pGL2-Basic (Promega, Madison, Wis.) and three NF-κB-binding sites from the major histocompatibility complex class I promoter. HeLa cells (1.5×10^5) in six-well tissue culture plates (Costar) were incubated for 24 h and then transfected with 10 μg of the luciferase reporter construct and 2 μg of a cytomegalovirus (CMV)–β-galactosidase reporter construct (Clontech, Palo Alto, Calif.) using LipofectAMINE (Gibco BRL). After an additional 24-h incubation, cells were either mock infected or infected with T3D at an MOI of 100 PFU per cell and incubated at 37°C for various intervals. The cells were resuspended in 1 ml of sonication buffer (91 mM dithiothreitol, 0.91 M K_2HPO_4 [pH 7.8]), centrifuged at 2,000 × *g* for 10 min, and resuspended in 100 μl of sonication buffer. The cells were then vortexed, frozen (−20°C) and thawed three times, and centrifuged at 14,000 × *g* for 10 min. Samples (10 μl) were assessed for luciferase activity after addition of 350 μl of luciferase assay buffer (85 mM dithiothreitol, 0.85 M K_2HPO_4 [pH 7.8], 50 mM ATP, 15 mM $MgSO_4$) by determining the optical density in a luminometer (Monolight 2010; Analytical Luminescence Laboratory). Samples were assayed for β-galactosidase activity using standard procedures (49) to normalize for transfection efficiency.

Proteasome inhibitor treatment. The proteasome inhibitor Z-L_3VS was obtained from Hidde Ploegh (10). HeLa cells were incubated at 37°C for 1 h with medium containing 5 μM Z-L_3VS. TNF-α at 20 ng per ml was added, and the cells were incubated at 37°C for 18 h, or the medium was removed and the cells were adsorbed at 4°C for 1 h with T3D at an MOI of 100 PFU per cell in gelatin saline containing 5 μM Z-L_3VS. Following adsorption, medium containing the proteasome inhibitor was added and the cells were incubated at 37°C for various intervals. Cells were harvested for EMSA or acridine orange staining assays.

Transient transfection of HeLa cells. The coding sequence of FLAG epitope-tagged human IκBα lacking amino acids 1 to 36 (IκBα-ΔN) (11) was inserted into the multiple-cloning site of pHook-2 (Invitrogen, Carlsbad, Calif.) to generate pHook-2/IκBα-ΔN. HeLa cells (7×10^5) in 60-mm dishes (Corning, Corning, N.Y.) were incubated at 37°C for 24 h and then transfected with either 5 μg of pHook-2/lacZ (Invitrogen) or 5 μg of pHook-2/IκBα-ΔN using LipofectAMINE PLUS reagent (Gibco BRL). Transfected cells were selected using Capture-Tec magnetic beads (Invitrogen) 24 h following infection and plated in 24-well plates for use in acridine orange staining assays.

Statistical analysis. Acridine orange staining data were tested using parametric statistical analysis with a two-sample *t* test. Statistical analysis was performed using Minitab statistical software (Addison-Wesley, Reading, Mass.).

RESULTS

Reovirus replicates efficiently and induces apoptosis in HeLa cells. To determine whether reovirus is capable of productively infecting HeLa cells, reovirus strain T3D was adsorbed to cells at an MOI of 1 PFU per cell and viral yields were determined 24 and 48 h after infection (Fig. 1A). T3D replicated efficiently in HeLa cells, producing yields of approximately 800 and 8,000 progeny virions per input 24 and 48 h following infection, respectively. To determine whether reovirus induces apoptosis of HeLa cells, T3D was adsorbed to cells at an MOI of 100 PFU per cell and apoptosis was assessed by acridine orange staining 24 and 48 h after infection (Fig. 1B). In previous work, we showed that cell death detected using acridine orange staining of infected L cells and Madin-Darby canine kidney (MDCK) epithelial cells correlates with ultrastructural changes characteristic of apoptosis and formation of oligonucleosome-length DNA ladders (46, 63). T3D infection of HeLa cells induced chromatin condensation and the morphological changes of apoptosis in approximately 70% of cells 24 h after infection and 80% of cells 48 h after infection. These results indicate that reovirus grows efficiently in HeLa cells and induces the death of these cells by apoptosis.

NF-κB is activated by reovirus. To determine whether NF-κB is activated following reovirus infection of HeLa cells, we used EMSAs to detect NF-κB in nuclear extracts prepared from reovirus-infected cells. HeLa cells were either mock infected or infected with reovirus strain T3D, and nuclear extracts were prepared at various times after viral adsorption. Extracts were incubated with a ^{32}P-labeled oligonucleotide consisting of the NF-κB consensus binding sequence and resolved in a nondenaturing polyacrylamide gel (Fig. 2A). Following infection with reovirus, proteins capable of shifting the radiolabeled oligonucleotide to a higher relative molecular

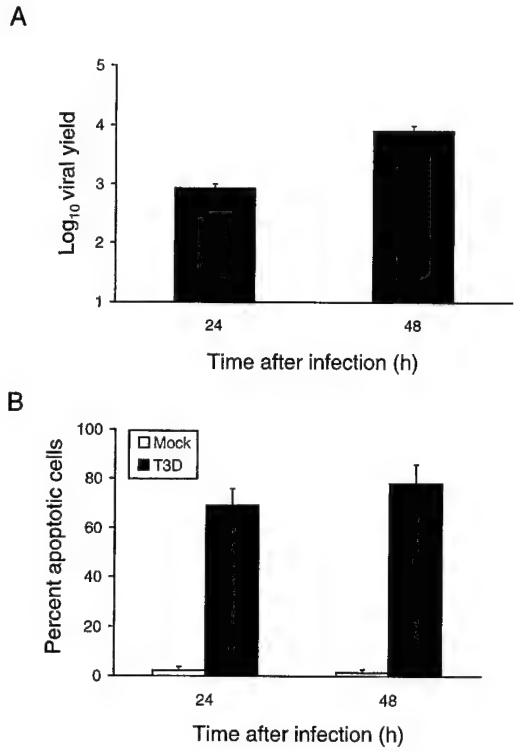

FIG. 1. (A) Growth of reovirus in HeLa cells. Cells (1×10^5) were infected with reovirus strain T3D at an MOI of 1 PFU per cell. After adsorption for 1 h, the inoculum was removed, fresh medium was added, and the cells were incubated at 37°C for 0, 24, or 48 h. The cells were frozen and thawed twice, and viral titers were determined by a plaque assay. The results are expressed as the mean viral yields, calculated by dividing the viral titer at 24 or 48 h by the viral titer at 0 h, for three independent experiments. Error bars indicate standard error of the mean. (B) Apoptosis induced by reovirus infection of HeLa cells. Cells (5×10^4) were either mock infected or infected with reovirus strain T3D at an MOI of 100 PFU per cell. After adsorption for 1 h, the cells were incubated at 37°C for 24 or 48 h and stained with acridine orange. The results are expressed as the mean percentage of cells undergoing apoptosis in three independent experiments. Error bars indicate standard error of the mean.

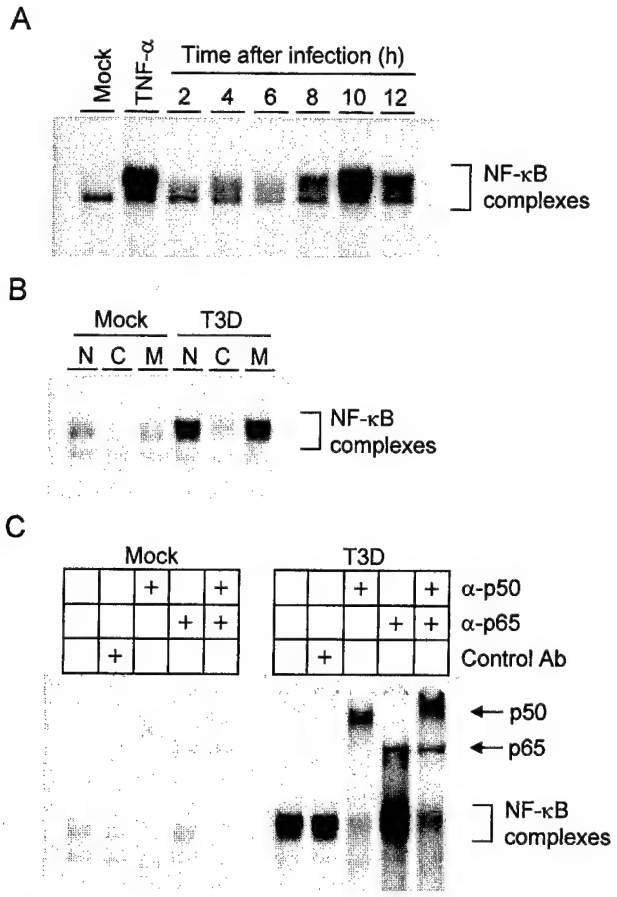

FIG. 2. (A) Time course of NF-κB gel shift activity in nuclear extracts prepared from reovirus-infected HeLa cells. Cells (5×10^6) were either mock infected or infected with T3D at an MOI of 100 PFU per cell and incubated at 37°C for the times shown. Uninfected cells also were treated with 20 ng of TNF-α per ml for 1 h. Nuclear extracts were prepared and incubated with a ^{32}P-labeled oligonucleotide consisting of the NF-κB consensus binding sequence. Incubation mixtures were resolved by acrylamide gel electrophoresis, dried, and exposed to film. NF-κB-containing complexes are indicated. (B) Specificity of NF-κB gel shift activity. Nuclear extracts were prepared as in panel A 10 h after viral adsorption. Extracts were incubated with ^{32}P-labeled NF-κB consensus oligonucleotide alone (lanes N), a 10-fold excess of unlabeled consensus probe (lanes C), or a 10-fold excess of unlabeled mutant probe consisting of the NF-κB consensus sequence with a point mutation that abolishes NF-κB binding (lanes M). NF-κB-containing complexes are indicated. (C) Identification of NF-κB family members activated by reovirus infection. Nuclear extracts were prepared as in panel A 10 h after viral adsorption. Extracts were incubated with no antibody, a control antibody (Ab), p50-specific antiserum, p65-specific antiserum, or both p50- and p65-specific antisera. NF-κB complexes not shifted by antibody and supershifted complexes containing p50 or p65 are indicated.

mass were increased in nuclear extracts. NF-κB activation was first detected at 4 h postinfection, peaked at 10 h postinfection, and was diminishing by 12 h postinfection. Activated complexes could not be detected in mock-infected cultures at any time point (data not shown). As assessed by EMSA, NF-κB was activated in L cells and MDCK cells with similar kinetics following reovirus infection (data not shown).

To confirm the specificity of NF-κB DNA-binding activity in these experiments, HeLa cells were either mock infected or infected with T3D at an MOI of 100 PFU per cell and nuclear extracts were prepared 10 h after adsorption. Nuclear extracts were incubated with a ^{32}P-labeled NF-κB consensus oligonucleotide in the presence of a 10-fold excess of either unlabeled consensus oligonucleotide or unlabeled mutant oligonucleotide (Fig. 2B). The mutant oligonucleotide consists of the NF-κB consensus sequence with a single point mutation that abolishes NF-κB binding. Binding of the radiolabeled probe was competed with unlabeled consensus oligonucleotide but not with mutant oligonucleotide. We conclude that the gel shift activity detected following reovirus infection is specific for sequences that are bound by NF-κB.

To identify NF-κB family members present in complexes activated following reovirus infection, nuclear extracts were prepared from mock-infected cells and cells infected with T3D 10 h after viral adsorption. The nuclear extracts were incubated with a p50-specific antiserum, a p65-specific antiserum, or both antisera prior to addition of the ^{32}P-labeled NF-κB consensus oligonucleotide (Fig. 2C). The addition of anti-p50 or anti-p65 antiserum or both antisera resulted in bands of higher relative molecular mass, indicating that both p50 and p65 are present in complexes activated following reovirus infection. These findings indicate that reovirus infection of HeLa cells results in nuclear translocation of NF-κB complexes and that these complexes contain NF-κB family members p50 and p65.

To determine whether NF-κB is capable of stimulating transcription following reovirus infection, we used a reporter gene construct containing NF-κB-binding sites to direct the expression of luciferase. Following transfection of HeLa cells with

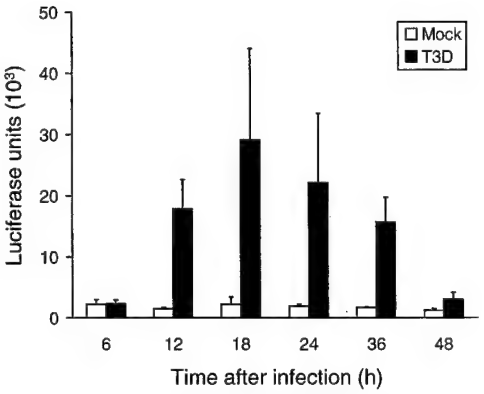

FIG. 3. NF-κB-dependent luciferase expression in reovirus-infected HeLa cells. Cells (1.5×10^5) were transfected with 10 μg of a luciferase reporter construct containing NF-κB binding sites. After 24 h, the cells were either mock infected or infected with T3D at an MOI of 100 PFU per cell and incubated at 37°C for the times shown. Cell extracts were prepared, and luciferase activity was determined. The results are expressed as the mean luciferase units in two independent experiments. Error bars indicate standard error of the mean.

this construct, cells were either mock infected or infected with T3D. After incubation for various intervals, cell extracts were prepared and assayed for luciferase activity (Fig. 3). T3D infection was associated with substantial NF-κB-dependent luciferase expression in comparison to mock-infected cells. Luciferase activity in infected cells was first detected between 6 and 12 h postinfection and was greatest 18 h postinfection, after which it declined and was nearly undetectable by 48 h postinfection. Transfection efficiencies were normalized by cotransfection of a β-galactosidase reporter construct driven by the CMV promoter. β-Galactosidase expression from the CMV reporter was not altered by reovirus infection (data not shown). These results indicate that reovirus infection of HeLa cells activates NF-κB-dependent transcription, which is consistent with the results obtained from biochemical experiments.

Proteasome inhibitor treatment inhibits reovirus-induced apoptosis. To determine the role of NF-κB activation in reovirus-induced apoptosis, HeLa cells were treated with Z-L_3VS, a synthetic inhibitor of proteasome function (10). Previous studies of other proteasome inhibitors have demonstrated that NF-κB activation induced by a variety of stimuli, including TNF-α, lipopolysaccharide, and phorbol esters, is blocked by treatment of cells with inhibitors of proteasome catalytic activity (36, 44). Since degradation of IκB and the subsequent release of NF-κB require proteasome activity (17), proteasome inhibitors lead to sequestration of NF-κB in the cytoplasm. To determine whether Z-L_3VS is capable of blocking NF-κB activation following reovirus infection, cells were cultured in the absence or presence of 5 μM Z-L_3VS and then either mock infected or infected with T3D at an MOI of 100 PFU per cell. Nuclear extracts were prepared 10 h following infection and used in an EMSA (Fig. 4A). Treatment of HeLa cells with Z-L_3VS abolished NF-κB activation following reovirus infection, which confirms that inhibition of proteasome function blocks nuclear translocation of NF-κB.

To determine the effect of blockade of NF-κB activation on reovirus-induced apoptosis, HeLa cells were cultured in the absence or presence of 5 μM Z-L_3VS and then either mock infected or infected with T3D at an MOI of 100 PFU per cell. Apoptosis was assessed using acridine orange staining 18 h after infection (Fig. 4B). This time point was chosen because more prolonged incubation with the proteasome inhibitor resulted in cytotoxicity. Approximately 20% of reovirus-infected

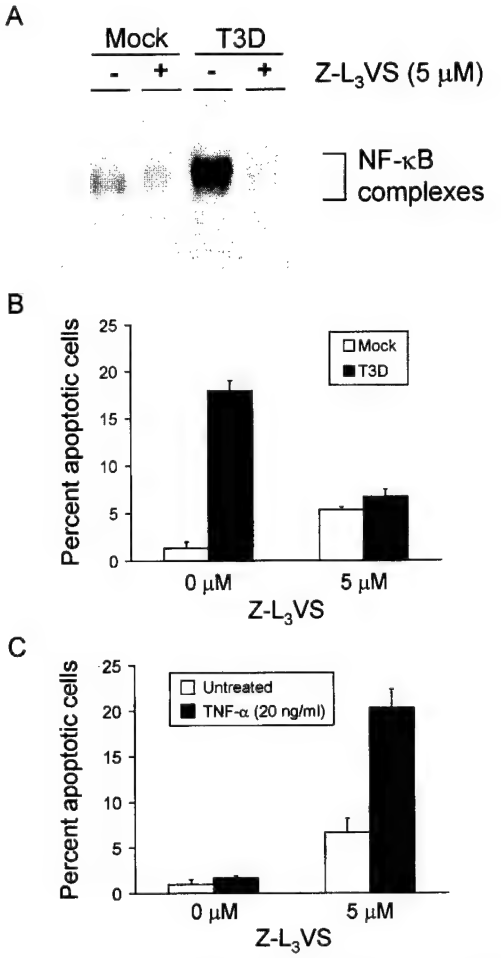

FIG. 4. (A) NF-κB gel shift activity in reovirus-infected cells cultured in the presence of Z-L_3VS. Cells (5×10^6) were either mock infected or infected with T3D at an MOI of 100 PFU per cell and cultured in the absence or presence of 5 μM Z-L_3VS. After incubation at 37°C for 10 h, nuclear extracts were prepared and incubated with a ^{32}P-labeled oligonucleotide consisting of the NF-κB consensus sequence. Incubation mixtures were resolved by acrylamide gel electrophoresis, dried, and exposed to film. NF-κB-containing complexes are indicated. (B) Quantitation of apoptosis in reovirus-infected HeLa cells cultured in the presence of Z-L_3VS. Cells (5×10^4) were either mock infected or infected with T3D at an MOI of 100 PFU per cell and cultured in the absence or presence of 5 μM Z-L_3VS. After incubation at 37°C for 18 h, the cells were stained with acridine orange. (C) Quantitation of apoptosis in TNF-α-treated HeLa cells cultured in the presence of Z-L_3VS. Cells (5×10^4) were either untreated or treated with 20 ng of TNF-α per ml and cultured in the absence or presence of 5 μM Z-L_3VS. After incubation at 37°C for 18 h, the cells were stained with acridine orange. The results of the experiments in panels B and C are expressed as the mean percentage of cells undergoing apoptosis in three independent experiments. Error bars indicate standard error of the mean.

cells cultured in the absence of the proteasome inhibitor were apoptotic 18 h after infection; however, only 6% of infected cells cultured in the presence of the proteasome inhibitor were apoptotic ($P = 0.005$). The level of apoptosis detected in infected cells cultured with Z-L_3VS did not significantly differ from that observed in uninfected cells cultured with the proteasome inhibitor ($P = 0.25$). As a control for the blockade of NF-κB using Z-L_3VS, cells also were treated with TNF-α (Fig. 4C), which has been shown to increase the levels of apoptosis in cells lacking functional NF-κB (6, 35, 65, 69). Apoptosis was increased in TNF-α-treated cells cultured in the presence of Z-L_3VS, suggesting that alterations in apoptosis induction mediated by the proteasome inhibitor are due to blockade of

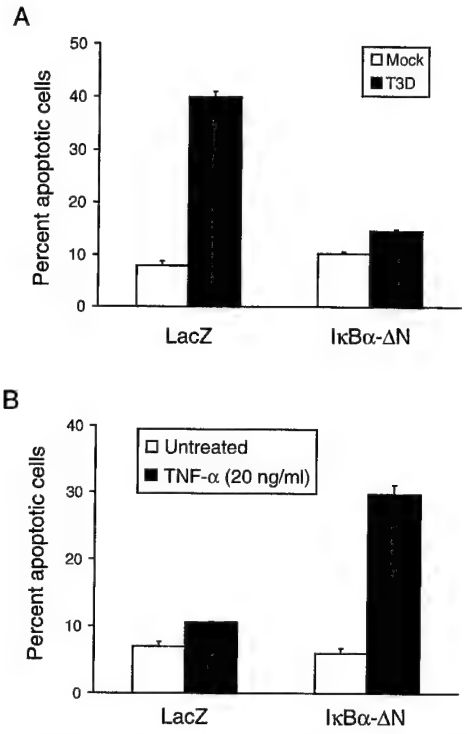

FIG. 5. Quantitation of apoptosis in HeLa cells transiently expressing IκBα-ΔN. Cells (1×10^6) were either transfected with 5 μg of pHook-2/IκBα-ΔN or 5 μg of pHook-2/lacZ. After 24 h, transfected cells were isolated using CaptureTec magnetic beads and plated in 24-well plates. (A) Transfected cells (2×10^4) were either mock infected or infected with T3D at an MOI of 100 PFU per cell. After incubation at 37°C for 24 h, the cells were stained with acridine orange. (B) Transfected cells (2×10^4) were either not treated or treated with 20 ng of TNF-α per ml. After incubation at 37°C for 24 h, the cells were stained with acridine orange. The results of the experiments in both panels are expressed as the mean percentage of cells undergoing apoptosis in three independent experiments. Error bars indicate standard error of the mean.

NF-κB. These results provide evidence that interference with signal-dependent degradation of IκB prevents reovirus-induced apoptosis.

Expression of a transdominant inhibitor of NF-κB inhibits reovirus-induced apoptosis. To exclude the possibility that exposure of cells to a proteasome inhibitor results in the blockade of apoptosis by inhibiting viral replication or by exerting other nonspecific effects, we tested whether transient transfection of a transdominant inhibitor of NF-κB, IκBα-ΔN, alters reovirus-induced apoptosis. HeLa cells were transfected with the pHook-2 plasmid containing human IκBα-ΔN appended at the amino terminus with a FLAG epitope. IκBα-ΔN is a 36-amino-acid amino-terminal truncation of IκBα that lacks the two serine residues required for IκBα degradation (12, 51, 61). IκBα-ΔN cannot be targeted for proteasome-mediated degradation and thus functions as a *trans*-dominant inhibitor of NF-κB. The pHook-2 plasmid allows the selection of transfected cells from a population of cells by virtue of coexpression of a cell surface marker that allows subsequent isolation using magnetic beads (19). Cells selected following transfection of either pHook-2/IκBα-ΔN or a control plasmid, pHook-2/lacZ, were either mock infected or infected with T3D at an MOI of 100 PFU per cell. Apoptosis was assessed using acridine orange staining 24 h after infection (Fig. 5A). Approximately 40% of pHook-2/lacZ-transfected cells were apoptotic following infection with reovirus. In sharp contrast, only 15% of pHook-2/IκBα-ΔN-transfected cells were apoptotic following reovirus infection ($P = 0.002$). This low level of apoptosis in the pHook-2/IκBα-ΔN-transfected cells was similar to the level of apoptosis in mock-infected cultures (approximately 10%). The percentage of apoptotic cells in mock-infected cultures was higher than routinely observed for untransfected cells, which is probably due to transfection and selection conditions. As a control, transfected cells also were treated with TNF-α (Fig. 5B), which has been shown to increase levels of apoptosis in cells lacking p65 (6) and in cells expressing mutant forms of IκBα (65, 69). Levels of apoptosis were increased following TNF-α treatment of cells transfected with pHook-2/IκBα-ΔN in comparison to cells transfected with pHook-2/lacZ. Therefore, it is likely that transfection with pHook-2/IκBα-ΔN effectively blocks NF-κB activation. Stable expression of mutant forms of IκB in L cells and MDCK cells also inhibits both NF-κB activation and apoptosis following reovirus infection (data not shown). These results demonstrate that expression of an NF-κB *trans*-dominant inhibitor blocks reovirus-induced apoptosis and further supports the hypothesis that NF-κB activation is required for apoptosis induced by reovirus infection.

Reovirus-induced apoptosis is inhibited in cell lines deficient for p50 or p65. Since both p50 and p65 are present in NF-κB complexes activated following reovirus infection, we performed experiments to specifically determine whether p50 or p65 is required for reovirus-induced apoptosis. Immortalized embryonic fibroblasts containing a null mutation in the gene encoding either the p50 or p65 subunit of NF-κB were infected with reovirus and assayed for NF-κB activation and apoptosis induction. To determine whether NF-κB complexes are activated following reovirus infection of the null cell lines, the p50−/− and p65−/− cell lines and their respective p50+/+ and p65+/+ littermate control cell lines were either mock infected or infected with T3D at an MOI of 100 PFU per cell. Nuclear extracts were prepared 6 h (p50+/+ and p50−/−) or 8 h (p65+/+ and p65−/−) following infection and used in EMSAs (Fig. 6A and 7A). The results demonstrate that NF-κB complexes are not activated in the p50−/− and p65−/− cell lines following infection. This result was anticipated based on the biochemical results with HeLa cells, which demonstrated that p50 and p65 are the primary constituents of NF-κB complexes activated by reovirus.

To determine whether reovirus is capable of inducing apoptosis in the mutant cell lines, p50+/+, p50−/−, p65+/+, and p65−/− cells were either mock infected or infected with T3D at an MOI of 100 PFU per cell. Apoptosis was assessed using acridine orange staining 48 h after infection (Fig. 6B and 7B). Reovirus infection of both p50+/+ and p65+/+ cell lines resulted in apoptosis of approximately 25% of cells. However, only 5% of p50−/− cells and 1% of p65−/− cells were apoptotic following infection. Although apoptosis was not abolished in p50-deficient cells, the levels of apoptosis were significantly reduced in comparison to those in p50-expressing control cells ($P = 0.013$). This result suggests that p50 serves as an enhancer of reovirus-induced apoptosis but is not absolutely required for this effect. Reovirus infection of p65-deficient cells resulted in levels of apoptosis indistinguishable from those of mock-infected cells ($P = 0.78$), which indicates a strict requirement for p65 in the signaling pathway that results in apoptosis following reovirus infection. Differences in p65+/+ and p65−/− cell apoptosis induced by reovirus were highly statistically significant ($P = 0.01$).

A previous study of the p50−/− and p65−/− cell lines demonstrated that p65 but not p50 is required to inhibit apoptosis induced by TNF-α (6), the opposite effect observed with reovirus infection. To confirm that p65−/− cells but not p50−/− cells are more sensitive to TNF-α-induced cell death,

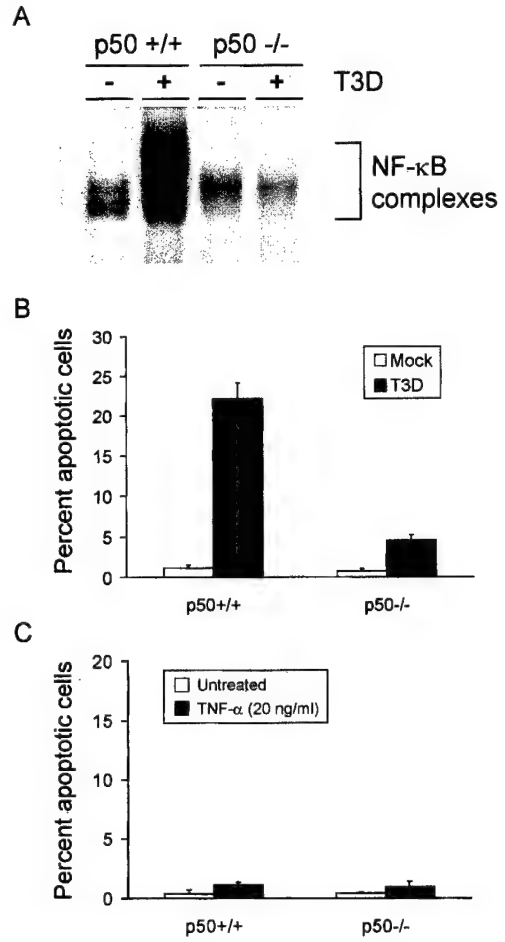

FIG. 6. (A) NF-κB gel shift activity in reovirus-infected p50+/+ and p50−/− immortalized fibroblast cells. Cells (5×10^6) were either mock infected or infected with T3D at an MOI of 100 PFU per cell. After incubation at 37°C for 6 h, nuclear extracts were prepared and incubated with a ^{32}P-labeled DNA probe consisting of the NF-κB consensus sequence. Incubation mixtures were resolved by acrylamide gel electrophoresis, dried, and exposed to film. NF-κB-containing complexes are indicated. (B) Quantitation of apoptosis in reovirus-infected p50+/+ and p50−/− cells. Cells (2.5×10^4) were either mock infected or infected with T3D at an MOI of 100 PFU per cell. After incubation at 37°C for 48 h, the cells were stained with acridine orange. (C) Quantitation of apoptosis in TNF-α-treated p50+/+ and p50−/− cells. Cells (2.5×10^4) were either untreated or treated with 20 ng of TNF-α per ml. After incubation at 37°C for 24 h, the cells were stained with acridine orange. The results of the experiments in panels B and C are expressed as the mean percentage of cells undergoing apoptosis in three independent experiments. Error bars indicate standard error of the mean.

the null and control cell lines were either not treated or treated with TNF-α (Fig. 6C and 7C). TNF-α treatment induced apoptosis of p65−/− cells but did not alter the viability of p50−/− or control cell lines. These results provide strong genetic evidence that both p50 and p65 are critical for mediating the apoptotic response triggered by reovirus infection and support the idea that reovirus and TNF-α engage NF-κB in fundamentally different ways to influence stimulus-induced cell death.

Growth of reovirus is diminished in cell lines deficient for p50 and p65. For some viruses, induction of apoptosis may lead to the activation of cellular signaling molecules required to render a cell fully permissive for virus replication. Apoptosis may also facilitate virus release and dissemination from infected cells, resulting in an increase in viral progeny. To determine whether NF-κB family members are required for maximal viral replication in cultured cells, yields of reovirus were determined after viral growth in the p50−/− and p65−/− cell lines and their respective p50+/+ and p65+/+ littermate control cell lines (Fig. 8). Cells were infected with T3D at an MOI of 1 PFU per cell, and viral yields were determined 24 and 48 h after infection. T3D replicated efficiently in all four cell lines; however, viral yields in the control cell lines were two- to fivefold greater, after 24 or 48 h of viral growth, than were the yields in their respective null cell lines. In p50+/+ cells, T3D produced yields of approximately 1,300 and 9,100 progeny virions per input 24 and 48 h following infection, respectively. However, in p50−/− cells, the yields of T3D were reduced to approximately 350 and 3,900 progeny per input 24 and 48 h following infection, respectively. Similarly, in p65+/+ cells,

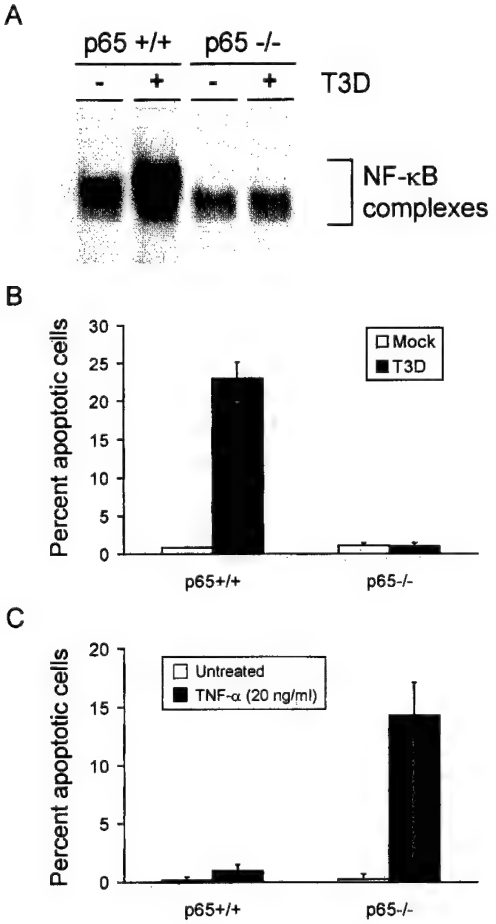

FIG. 7. (A) NF-κB gel shift activity in reovirus-infected p65+/+ and p65−/− immortalized fibroblast cells. Cells (5×10^6) were either mock infected or infected with T3D at an MOI of 100 PFU per cell. After incubation at 37°C for 8 h, nuclear extracts were prepared and incubated with a ^{32}P-labeled DNA probe consisting of the NF-κB consensus sequence. Incubation mixtures were resolved by acrylamide gel electrophoresis, dried, and exposed to film. NF-κB-containing complexes are indicated. (B) Quantitation of apoptosis in reovirus-infected p65+/+ and p65−/− cells. Cells (2.5×10^4) were either mock infected or infected with T3D at an MOI of 100 PFU per cell. After incubation at 37°C for 48 h, the cells were stained with acridine orange. (C) Quantitation of apoptosis in TNF-α-treated p65+/+ and p65−/− cells. Cells (2.5×10^4) were either untreated or treated with 20 ng of TNF-α per ml. After incubation at 37°C for 24 h, the cells were stained with acridine orange. The results of the experiments in panels B and C are expressed as the mean percentage of cells undergoing apoptosis in three independent experiments. Error bars indicate standard error of the mean.

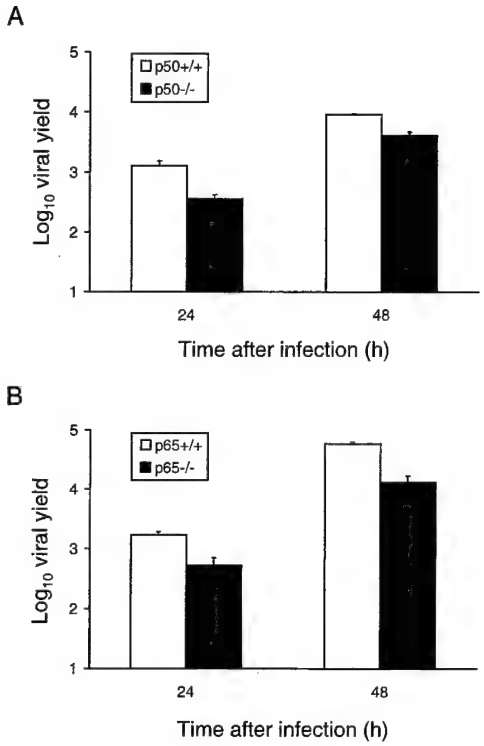

FIG. 8. Growth of reovirus in p50−/− and p65−/− immortalized fibroblast cells. p50+/+ and p50−/− cells (A) or p65+/+ and p65−/− cells (B) (2.5×10^4 cells per experiment) were infected with T3D at an MOI of 1 PFU per cell. After adsorption for 1 h, the inoculum was removed, fresh medium was added, and the cells were incubated at 37°C for 0, 24, or 48 h. The cells were frozen and thawed twice, and viral titers were determined by a plaque assay. The results are presented as the mean viral yields (viral titer at 24 or 48 h divided by viral titer at 0 h) in three independent experiments. Error bars indicate standard error of the mean.

T3D produced yields of approximately 1,700 and 57,500 progeny per input 24 and 48 h following infection, respectively. However, in p65−/− cells, the yields of T3D were reduced to approximately 500 and 12,900 progeny per input 24 and 48 h following infection, respectively. Similar two- to fivefold reductions in viral yields were observed in the p50−/− and p65−/− cell lines relative to the control cell lines when cells were infected at an MOI of 100 PFU per cell (data not shown). These results suggest that expression of p50 and p65 confers a modest viral growth advantage. The capacity of p50+/+ and p65+/+ cells to undergo apoptosis following reovirus infection may directly enhance viral replication, or expression of p50 and p65 may allow a more permissive cellular environment to achieve maximal viral growth.

DISCUSSION

Mammalian reoviruses have served as a useful experimental system for studies of viral pathogenesis, and studies of these viruses have provided important insights into how viruses interact with host cells (68). In this study, we demonstrate that NF-κB is activated following infection of cultured cells with reovirus. This conclusion is supported by two lines of evidence. First, reovirus infection of HeLa cells and immortalized cell lines derived from murine embryonic fibroblasts leads to nuclear translocation of NF-κB complexes containing the p50 and p65 subunits. Second, reovirus infection of HeLa cells induces NF-κB-directed expression of a luciferase reporter gene. Maximal luciferase activity follows the peak of NF-κB gel shift activity, as would be expected to allow NF-κB-directed gene expression. Thus, reovirus infection is capable of functional activation of NF-κB.

Our results using proteasome inhibitor Z-L_3VS and transient expression of mutant forms of IκBα suggest that reovirus-induced activation of NF-κB involves targeted degradation of IκBα by the 26S proteasome. However, the precise mechanism by which reovirus activates NF-κB remains unknown. We consider it unlikely that NF-κB activation is triggered solely by attachment of the virus to its cognate cellular receptor, because peak NF-κB activity follows reovirus adsorption by several hours. Activation of NF-κB in response to physiologic receptor-ligand interactions occurs with more rapid kinetics (66). Therefore, we suspect that reovirus transcription or translation is a prerequisite for access to the host NF-κB pathway, which is more consistent with the delayed response observed in our studies. It is also possible that reovirus infection induces a soluble factor that mediates activation of NF-κB, which also would account for the delay in NF-κB activation.

Prior studies have firmly established that NF-κB activation can be achieved by a broad spectrum of biochemical inducing cues, resulting in either enhancement (1, 29, 32) or inhibition (6, 8, 65) of programmed cell death (reviewed in reference 55). Using a proteasome inhibitor and a *trans*-dominant inhibitor of NF-κB, we demonstrated that interference with the NF-κB pathway leads to inhibition of reovirus-induced apoptosis. These findings strongly suggest that NF-κB enhances apoptosis in response to reovirus infection. In support of this contention, cell lines deficient for either p50 or p65, the primary constituents of NF-κB complexes activated by reovirus, are significantly more resistant to reovirus-induced apoptosis than are control cell lines. In fact, fibroblasts deficient in p65 expression do not undergo apoptosis in response to reovirus infection over an observation period of 48 h. These results provide compelling evidence that NF-κB plays an essential role in the mechanism by which reovirus triggers an apoptotic program in infected cells.

In contrast to our finding that NF-κB functions as a proapoptotic factor during reovirus infection of cultured cells, NF-κB plays an antiapoptotic role in cells treated with TNF-α (6, 35, 65, 69) (Fig. 4 to 7). Engagement of the TNF receptor by TNF-α induces protein-protein interactions that lead directly to the activation of NF-κB (30), which results in inhibition of apoptosis (6, 35, 65, 69). Since activation of NF-κB by reovirus is not likely to occur directly following receptor ligation, it is possible that the mechanism that promotes activation of NF-κB by reovirus explains its proapoptotic effects. Alternatively, reovirus infection and TNF-α receptor engagement may induce different auxiliary factors that influence the effects of NF-κB within a given cell type.

The requirement for NF-κB activation in reovirus-induced apoptosis suggests that NF-κB functions to increase the expression of proapoptotic genes. Several genes encoding proteins involved in mediating apoptosis induced by a variety of stimuli are regulated by NF-κB and contain NF-κB response elements in their promoters. Such NF-κB-responsive proapoptotic proteins include p53 (70), caspase-1 (14), and FasL (58). Activation of NF-κB following reovirus infection may induce the expression of one or more of these genes or other proapoptotic genes, which include death receptors and their ligands, such as DR4, DR5, and TRAIL; effector or initiator caspases, such as caspase-3 and caspase-9; and prodeath Bcl-2 family members, such as Bax, Bik, and Bad. In a previous study, we demonstrated that inhibitors of calpain, a calcium-dependent papain-like cysteine protease, block reovirus-induced apopto-

sis (21). NF-κB may function to upregulate the expression of calpain activator proteins (22, 48, 53) or growth factors (15, 40), which have been shown to increase calpain activity. NF-κB also may be involved in regulating genes that control cellular calcium flux, which is required for calpain activation (57). It is also possible that NF-κB induces the expression of transcription factors that in turn augment the transcription of proapoptotic genes not directly under the control of NF-κB.

Why would reovirus activate NF-κB? One possibility is that induction of apoptosis of infected cells would reduce host inflammatory responses, potentially leading to increased dissemination of the virus. Thus, viruses capable of this response would have a clear selective advantage. Given the well-established role of NF-κB in signal-induced cell growth pathways (reviewed in reference 66), a second possibility is that activation of NF-κB produces a cellular environment that is more permissive for reovirus replication. Reovirus yields are substantially higher in rapidly dividing or transformed cells (24, 56, 59), which suggests that cellular factors associated with cell growth augment viral replication. Reovirus-induced NF-κB activation might lead to expression of growth-associated cellular genes that promote more efficient viral nucleic acid or protein synthesis, intracellular transport of viral proteins, or assembly and release of progeny virions. In support of this idea, we found that reovirus yields are decreased in both p50−/− and p65−/− cells relative to control cells.

Other viruses induce NF-κB activation (13, 34, 37, 64, 72), and in some cases NF-κB is required for maximal viral replication. For instance, the long terminal repeat of human immunodeficiency virus contains κB response elements, and activation of NF-κB directly stimulates viral gene expression (16, 18). The human T-cell leukemia virus Tax protein induces NF-κB activation (9, 72), which in turn induces the expression of cellular genes that promote human T-cell leukemia virus replication (5, 28, 33, 39). Thus, the NF-κB signaling pathway may be a common pathway by which viruses confer an optimum environment to achieve their replication.

The results reported here establish that NF-κB is activated following reovirus infection and demonstrate that activation of NF-κB is required for reovirus-induced apoptosis. Most RNA-containing viruses, such as reovirus, are thought to replicate independently of the nucleus. Our results, however, clearly show that infection with an RNA-containing cytoplasmic virus triggers a signal transduction pathway involving nuclear components, which leads to cellular gene expression. Activation of this signaling pathway is critical for cell death caused by reovirus and probably contributes to reovirus-induced pathology (42; DeBiasi et al., Abstr. Am. Soc. Virol. 18th Annu. Meet. 1999). Understanding the signaling pathways used by reovirus to induce cellular gene expression and apoptosis will contribute important new information about mechanisms by which viruses produce cell death and disease.

ACKNOWLEDGMENTS

We thank David Baltimore for the NF-κB null and control cell lines and Hidde Ploegh for the proteasome inhibitor. We are grateful to Zhi-Liang Chu, David Scherer, and Alexander Hoffman for expert advice. We thank Erik Barton, Jim Chappell, and Tibor Valyi-Nagy for careful review of the manuscript.

This work was supported by Public Health Service awards T32 GM07347 from the National Institute of General Medical Studies for the Vanderbilt Medical Scientist Training Program (S.E.R.), AI33839 from the National Institutes of Allergy and Infectious Diseases (D.W.B.), AG14071 from the National Institute on Aging (K.L.T.), and AI38296 from the National Institute of Allergy and Infectious Diseases (J.L.C. and T.S.D.); Department of Veterans Affairs Merit and REAP Awards (K.L.T.); U.S. Army grant DAMD17-98-1-8614 (K.L.T.); and the Elizabeth B. Lamb Center for Pediatric Research (J.L.C. and T.S.D.). Additional support was provided by Public Health Service awards CA68485 for the Vanderbilt Cancer Center and DK20593 for the Vanderbilt Diabetes Research and Training Center.

REFERENCES

1. **Abbadie, C., N. Kabrun, F. Bouali, B. Vandenbunder, and P. Enrietto.** 1993. High levels of *c-rel* expression are associated with programmed cell death in the developing avian embryo and in bone marrow cells *in vitro*. Cell **75:**899–912.
2. **Ashkenazi, A., and V. M. Dixit.** 1998. Death receptors: signaling and modulation. Science **281:**1305–1308.
3. **Baeuerle, P., and D. Baltimore.** 1988. IκB: a specific inhibitor of the NF-κB transcription factor. Science **242:**540–546.
4. **Baeuerle, P., and D. Baltimore.** 1989. A 65-kD subunit of active NF-κB is required for inhibition of NF-κB by IκB. Genes Dev. **3:**1689–1698.
5. **Ballard, D. W., E. Bohnlein, J. W. Lowenthal, Y. Wano, B. R. Franza, and W. C. Greene.** 1988. HTLV-I tax induces cellular proteins that activate the kappa B element in the IL-2 receptor alpha gene. Science **241:**1652–1655.
6. **Beg, A., and D. Baltimore.** 1996. An essential role for NF-κB in preventing TNF-α-induced cell death. Science **274:**782–784.
7. **Beg, A. A., S. M. Ruben, R. I. Scheinman, S. Haskill, C. A. Rosen, and A. J. Baldwin.** 1992. IκB interacts with the nuclear localization sequences of the subunits of NF-κB: a mechanism for cytoplasmic retention. Genes Dev. **6:**1899–1913.
8. **Beg, A. A., W. C. Sha, R. T. Bronson, S. Ghosh, and D. Baltimore.** 1995. Embryonic lethality and liver degeneration in mice lacking the RelA component of NF-κB. Nature **376:**167–170.
9. **Beraud, C., and W. C. Greene.** 1996. Interaction of HTLV-1 Tax with human proteasome: implications for NF-kappa B induction. J. Acquired Immunodefic. Syndr. **13**(Suppl. 1)**:**S76–S84.
10. **Bogyo, M., J. McMaster, M. Gaczynska, D. Tortorella, A. Goldberg, and H. Ploegh.** 1997. Covalent modification of the active site threonine of proteasomal beta subunits and the *Escherichia coli* homolog HslV by a new class of inhibitors. Proc. Natl. Acad. Sci. U.S.A. **94:**6629–6634.
11. **Brockman, J. A., D. C. Scherer, T. A. McKinsey, S. M. Hall, X. Qi, W. Y. Lee, and D. W. Ballard.** 1995. Coupling of a signal response domain in IκBα to multiple pathways for NF-κB activation. Mol. Cell. Biol. **15:**2809–2818.
12. **Brown, K., S. Gerstberger, L. Carlson, G. Franzoso, and U. Siebenlist.** 1995. Control of I kappa B-alpha proteolysis by site-specific, signal-induced phosphorylation. Science **267:**1485–1488.
13. **Bussfeld, D., M. Bacher, A. Mortiz, D. Gemsa, and H. Sprenger.** 1997. Expression of transcription factor genes after influenza A virus infection. Immunobiology **198:**291–298.
14. **Casano, F., A. Rolando, J. Mudgett, and S. Molineaux.** 1994. The structure and complete nucleotide sequence of the murine gene encoding interleukin-1 beta converting enzyme (ICE). Genomics **20:**474–481.
15. **Chakrabarti, A. K., T. Neuberger, T. Russell, N. L. Banik, and G. H. DeVries.** 1997. Immunolocalization of cytoplasmic and myelin mCalpain in transfected Schwann cells. II. Effect of withdrawal of growth factors. J. Neurosci. Res. **47:**609–616.
16. **Chen, B. K., M. B. Feinberg, and D. Baltimore.** 1997. The kappaB sites in the human immunodeficiency virus type 1 long terminal repeat enhance virus replication yet are not absolutely required for viral growth. J. Virol. **71:**5495–5504.
17. **Chen, Z., J. Hagler, V. J. Palombella, F. Melandri, D. Scherer, D. Ballard, and T. Maniatis.** 1995. Signal-induced site-specific phosphorylation targets I kappa B alpha to the ubiquitin-proteasome pathway. Genes Dev. **9:**1585–1597.
18. **Chene, L., M. T. Nugeyre, F. Barre-Sinoussi, and N. Israel.** 1999. High-level replication of human immunodeficiency virus in thymocytes requires NF-kappaB activation through interaction with thymic epithelial cells. J. Virol. **73:**2064–2073.
19. **Chesnut, J., A. Baytan, M. Russell, M. Chang, A. Bernard, I. Maxwell, and J. Hoeffler.** 1996. Selective isolation of transiently transfected cells from a mammalian cell population with vectors expressing a membrane anchored single-chain antibody. J. Immunol. Methods **193:**17–27.
20. **Cohen, J. J.** 1991. Programmed cell death in the immune system. Adv. Immunol. **50:**55–85.
21. **DeBiasi, R. L., M. K. T. Squier, B. Pike, M. Wynes, T. S. Dermody, J. J. Cohen, and K. L. Tyler.** 1999. Reovirus-induced apoptosis is preceded by increased cellular calpain activity and is blocked by calpain inhibitors. J. Virol. **73:**695–701.
22. **DeMartino, G. N., and D. K. Blumenthal.** 1982. Identification and partial purification of a factor that stimulates calcium-dependent proteases. Biochemistry **21:**4297–4303.
23. **Duke, R. C., and J. J. Cohen.** 1992. Morphological and biochemical assays of apoptosis, p. 17.1–17.16. *In* J. E. Coligan (ed.), Current Protocols in Immunology, Wiley & Sons, New York, N.Y.
24. **Duncan, M. R., S. M. Stanish, and D. C. Cox.** 1978. Differential sensitivity of normal and transformed human cells to reovirus infection. J. Virol. **28:**444–449.

25. **Ernst, H., and A. J. Shatkin.** 1985. Reovirus hemagglutinin mRNA codes for two polypeptides in overlapping reading frames. Proc. Natl. Acad. Sci. USA **82:**48–52.
26. **Furlong, D. B., M. L. Nibert, and B. N. Fields.** 1988. Sigma 1 protein of mammalian reoviruses extends from the surfaces of viral particles. J. Virol. **62:**246–256.
27. **Ghosh, S., A. Gifford, L. Riviere, P. Tempst, G. Nolan, and D. Baltimore.** 1990. Cloning of the p50 DNA binding subunit of NF-κB: homology to *rel* and *dorsal*. Cell **62:**1019–1029.
28. **Greene, W. C., E. Bohnlein, and D. W. Ballard.** 1989. HIV-1, HTLV-1 and normal T-cell growth: transcriptional strategies and surprises. Immunol. Today **10:**272–278.
29. **Grimm, S., M. K. A. Bauer, P. A. Baeuerle, and K. Schulze-Osthoff.** 1996. Bcl-2 down-regulates the activity of transcription factor NF-κB induced upon apoptosis. J. Cell Biol. **134:**13–23.
30. **Hsu, H., J. Xiong, and D. V. Goeddel.** 1995. The TNF receptor 1-associated protein TRADD signals cell death and NF-κB activation. Cell **82:**495–504.
31. **Jacobs, B. L., and C. E. Samuel.** 1985. Biosynthesis of reovirus-specified polypeptides: the reovirus S1 mRNA encodes two primary translation products. Virology **143:**63–74.
32. **Jung, M., Y. Zhang, S. Lee, and A. Dritschilo.** 1995. Correction of radiation sensitivity in ataxia telangiectasia cells by a truncated IκB-α. Science **268:** 1619–1621.
33. **Leung, K., and G. J. Nabel.** 1988. HTLV-1 transactivator induces interleukin-2 receptor expression through an NF-kappa B-like factor. Nature **333:** 776–778.
34. **Lin, K. I., S. H. Lee, R. Narayanan, J. Baraban, J. Hardwick, and R. Ratan.** 1995. Thiol agents and Bcl-2 identify an alphavirus-induced apoptotic pathway that requires activation of the transcription factor NF-kappa B. J. Cell Biol. **131:**1149–1161.
35. **Liu, Z.-G., H. Hsu, D. Goeddel, and M. Karin.** 1996. Dissection of TNF receptor 1 effector functions: JNK activation is not linked to apoptosis while NF-κB activation prevents cell death. Cell **87:**565–576.
36. **Lum, R., S. Kerwar, S. Meyer, M. Nelson, S. Schow, D. Shiffman, M. Wick, and A. Joly.** 1998. A new structural class of proteasome inhibitors that prevent NF-kappa B activation. Biochem. Pharmacol. **55:**1391–1397.
37. **Marianneau, P., A. Cardona, L. Edelman, V. Deubel, and P. Despres.** 1997. Dengue virus replication in human hepatoma cells activates NF-κB, which in turn induces apoptotic cell death. J. Virol. **71:**3244–3249.
38. **May, M. J., and S. Ghosh.** 1997. Rel/NF-kappa B and I kappa B proteins: an overview. Semin. Cancer Biol. **8:**63–73.
39. **Mesnard, J. M., and C. Devaux.** 1999. Multiple control levels of cell proliferation by human T-cell leukemia virus type 1 Tax protein. Virology **257:** 277–284.
40. **Neuberger, T., A. K. Chakrabarti, T. Russell, G. H. DeVreis, E. L. Hogan, and N. L. Banik.** 1997. Immunolocalization of cytoplasmic and myelin mCalpain in transfected Schwann cells. I. Effect of treatment with growth factors. J. Neurosci. Res. **47:**521–530.
41. **Nibert, M. L., L. A. Schiff, and B. N. Fields.** 1996. Reoviruses and their replication, p. 1557–1596. *In* B. N. Fields, D. M. Knipe, and P. M. Howley (ed.), Fields virology, 3rd ed. Lippincott-Raven, Philadelphia, Pa.
42. **Oberhaus, S. M., R. L. Smith, G. H. Clayton, T. S. Dermody, and K. L. Tyler.** 1997. Reovirus infection and tissue injury in the mouse central nervous system are associated with apoptosis. J. Virol. **71:**2100–2106.
43. **O'Brien, V.** 1998. Viruses and apoptosis. J. Gen. Virol. **79:**1833–1845.
44. **Palombella, V., O. Rando, A. Goldberg, and T. Maniatis.** 1994. The ubiquitin-proteasome pathway is required for processing the NF-kappa B1 precursor protein and the activation of NF-kappa B. Cell **78:**773–785.
45. **Razvi, E. S., and R. M. Welsh.** 1995. Apoptosis in viral infections. Adv. Virus Res. **45:**1–60.
46. **Rodgers, S. E., E. S. Barton, S. M. Oberhaus, B. Pike, C. A. Gibson, K. L. Tyler, and T. S. Dermody.** 1997. Reovirus-induced apoptosis of MDCK cells is not linked to viral yield and is blocked by Bcl-2. J. Virol. **71:**2540–2546.
47. **Rodgers, S. E., J. L. Connolly, J. D. Chappell, and T. S. Dermody.** 1998. Reovirus growth in cell culture does not require the full complement of viral proteins: identification of a σ1s-null mutant. J. Virol. **72:**8597–8604.
48. **Salamino, F., R. DeTullio, P. Mengotti, P. L. Viotti, E. Melloni, and S. Pontremoli.** 1993. Site-directed activation of calpain is promoted by a membrane-associated natural activator protein. Biochem. J. **290:**191–197.
49. **Sambrook, J., E. F. Fritsch, and T. Maniatis.** 1989. Molecular cloning: a laboratory manual, 2nd ed. Cold Spring Harbor Laboratory, Cold Spring Harbor, N.Y.
50. **Sarkar, G., J. Pelletier, R. Bassel-Duby, A. Jayasuriya, B. N. Fields, and N. Sonenberg.** 1985. Identification of a new polypeptide coded by reovirus gene S1. J. Virol. **54:**720–725.
51. **Scherer, D. C., J. A. Brockman, Z. Chen, T. Maniatis, and D. W. Ballard.** 1995. Signal-induced degradation of I kappa B alpha requires site-specific ubiquitination. Proc. Natl. Acad. Sci. USA **92:**11259–11263.
52. **Shen, Y., and T. E. Shenk.** 1995. Viruses and apoptosis. Curr. Opin. Genet. Dev. **5:**105–111.
53. **Shiba, R., H. Ariyoshi, Y. Yano, T. Kawasaki, M. Sakon, J. Kambayashi, and T. Mori.** 1992. Purification and characterization of a calpain activator from human platelets. Biochem. Biophys. Res. Commun. **182:**461–465.
54. **Smith, R. E., H. J. Zweerink, and W. K. Joklik.** 1969. Polypeptide components of virions, top components and cores of reovirus type 3. Virology **39:**791–810.
55. **Sonenshein, G. E.** 1997. Rel/NF-κB transcription factors and the control of apoptosis. Semin. Cancer Biol. **8:**113–119.
56. **Strong, J. E., and P. W. Lee.** 1996. The v-*erbB* oncogene confers enhanced cellular susceptibility to reovirus infection. J. Virol. **70:**612–616.
57. **Suzuki, K., T. C. Saido, and S. Hirai.** 1992. Modulation of cellular signals by calpain. Ann. N. Y. Acad. Sci. **674:**218–227.
58. **Takahashi, T., M. Tanaka, J. Inazawa, T. Abe, T. Suda, and S. Nagata.** 1994. Human Fas ligand: gene structure, chromosomal location and species specificity. Int. Immunol. **6:**1567–1574.
59. **Taterka, J., M. Sugcliffe, and D. H. Rubin.** 1994. Selective reovirus infection of murine hepatocarcinoma cells during cell division. A model of viral liver infection. J. Clin. Investig. **94:**353–360.
60. **Teodoro, J. G., and P. E. Branton.** 1997. Regulation of apoptosis by viral gene products. J. Virol. **71:**1739–1746.
61. **Traenckner, E. B., H. L. Pahl, T. Henkel, K. N. Schmidt, S. Wilk, and P. A. Baeuerle.** 1995. Phosphorylation of human I kappa B-alpha on serines 32 and 36 controls I kappa B-alpha proteolysis and NF-kappa B activation in response to diverse stimuli. EMBO J. **14:**2876–2883.
62. **Tyler, K. L., and B. N. Fields.** 1996. Reoviruses, p. 1597–1623. *In* B. N. Fields, D. M. Knipe, and P. M. Howley (ed.), Fields Virology, 3rd ed. Lippincott-Raven, Philadelphia, Pa.
63. **Tyler, K. L., M. K. T. Squier, S. E. Rodgers, B. E. Schneider, S. M. Oberhaus, T. A. Grdina, J. J. Cohen, and T. S. Dermody.** 1995. Differences in the capacity of reovirus strains to induce apoptosis are determined by viral attachment protein σ1. J. Virol. **69:**6972–6979.
64. **Umansky, V., V. A. Shatrov, V. Lehmann, and V. Schirrmacher.** 1996. Induction of NO synthesis in macrophages by Newcastle disease virus is associated with activation of nuclear factor-kappa B. Int. Immunol. **8:**491–498.
65. **Van Antwerp, D., S. Martin, T. Kafri, D. Green, and I. Verma.** 1996. Suppression of TNF-α-induced apoptosis by NF-κB. Science **274:**787–789.
66. **Verma, I. M., J. K. Stevenson, E. M. Schwarz, D. Van Antwerp, and S. Miyamoto.** 1995. Rel/NF-kappa B/I kappa B family: intimate tales of association and disassociation. Genes Dev. **9:**2723–2735.
67. **Virgin, H. W., IV, R. Bassel-Duby, B. N. Fields, and K. L. Tyler.** 1988. Antibody protects against lethal infection with the neurally spreading reovirus type 3 (Dearing). J. Virol. **62:**4594–4604.
68. **Virgin, H. W., K. L. Tyler, and T. S. Dermody.** 1997. Reovirus, p. 669–699. *In* N. Nathanson (ed.), Viral pathogenesis. Lippincott-Raven, New York, N.Y.
69. **Wang, C.-Y., M. Mayo, and A. Baldwin.** 1996. TNF- and cancer therapy-induced apoptosis: potentiation by inhibition of NF-κB. Science **274:**784–787.
70. **Wu, H., and G. Lozano.** 1994. NF-kappa B activation of p53. A potential mechanism for suppressing cell growth in response to stress. J. Biol. Chem. **269:**20067–20074.
71. **Wyllie, A. H.** 1997. Apoptosis: an overview. Br. Med. Bull. **53:**451–465.
72. **Yoshida, M.** 1996. Molecular biology of HTLV-I: recent progress. J. Acquired Immune Defic. Syndr. **13**(Suppl. 1)**:**S63–S68.

pgs. 3+4 must face

AUTHOR: SEE QUERY PAGE 1

JOURNAL OF VIROLOGY, Oct. 2000, p. 000–000
0022-538X/00/$04.00+0

Vol. 74, No. 20

Reovirus-Induced G_2/M Cell Cycle Arrest Requires σ1s and Occurs in the Absence of Apoptosis

GEORGE J. POGGIOLI,[1] CHRISTOPHER KEEFER,[2] JODI L. CONNOLLY,[3,4] TERENCE S. DERMODY,[2,3,4] AND KENNETH L. TYLER[1,5,6,7,8]*

Departments of Neurology,[5] Medicine,[6] Microbiology,[1] and Immunology,[7] University of Colorado Health Sciences Center, and Neurology Service, Denver Veterans Affairs Medical Center,[8] Denver, Colorado 80220, and Departments of Pediatrics[2] and Microbiology and Immunology[3] and Elizabeth B. Lamb Center for Pediatric Research,[4] Vanderbilt University School of Medicine, Nashville, Tennessee 37232

Received 1 May 2000/Accepted 18 July 2000

Serotype-specific differences in the capacity of reovirus strains to inhibit proliferation of murine L929 cells correlate with the capacity to induce apoptosis. The prototype serotype 3 reovirus strains Abney (T3A) and Dearing (T3D) inhibit cellular proliferation and induce apoptosis to a greater extent than the prototype serotype 1 reovirus strain Lang (T1L). We now show that reovirus-induced inhibition of cellular proliferation results from a G_2/M cell cycle arrest. Using T1L × T3D reassortant viruses, we found that strain-specific differences in the capacity to induce G_2/M arrest, like the differences in the capacity to induce apoptosis, are determined by the viral S1 gene. The S1 gene is bicistronic, encoding the viral attachment protein σ1 and the nonstructural protein σ1s. A σ1s-deficient reovirus strain, T3C84-MA, fails to induce G_2/M arrest, yet retains the capacity to induce apoptosis, which indicates that σ1s is required for reovirus-induced G_2/M arrest. Expression of σ1s in C127 cells increases the percentage of cells in the G_2/M phase of the cell cycle, supporting a role for this protein in reovirus-induced G_2/M arrest. Inhibition of reovirus-induced apoptosis failed to prevent virus-induced G_2/M arrest, indicating that G_2/M arrest is not the result of apoptosis related DNA damage and suggests that these two processes occur through distinct pathways.

Reovirus infection of cultured cells results in inhibition of cellular proliferation (10, 17–19, 21, 24–27, 38, 40, 41, 44). Serotype 3 prototype strains type 3 Abney (T3A) and type 3 Dearing (T3D) inhibit cellular DNA synthesis to a greater extent than the serotype 1 prototype strain type 1 Lang (T1L) (40, 44). Studies using T1L × T3A and T1L × T3D reassortant viruses indicate that the S1 gene is the primary determinant of DNA synthesis inhibition (40, 44). Earlier studies suggested that reovirus-induced inhibition of cellular proliferation results from inhibition of the initiation of DNA synthesis, consistent with a G_1-S transition block (10, 19, 26, 27, 38).

Reovirus infection also results in apoptosis (11, 36, 37, 44, 45). Reovirus strains T3A and T3D induce apoptosis to substantially greater extent than T1L (44, 45). A significant correlation exists between the capacities of both T1L × T3A (r = 0.937) and T1L × T3D (r = 0.772) reassortant viruses and reovirus field isolate strains (r = 0.851) to inhibit cellular proliferation and induce apoptosis (44). Like strain-specific differences in DNA synthesis inhibition, strain-specific differences in apoptosis induction also segregate with the S1 gene (36, 44, 45).

The viral S1 gene segment is bicistronic, encoding the viral attachment protein, σ1, and a non-virion-associated protein with no known function, σ1s, from overlapping reading frames (20, 30, 39). Using a σ1s-deficient virus strain, it was shown that σ1s is not required for reovirus growth in cell culture and is dispensable for the induction of apoptosis (37). These observations in conjunction with the genetic mapping studies suggest that σ1s is the primary determinant of strain-specific differences in apoptosis induction. The S1 gene product associated with reovirus-induced inhibition of cellular DNA synthesis has not been identified.

We conducted experiments to further investigate the relationship between reovirus-induced cellular DNA synthesis inhibition and apoptosis. We found that inhibition of cellular proliferation in response to reovirus infection is caused by an arrest in the G_2/M phase of the cell cycle. Reovirus strains differ in the capacity to induce G_2/M arrest, and we used reassortant viruses to demonstrate that these differences segregate with the S1 gene. A reovirus σ1s mutant fails to induce G_2/M arrest but retains the capacity to induce apoptosis. Inducible expression of σ1s results in the accumulation of cells in G_2/M phase. Inhibition of reovirus-induced apoptosis does not affect reovirus-induced G_2/M arrest. These results indicate that the σ1s protein is required for reovirus-induced G_2/M arrest and suggest that reovirus-induced inhibition of cellular proliferation and induction of apoptosis involve independent pathways.

MATERIALS AND METHODS

Cells and viruses. Spinner-adapted mouse L929 cells (ATCC CCL1) were grown in Joklik's modified Eagle's minimal essential medium (JMEM) supplemented to contain 5% heat-inactivated fetal bovine serum (Gibco BRL, Gaithersburg, Md.) and 2 mM L-glutamine (Gibco). Human embryonic kidney (HEK293) cells (ATCC CRL1573), Madin-Darby canine kidney (MDCK) cells (ATCC CCL34), C127 cells (ATCC CRL1616), and HeLa cells (ATCC CCL2) were grown in Dulbecco's modified Eagle's medium (DMEM) supplemented to contain 10% heat-inactivated fetal bovine serum (HEK293, MDCK, and C127) or 10% non-heat-inactivated fetal bovine serum (HeLa), 2 mM L-glutamine, and 100 U of penicillin and 100 μg of streptomycin per ml (Gibco). IκB-ΔN2 cells are HEK293 cells expressing a strong dominant-negative IκB mutant lacking the phosphorylation sites that regulate signal-dependent activation of NF-κB (7).

Reovirus strains T1L, T3A, and T3D are laboratory stocks. T1L × T3D reassortant viruses were grown from stocks originally isolated by Kevin Coombs, Bernard Fields, and Max Nibert (4, 9). The reovirus field-isolate strain type 3 clone 84 (T3C84) was isolated from a human host, and T3C84-MA was isolated

* Corresponding author. Mailing address: Department of Neurology (B-182), University of Colorado Health Sciences Center, 4200 E. 9th Ave., Denver, CO 80262. Phone: (303) 393-2874. Fax: (303) 393-4686. E-mail: Ken.Tyler@UCHSC.edu.

AUTHOR: Publication of this article cannot proceed without the signature of the person who read and corrected the proof on behalf of all the authors:

signature _____ date _____

Orig. Op.	OPERATOR:	Session	PROOF:	PE's:	AA's:	COMMENTS	ARTNO:
1st jsf, 2nd sbd-s	seayb	3					

zjs= zjss=

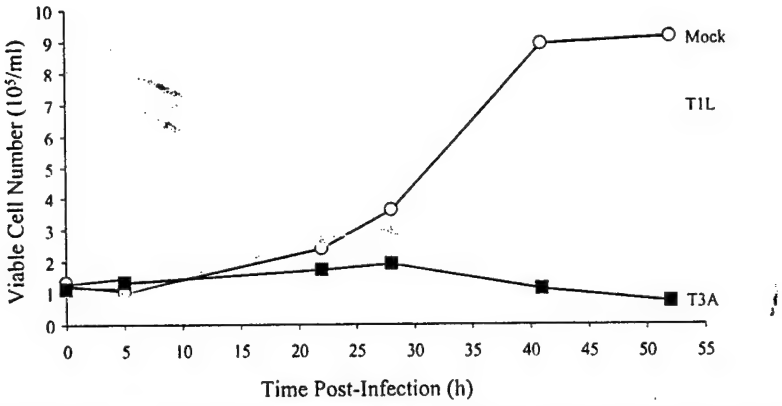

FIG. 1. Reovirus inhibits cellular proliferation. Asynchronous, subconfluent monolayers of L929 cells were either mock infected (circles) or infected with T1L (triangles) or T3A (squares) at an MOI of 100 PFU per cell. Cells were harvested at the indicated times postinfection and counted. Cells that excluded trypan blue were scored as viable. Results are presented as the number of viable cells × 10^5 per ml. The results from a representative experiment of three independent experiments are shown.

as previously described (6, 12). Viral strains were plaque purified and passaged two to three times in L929 cells to generate working stocks as previously described (43).

Isolation and characterization of T3C84-MA/σ1s+. T3C84-MA/σ1s+ was isolated following serial passage of T3C84 in MEL cells as previously described (6). To isolate a sialic acid binding MEL cell-adapted variant derived from T3C84 that retains the capacity to express σ1s, virus isolates from a fifth-passage MEL cell lysate stock were plaque purified twice on L929 cell monolayers. Plaques were amplified twice in L929 cell cultures and used to infect L929 cells (10^7) at a multiplicity of infection (MOI) of 10 PFU per cell. Cytoplasmic extracts were prepared 24 h following infection as previously described (8). Protein (100 μg) was electrophoresed in a 14% sodium dodecyl sulfate-polyacrylamide gel and transferred to a nitrocellulose membrane. An immunoblot for σ1s was performed as previously described (37). The S1 gene of a fifth-passage isolate that expresses σ1s, termed T3C84-MA/σ1s+, was sequenced as previously described (6). T3C84-MA/σ1s+ contains the mutation at nucleotide 616 that results in a tryptophan-to-arginine substitution at residue 202 of the σ1 protein, which is also present in the S1 gene of T3C84-MA and confers the capacity to bind sialic acid but does not contain the mutation that results in the introduction of a stop codon following amino acid six in the σ1s protein.

Cellular proliferation. L929 cells were seeded in six-well plates (Costar, Cambridge, Mass.) at 10^5 cells per well in a volume of 2.5 ml in JMEM supplemented to contain nonessential amino acids, 5% fetal bovine serum, 2 mM L-glutamine, 100 U of penicillin per ml, and 100 μg of streptomycin per ml. After 24 h of incubation, when cells were 10 to 20% confluent, the medium was removed, and cells were infected with viral strains at an MOI of 100 PFU per cell in a volume of 100 μl at 37°C for 1 h. After viral infection, 2.5 ml of fresh medium was added to each well. At various times postinfection, cells were harvested, resuspended in 2 ml of phosphate-buffered saline (PBS), and counted using a hemacytometer. Cell viability was determined by trypan blue exclusion. Results are presented as the viable cell numbers per milliliter.

Flow cytometry. L929, HEK293, MDCK, and HeLa cells were seeded in either 12-well plates (Costar) at 10^5 cells per well in a volume of 1 ml per well or 24-well plates (Costar) at 3.7×10^4 cells per well in a volume of 0.5 ml per well and then infected with reovirus as described above. Cells were harvested, washed once with PBS, and stained at 4°C overnight with Krishan's stain containing 3.8 mM trisodium citrate (Sigma Chemical Co., St. Louis, Mo.), 70 μM propidium iodide (Sigma), 0.01% Nonidet P-40 (Sigma), and 0.01 mg of RNase A (Boehringer Mannheim Co., Indianapolis, Ind.) per ml (33). Cell cycle analysis was performed using a Coulter Epics XL flow cytometer (Beckman-Coulter, Hialeah, Fla.). Alignment of the instrument was verified daily using DNA check beads (Coulter). Peak versus integral gating was used to exclude doublet events from the analysis. Data were collected for 10,000 events. The Modfit LT program (Verity Software House, Topsham, Maine) was used for cell cycle modeling.

Cell synchronization. L929 cells were seeded in 24-well plates at 3.7×10^4 cells per well in a volume of 0.5 ml per well. After 24 h, cells were treated with 1 μM amethopterin (methotrexate) (Sigma) and 50 μM adenosine (Sigma) for 16 h. Cells were washed twice with PBS, infected with reovirus, and incubated with fresh JMEM supplemented to contain 5% heat-inactivated fetal bovine serum, 2 mM L-glutamine, and 2 mg of thymidine (Sigma) per ml. At various times after infection, cells were harvested, washed once with PBS, and stained at 4°C overnight with Krishan's stain as described above.

Quantitation of apoptosis by acridine orange staining. L929, HEK293, MDCK, and HeLa cells were seeded and infected with reovirus as described above. The percentage of apoptotic cells was determined at 48 h postinfection as previously described (16, 45). Cells were harvested, washed once with PBS, resuspended in 25 μl of cell culture medium, and stained with 1 μl of a dye solution containing 100 μg of acridine orange (Sigma) per ml and 100 μg of ethidium bromide (Sigma) per ml. Cells were examined by epifluorescence microscopy (Nikon Labophot-2; B-2A filter; excitation, 450 to 490 nm; barrier, 520 nm; dichroic mirror, 505 nm) and scored as apoptotic if their nuclei contained uniformly stained condensed or fragmented chromatin (16, 45).

Apoptosis inhibitors. L929 cells were seeded in 24-well plates at 3.7×10^4 cells per well in a volume of 0.5 ml per well. After 24 h of incubation, cells were incubated with the calpain inhibitor PD150606 (Parke-Davis Pharmaceutical Research, Ann Arbor, Mich.) (50 μM, L929 cell), the caspase 3 inhibitor DEVD-CHO (Clontech, Palo Alto, Calif.) (100 μM, HEK293), or anti-TRAIL antibody (Affinity Bioreagents, Golden, Colo.) (30 μM, HEK293) for 1 h. Cells were then infected with T3A at an MOI of 100 PFU per cell at 37°C for 1 h. Following infection, media containing the apoptosis inhibitor was added. Cells were harvested and analyzed for either apoptosis or cell cycle arrest at 48 h postinfection.

Inducible expression of σ1s. C127 stable transformants expressing T3D σ1s (BPX6-2) from the mouse metallothionein promoter and vector control (BPV-12) were provided by Aaron Shatkin (21). BPX-6 and BPV-12 cells were seeded in 24-well plates at 3.0×10^4 cells per well in a volume of 0.5 ml per well. After 24 h of incubation, cells were incubated with 1 μM $CdCl_2$ to induce σ1s expression (22) and harvested at various times postinduction for cell cycle analysis.

RESULTS

Reovirus strains T1L and T3A differ in the capacity to inhibit cellular proliferation. We have previously shown that T1 and T3 reovirus strains differ in the capacity to inhibit cellular DNA synthesis as measured by [^{3}H]thymidine incorporation (40, 44). To determine whether reovirus-induced DNA synthesis inhibition is associated with inhibition of cellular proliferation, we infected L929 cells with either T1L or T3A at an MOI of 100 PFU per cell. At various intervals after infection, viable cells were counted (Fig. 1). Infection with T3A resulted in complete inhibition of cellular proliferation. A modest reduction in proliferation was observed for cells infected with T1L compared to mock-infected controls. Therefore, strain-specific differences in inhibition of cellular proliferation parallel those previously reported for DNA synthesis inhibition.

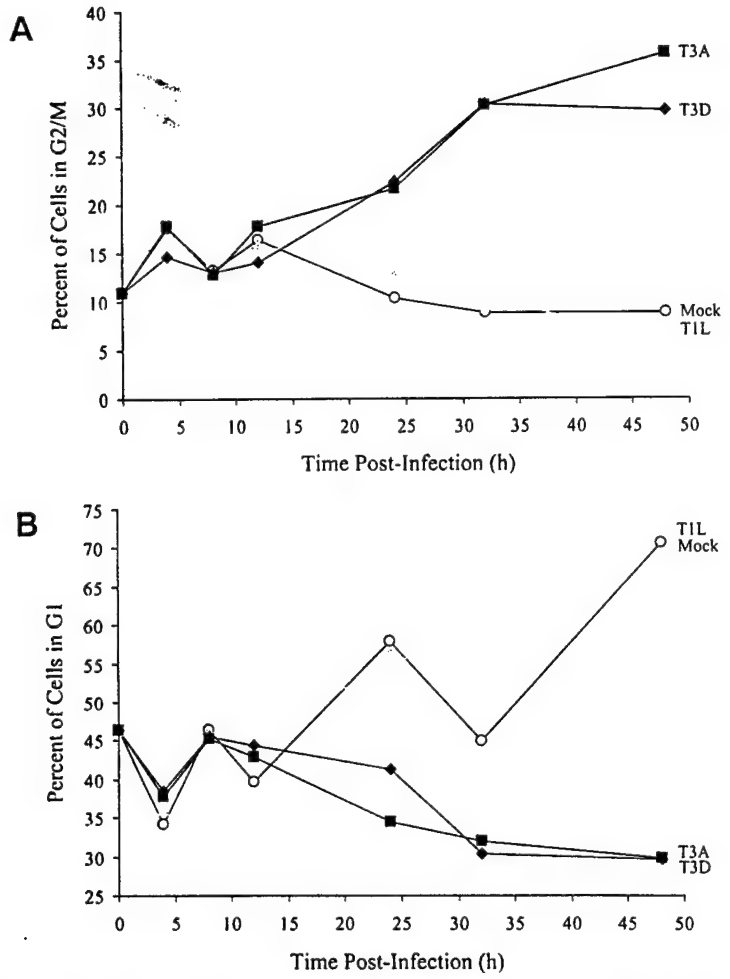

FIG. 2. T3 reovirus induces an increase in the percentage of cells in the G_2/M phase of the cell cycle. Asynchronous, subconfluent monolayers of L929 cells were either mock infected (circles) or infected with T1L (triangles), T3A (squares), or T3D (diamonds) at an MOI of 100 PFU per cell. Cells were harvested at the indicated times postinfection, stained with Krishan's stain, and analyzed for DNA content using flow cytometry. Results are presented as the percentage of cells in G_2/M phase (A) or G_1 phase (B) of the cell cycle. Results of a representative experiment of three independent experiments are shown. (C) L929 cells were synchronized with 1 μM methotrexate and 50 μM adenosine for 16 h. Cells were released using fresh media containing 2 mg of thymidine per ml and either mock infected or infected with T1L or T3A at an MOI of 100 PFU per cell. Cells were harvested at the indicated times postinfection, stained with Krishan's stain, and analyzed for DNA content using flow cytometry. Results are presented as the cell cycle distribution following either mock, T1L, or T3A infection at the indicated times postinfection.

T3 reoviruses induce G_2/M arrest. To identify the phase in the cell cycle that T3 reoviruses inhibit cellular proliferation, we analyzed reovirus-infected cells using flow cytometry. L929 cells were infected with T1L, T3A, or T3D at an MOI of 100 PFU per cell and stained with Krishan's stain (33) containing propidium iodide to determine cellular DNA content at various intervals postinfection. The results were converted to the percentage of cells in G_2/M phase of the cell cycle using Modfit LT software (Fig. 2). Infection with either T3A or T3D resulted in a substantial increase in the percentage of cells in the G_2/M phase of the cell cycle compared to T1L-infected or mock-infected cells by 24 h postinfection (Fig. 2A). There also was a corresponding decrease in the percentage of cells in G_1 phase following infection with either T3A or T3D compared to T1L-infected or mock-infected cells (Fig. 2B). To confirm these results, L929 cells were synchronized with methotrexate prior to reovirus infection and assessed for cell cycle progression (Fig. 2C). Similar to findings with unsynchronized cells, T3A induced a significant increase in the proportion of cells in the G_2/M phase of the cell cycle compared to T1L or mock infection. The increase in the proportion of cells in G_2/M was first seen at 12 h postinfection and was maintained throughout the observation period (48 h). These findings indicate that the inhibition of proliferation induced by T3 reoviruses is caused

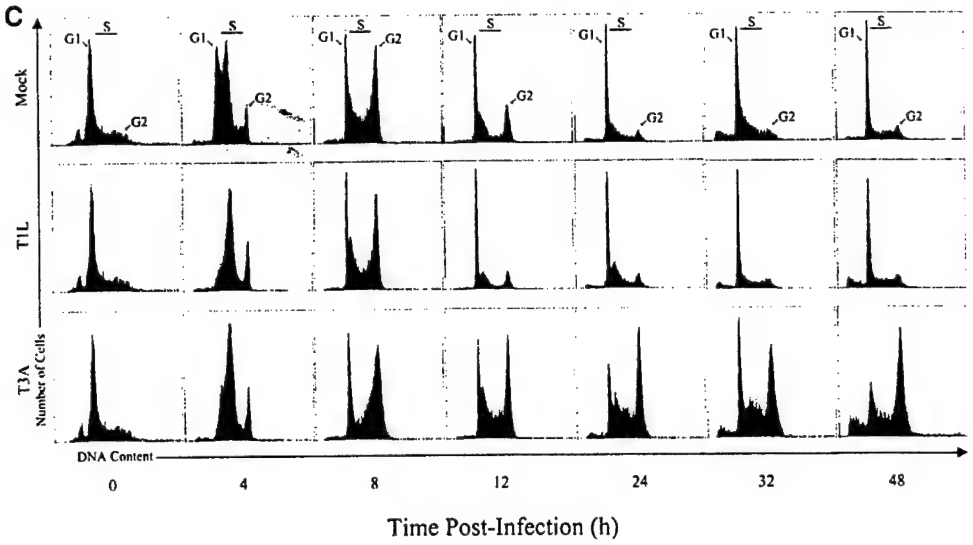

FIG. 2—*Continued.*

by a block in the G_2/M phase of the cell cycle. Following T1L or mock infection, cells traverse the cell cycle, proliferate, and reenter the cell cycle. Conversely, T3-infected cells enter the cell cycle, stall in G_2/M phase, and do not proliferate.

T3 reovirus-induced G_2/M arrest is dose dependent. To investigate the relationship between MOI and the induction of G_2/M arrest, we infected L929 cells with T3A at MOIs of 1, 10, and 100 PFU per cell. Cells were harvested at 48 h postinfection, stained with Krishan's stain (33), and analyzed for DNA content by flow cytometry (Fig. 3). T3A infection induced a greater percentage of cells in G_2/M than mock infection at each MOI tested, and the effect was dose dependent.

G_2/M arrest occurs in a variety of cell lines following T3 reovirus infection. To determine whether the capacity of reovirus to block cell cycle progression is cell type dependent, L929, MDCK, C127, HEK293, and HeLa cells were either mock infected or infected with T1L or T3A at an MOI of 100 PFU per cell. Cells were harvested at 48 h postinfection, stained with Krishan's stain (33), and analyzed for DNA content by flow cytometry (Fig. 4). T3A infection induced a greater percentage of cells in G_2/M than either T1L or mock infection in all cell lines tested. However, the magnitude of the strain-specific difference was greatest in L929 (Fig. 4A), MDCK (Fig. 4B), and C127 (Fig. 4C) cells. Therefore, reovirus-induced G_2/M arrest is not cell type specific and likely requires non-cell-type-specific factors to mediate G_2/M arrest.

T3 reovirus G_2/M arrest phenotype is dominant. To determine whether G_2/M arrest resulting from T3 reovirus infection could be overcome by T1 reovirus infection, we coinfected L929 cells with equivalent MOIs of T1L and T3A and measured the percentage of cells in G_2/M by flow cytometry at 48 h postinfection. The percentage of cells in G_2/M after coinfection with T1L and T3A was identical to that of T3A alone and significantly greater than that of T1L alone (Fig. 5). These results indicate that the G_2/M arrest phenotype of T3 reovirus is dominant.

G_2/M arrest by T1L × T3D reassortant viruses. To identify viral genes associated with differences in the capacity of T1L and T3D to induce G_2/M arrest, we tested 12 T1L × T3D reassortant viruses for the capacity to induce G_2/M arrest in unsynchronized and synchronized L929 cells (Table 1). The results demonstrate a significant association between the capacity of reassortant viruses to induce G_2/M arrest in unsynchronized L929 cells and the S1 gene segment (Student t test, $P = 0.004$; Mann-Whitney, $P = 0.007$). No other viral genes were significantly associated with G_2/M arrest in this analysis (t test and Mann-Whitney, all $P > 0.05$). However, when L929 cells were synchronized prior to infection, the results demonstrate a significant association between the capacity of reassortant viruses to induce G_2/M arrest and the derivation of the S1

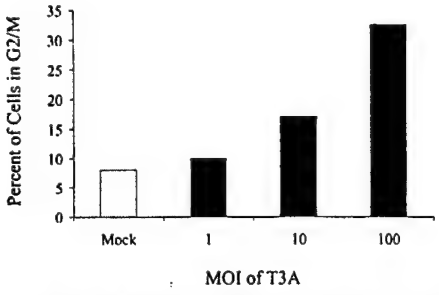

FIG. 3. G_2/M arrest induced by T3 reovirus is dose dependent. Asynchronous, subconfluent monolayers of L929 cells were either mock infected or infected with T3A at MOIs of 1, 10, and 100 PFU per cell. Cells were harvested at 48 h postinfection, stained with Krishan's stain, and analyzed for DNA content using flow cytometry. Results are presented as the percentage of cells in G_2/M phase.

Orig. Op.	OPERATOR:	Session	PROOF:	PE's:	AA's:	COMMENTS	ARTNO:
1st jsf, 2nd sbd-s	seayb	3					

zjs= zjss=

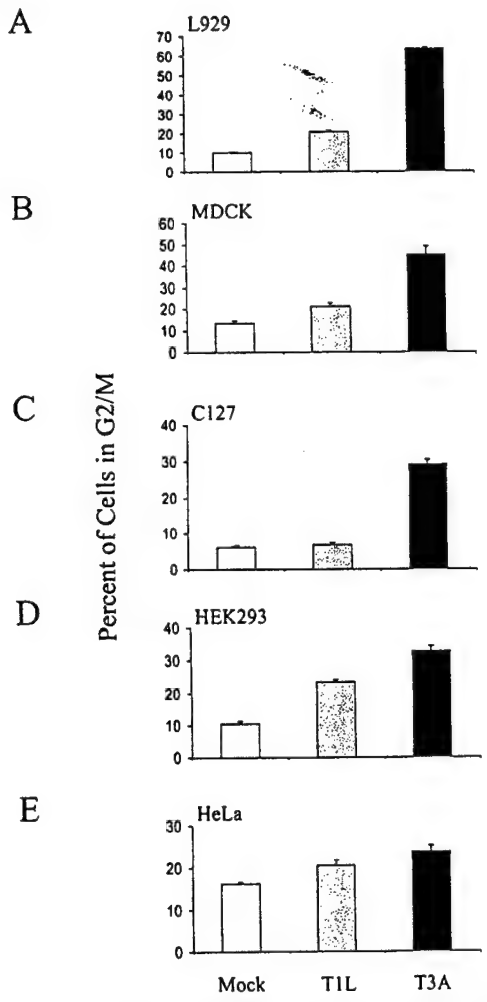

FIG. 4. T3 reovirus induces G_2/M arrest in murine, canine, and human cells. Asynchronous, subconfluent monolayers of L929 (A), MDCK (B), C127 (C), HEK293 (D), and HeLa (E) cells were either mock infected (white) or infected with T1L (gray) or T3A (black) at an MOI of 100 PFU per cell. Cells were harvested at 48 h postinfection, stained with Krishan's stain, and analyzed for DNA content using flow cytometry. Results are presented as the mean percentage of cells in G_2/M phase for three independent experiments. The error bars indicate the standard errors of the mean. A significantly greater percentage of T3A-infected cells were in G_2/M than mock-infected cells in all cell lines tested ($P < 0.01$ to 0.001). A significantly greater percentage of T3A-infected cells were in G_2/M than T1L-infected cells in all cell lines tested ($P < 0.01$ to 0.001) except HeLa. A significantly greater percentage of T1L-infected cells were in G_2/M than mock-infected cells in L929 and HEK293 cells ($P < 0.001$).

gene segment (*t* test, $P = 0.007$; Mann-Whitney, $P = 0.016$) and the M2 gene segment (*t* test, $P = 0.007$; Mann-Whitney, $P = 0.016$). We used parametric stepwise linear regression analysis to determine whether the S1 and M2 genes contributed independently to the capacity of T1L × T3D reassortant viruses to induce G_2/M arrest. We obtained R^2 values of 91.3 and 96.7% for the regression equation using all 10 reovirus genes for unsynchronized and synchronized L929 cells, respectively: 52.2% ($P = 0.004$) for S1 in unsynchronized L929 cells and 84.9% ($P < 0.001$) for S1 and M2 and 53.5% ($P = 0.007$) for the S1 gene alone in synchronized L929 cells. These results indicate that the S1 gene segment is the primary determinant of strain-specific differences in reovirus-induced G_2/M arrest.

G_2/M arrest induced by T3 reovirus. The S1 gene segment encodes two proteins, the viral attachment protein σ1 and the nonstructural protein σ1s (20, 30, 39). To determine whether σ1s is required for G_2/M arrest, we infected L929 cells with reovirus strain T3C84-MA, which does not express σ1s (37) (Fig. 6). The percentage of cells in G_2/M following infection with T3C84-MA was significantly less than the percentage of cells in G_2/M following infection with the σ1s-expressing parental virus, T3C84. T3C84-MA failed to induce G_2/M arrest, even at an MOI 10-fold greater than T3C84. T3C84-MA/σ1s+, a MEL-cell-adapted strain that does not contain the point mutation in S1 that results in an early stop codon in σ1s but contains the tryptophan-to-arginine substitution at position 202 in σ1, induced a level of G_2/M arrest that was significantly greater than T3C84-MA at an MOI of 100 in L929 cells ($P = 0.002$; percentage of cells in G_2/M following T3C84-MA/σ1s+ infection, 23.02 ± 1.1%). These findings indicate that functional σ1s is required for reovirus-induced G_2/M arrest.

Expression of T3 σ1s induces an increase in the percentage of cells in G_2/M phase. To determine whether σ1s alone is sufficient to induce the accumulation of cells in G_2/M phase, we analyzed the DNA content of C127 cells engineered to express the T3D σ1s protein. Expression of σ1s from the mouse metallothionein promoter was induced by 1 μM $CdCl_2$ (21) however, levels of σ1s were substantially less than levels found following natural virus infection (data not shown). The percentage of cells in G_2/M following induction was significantly greater in cells expressing σ1s than in vector control cells at 45 and 55 h postinduction ($P = 0.03$ and $P = 0.005$, respectively) (Fig. 7). These results provide additional evidence that σ1s expression is involved in the accumulation of cells in the G_2/M phase of the cell cycle.

Reovirus-induced apoptosis can be dissociated from reovirus-induced G_2/M arrest. Previous studies indicate that the capacity of reovirus to inhibit DNA synthesis correlates with the capacity to induce apoptosis (44). Like strain-specific differences in reovirus-induced G_2/M arrest, differences in the capacity of reovirus strains to inhibit DNA synthesis and induce apoptosis are determined by the S1 gene (40, 44). To determine whether apoptosis-associated disruption of cellular DNA is required for reovirus-induced inhibition of cellular proliferation, L929 cells or HEK293 cells were either mock infected or infected with T3A in the presence or absence of inhibitors of reovirus-induced apoptosis (7, 8, 11). Treatment of cells with the calpain inhibitor PD150606 (11), the caspase inhibitor DEVD-CHO (●. ●. Kominsky, personal communication), or anti-TRAIL antibody (7) blocks reovirus-induced apoptosis, as does expression of an IκB mutant that blocks NF-κB activation (7, 8). G_2/M arrest was evaluated by flow cytometry at 48 h postinfection (Fig. 8). Treatment with the calpain inhibitor PD150606 (Fig. 8A), the caspase 3 inhibitor DEVD-CHO (Fig. 8B), or anti-TRAIL antibody (Fig. 8C) using conditions that inhibit reovirus-induced apoptosis, had no effect on T3A-induced G_2/M arrest, nor did inhibition of NF-κB by expression of a dominant-negative IκB (7, 8) (Fig. 8D). Therefore, inhibitors of reovirus-induced apoptosis do not inhibit reovirus-induced G_2/M arrest. These findings indicate that apoptosis induced DNA damage is not required for reovirus-induced G_2/M arrest.

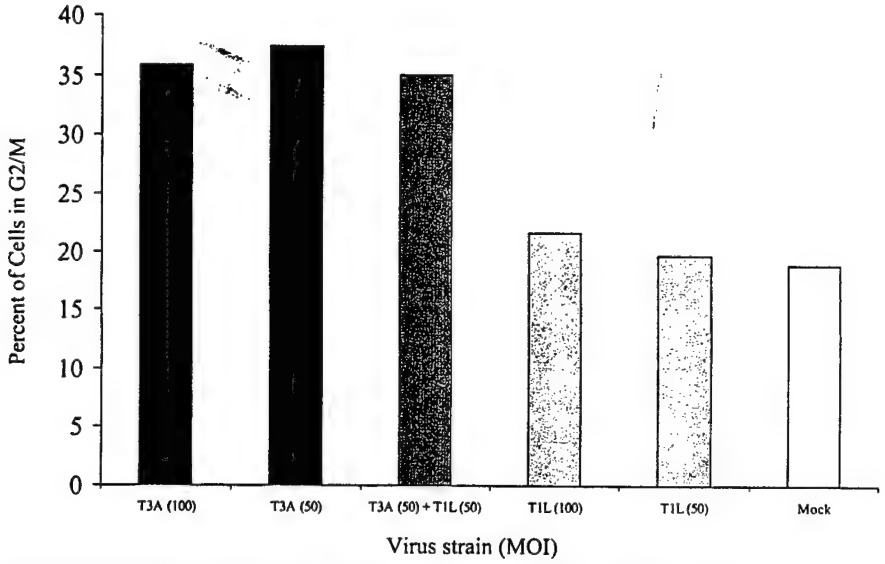

FIG. 5. T3A-induced G_2/M arrest phenotype is dominant. L929 cells were either mock infected (white), coinfected with equivalent MOIs of T1L and T3A (the MOI of each virus was 50 PFU per cell) (dark gray), or infected with T1L (light gray) or T3A (black) alone at MOIs of 50 or 100 PFU per cell. L929 cells were harvested at 48 h postinfection and analyzed using flow cytometry. The results are presented as the percentage of cells in the G_2/M phase of the cell cycle.

DISCUSSION

T3 reovirus strains inhibit host cell proliferation, as measured by cellular DNA synthesis inhibition, to a substantially greater extent than T1 reovirus strains (40, 44). It has been suggested, based on extrapolation of results obtained using [^{3}H]thymidine incorporation, that T3 reoviruses induce cell cycle arrest at the G_1-to-S transition. We now show, using flow cytometry to directly analyze cell cycle progression in reovirus-infected cells, that reovirus-induced inhibition of cellular pro-

TABLE 1. Capacities of T1L × T3D reassortant viruses to induce G_2/M arrest

Virus strain	Genome segment[a]										% Cells in G_2/M[b]	
	L1	L2	L3	M1	M2	M3	S1	S2	S3	S4	Unsynchronized	Synchronized
EB138	3D	1L	1L	3D	3D	1L	3D	3D	1L	1L	ND	24.56
EB28	3D	3D	1L	3D	3D	3D	3D	1L	3D	3D	38.13	28.59
KC150	3D	1L	1L	1L	3D	1L	3D	3D	1L	3D	33.91	36.47
EB97	3D	3D	1L	3D	3D	3D	3D	3D	3D	1L	30.30	28.35
G2	1L	3D	1L	1L	1L	1L	3D	1L	1L	1L	29.09	13.92
H41	3D	3D	1L	1L	1L	3D	1L	1L	3D	1L	26.56	ND
T3D	3D	3D	3D	3D	3D	3D	3D	3D	3D	3D	25.71	38.51
H15	1L	3D	3D	1L	3D	3D	3D	3D	3D	1L	24.95	31.63
EB127	3D	3D	1L	1L	3D	1L	1L	3D	3D	1L	23.54	ND
H9	3D	3D	1L	3D	1L	1L	3D	3D	3D	3D	23.11	17.17
EB85	1L	1L	1L	1L	1L	3D	1L	3D	1L	1L	21.88	ND
T1L	1L	1L	1L	1L	1L	1L	1L	1L	1L	1L	19.23	5.56
EB145	3D	3D	3D	3D	3D	1L	1L	3D	3D	3D	15.72	14.72
EB121	3D	3D	1L	3D	1L	3D	1L	3D	3D	3D	14.98	9.45
EB1	1L	3D	1L	1L	3D	1L	1L	1L	3D	1L	11.89	16.19
Significance (P)[c]												
Unsynchronized L cells												
t test	0.30	0.84	0.60	0.85	0.46	0.36	**0.004**	0.78	0.58	0.66		
MW	0.30	1	0.77	0.95	0.41	0.38	**0.007**	0.80	0.73	0.85		
Synchronized L cells												
t test	0.25	1	0.27	0.73	**0.007**	0.16	**0.007**	0.18	0.67	0.53		
MW	0.28	1	0.28	0.76	**0.016**	0.2	**0.016**	0.21	0.57	0.48		

[a] The parental origin of each genome segment in the reassortants strains: 1L, genome segment derived from T1L; 3D, genome segment derived from T3D.
[b] Unsynchronized or synchronized L cells were infected with viral strains at an MOI of 100 PFU per cell and analyzed by flow cytometry at 48 h postinfection. ND, not determined.
[c] As determined by two-sample parametric Student t test (t test) and Mann-Whitney nonparametric analysis (MW). Values in boldface are ●●●.

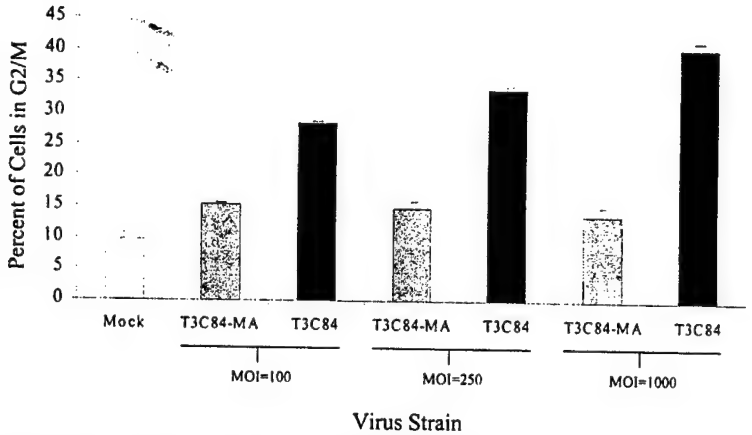

FIG. 6. Reovirus-induced G_2/M arrest requires σ1s. L929 cells were either mock infected (white) or infected with wild-type T3C84 (black) or σ1s-null mutant T3C84-MA (gray) at MOIs of 100, 250, or 1,000 PFU per cell. Cells were harvested 48 h postinfection, stained with Krishan's stain, and analyzed using flow cytometry. The results are presented as the mean percentage of cells in G_2/M phase of the cell cycle for six independent experiments at an MOI of 100 and three independent experiments at MOIs of 250 and 1,000. The error bars indicate the standard errors of the mean. A significantly greater percentage of T3C84-infected cells were in G_2/M than T3C84-MA-infected cells at each MOI tested ($P < 0.001$).

liferation results from G_2/M arrest. This effect is not cell type specific and is dominant in strains that block cell cycle progression.

Differences in the capacity of reovirus strains to inhibit cellular proliferation are determined by the viral S1 gene (40, 44). Our results indicate that the same is true for G_2/M arrest. The reovirus S1 gene is bicistronic, encoding the structural protein σ1 and the nonstructural protein σ1s using overlapping, alternative reading frames (20, 30, 39). As a result of this coding strategy, there is no sequence similarity between the σ1 and σ1s proteins (12). To determine which of the two S1-encoded proteins are required for G_2/M arrest, we examined the capacity of the σ1s null mutant T3C84-MA to induce G_2/M arrest. T3C84-MA and its σ1s expressing parent, T3C84, produce equivalent yields of viral progeny in L929 cells, and both viruses are equally effective in inducing apoptosis (37). However, T3C84-MA fails to induce G_2/M arrest. This finding suggests that σ1s is required for blockade of cell cycle progression following T3 reovirus infection. However, it is also possible that differences in the capacity of T3C84 and T3C84-MA to induce cell cycle arrest are influenced by other sequence differences. The mutation in the S1 gene that introduces a termination codon in the σ1s open reading frame also results in a lysine-to-isoleucine substitution at residue 26 in the deduced amino acid sequence of σ1. The T3C84-MA S1 gene also contains an additional mutation that results in a tryptophan-to-arginine substitution at residue 202 in σ1, which determines the capacity of this strain to bind sialic acid. To exclude the possibility that sialic acid binding influences cell cycle arrest, we isolated and characterized an additional T3C84-MA variant, T3C84-MA/σ1s+, that binds to sialic acid and expresses σ1s. In contrast to T3C84-MA, which binds sialic acid but does not express σ1s, T3C84-MA/σ1s+ induces G_2/M arrest. Therefore, it is unlikely that the capacity to bind sialic acid influences the efficiency of cell cycle arrest induced by T3 reoviruses (12).

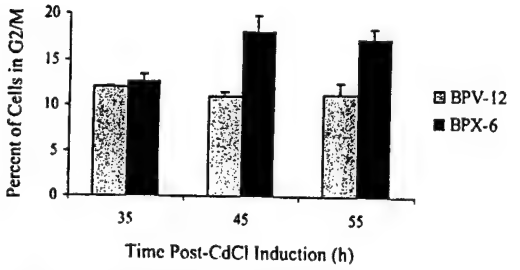

FIG. 7. σ1s expression induces an increase in the percentage of cells in G_2/M phase. C127 cells stably transfected with σ1s (BPX-6) or vector control (BPV-12) under the control of the mouse metallothionein promoter were induced with $CdCl_2$, harvested at the indicated times postinduction, and analyzed for DNA content by flow cytometry. The results are presented as the mean percentage of cells in the G_2/M phase of the cell cycle for three to six independent experiments. The error bars indicate the standard errors of the mean. The percentage of cells in G_2/M was significantly greater in the σ1s-expressing cells than in the vector-control cells at 45 h ($P = 0.03$, $n = 4$) and 55 h ($P = 0.005$, $n = 6$) postinduction.

To corroborate findings made using viruses that vary in σ1s expression, we also tested the capacity of cells engineered to express σ1s under the control of an inducible promoter to undergo cell cycle arrest. Following induction of σ1s expression, we observed an increase in the percentage of cells in the G_2/M phase of the cell cycle, which suggests that σ1s is capable of mediating cell cycle blockade at the G_2/M checkpoint. This observation suggests that the reovirus σ1s protein is similar to the human immunodeficiency virus (HIV) Vpr protein (2, 28, 31, 35) or the human papillomavirus (HPV) E2 protein (23), which similarly block cell cycle progression at the G_2/M boundary. Thus, our findings indicate that reovirus-induced G_2/M arrest requires σ1s and provide the first evidence of a functional role for this nonstructural protein.

We have previously shown that the capacity of reovirus to induce apoptosis correlates with the capacity to inhibit cellular proliferation and that both properties are determined by the viral S1 gene (44). Our results clearly show that G_2/M arrest can occur in cells treated with potent inhibitors of reovirus-

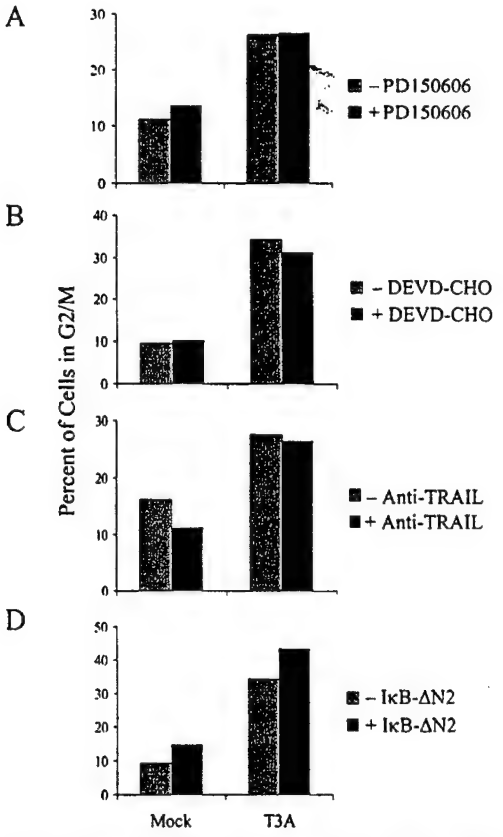

FIG. 8. Inhibitors of reovirus-induced apoptosis do not inhibit reovirus-induced G_2/M arrest. (A) Effect of calpain inhibitor PD150606 on T3A-induced G_2/M arrest. L929 cells were treated with either 25 μM calpain inhibitor PD150606 or an ethanol control and then either mock infected or infected with T3A at an MOI of 100 PFU per cell. (B) Effect of caspase 3 inhibitor DEVD-CHO on T3A-induced G_2/M arrest. HEK293 cells were treated with either 100 μM caspase 3 inhibitor DEVD-CHO or a dimethyl sulfoxide control and then either mock infected or infected with T3A at an MOI of 100 PFU per cell. (C) Effect of anti-TRAIL antibodies on T3A-induced G_2/M arrest. HEK293 cells were treated with either 30 μg of an anti-TRAIL antibody per ml or mock treated as a control and then either mock infected or infected with T3A at an MOI of 100 PFU per cell. (D) Effect of NF-κB inhibition on T3A-induced G_2/M arrest. HEK293 cells expressing a dominant-negative form of IκB (IκB-ΔN2) to inhibit NF-κB activation or untransfected HEK293 cells were either mock infected or infected with T3A at an MOI of 100 PFU per cell. In all cases, G_2/M arrest was assessed 48 h postinfection.

induced apoptosis. These findings indicate that the induction of G_2/M arrest and apoptosis by reovirus are functionally independent at some stage following infection. Moreover, although strain-specific differences in reovirus-induced G_2/M arrest and apoptosis induction segregate with the viral S1 gene, each property is determined by a different S1 gene product. Strain-specific differences in reovirus-induced G_2/M arrest are determined by σ1s, whereas differences in reovirus-induced apoptosis are determined by σ1 (36, 45). The induction of G_2/M arrest by HIV Vpr is apparently required for Vpr-induced apoptosis (42), whereas reovirus-induced apoptosis can occur in the absence of G_2/M arrest (37). These findings suggest that viruses may utilize different mechanisms to induce G_2/M arrest and apoptosis.

The G_2/M transition is regulated by the kinase cdc2/cdk1 (13–15, 32, 34). Expression of HIV Vpr (28, 35) or HPV E2 protein (23) results in inhibition or delayed activation of cdc2 kinase activity resulting in an accumulation of cells in the G_2/M phase of the cell cycle. In contrast, the baculovirus *Autographa californica* nuclear polyhydrosis virus (AcNPV) (3) and herpes simplex virus (HSV) (1, 29) induce G_2/M arrest by a mechanism that is cdc2 independent since cells infected with either of these viruses maintain high levels of cdc2 kinase activity. HIV, HPV, AcNPV, and HSV require a nuclear phase to replicate, whereas reovirus replicates in the cytoplasm. T3 σ1s has been detected in the nucleus as well as in the cytoplasm following reovirus infection (5, 37), and it is possible that this nuclear localization is required for reovirus-induced G_2/M arrest. Future studies will be aimed at identifying which cell cycle regulatory proteins are involved in reovirus-induced cell cycle perturbation, the role of cellular localization of σ1s in this process, and the significance of cell cycle arrest in reovirus-induced cytopathology and pathogenesis.

ACKNOWLEDGMENTS

This work was supported by Public Health Service grant 1RO1AG14071 from the National Institute of Aging, Merit and REAP grants from the Department of Veterans Affairs, and a U.S. Army Medical Research and Material Command grant (USAMRMC 98293015) (K.L.T.). This work also was supported by Public Health Service grant AI38296 from the National Institute of Allergy and Infectious Diseases and the Elizabeth B. Lamb Center for Pediatric Research (T.S.D.).

The University of Colorado Cancer Center provided core flow cytometry facilities.

REFERENCES

1. **Advani, S. J., R. Brandimarti, R. R. Weichselbaum, and B. Roizman.** 2000. The disappearance of cyclins A and B and the increase in activity of the G(2)/M-phase cellular kinase cdc2 in herpes simplex virus 1-infected cells require expression of the alpha22/U(S)1.5 and U(L)13 viral genes. J. Virol. 74:8–15.
2. **Bartz, S. R., M. E. Rogel, and M. Emerman.** 1996. Human immunodeficiency virus type 1 cell cycle control: Vpr is cytostatic and mediates G_2 accumulation by a mechanism which differs from DNA damage checkpoint control. J. Virol. 70:2324–2331.
3. **Braunagel, S. C., R. Parr, M. Belyavskyi, and M. D. Summers.** 1998. *Autographa californica* nucleopolyhedrovirus infection results in Sf9 cell cycle arrest at G2/M phase. Virology 244:195–211.
4. **Brown, E. G., M. L. Nibert, and B. N. Fields.** 1983. The L2 gene of reovirus serotype 3 controls the capacity to interfere, accumulate deletions and establish persistent infection, p. 275–287. *In* R. W. Compans and D. H. L. Bishop (ed.), Double-stranded RNA viruses. Elsevier, New York, N.Y.
5. **Ceruzzi, M., and A. J. Shatkin.** 1986. Expression of reovirus p14 in bacteria and identification in the cytoplasm of infected mouse L cells. Virology 153:35–45.
6. **Chappell, J. D., V. L. Gunn, J. D. Wetzel, G. S. Baer, and T. S. Dermody.** 1997. Mutations in type 3 reovirus that determine binding to sialic acid are contained in the fibrous tail domain of viral attachment protein sigma1. J. Virol. 71:1834–1841.
7. **Clarke, P., S. M. Meintzer, G. Spencer, C. Widmann, T. P. Garrington, G. L. Johnson, and K. L. Tyler.** TRAIL mediated apoptosis is induced in cells following infection with reovirus. J. Virol., in press.
8. **Connolly, J. L., S. E. Rodgers, P. Clarke, D. W. Ballard, L. D. Kerr, K. L. Tyler, and T. S. Dermody.** 2000. Reovirus-induced apoptosis requires activation of transcription factor NF-κB. J. Virol. 74:2981–2989.
9. **Coombs, K. M., B. N. Fields, and S. C. Harrison.** 1990. Crystallization of the reovirus type 3 Dearing core. Crystal packing is determined by the lambda 2 protein. J. Mol. Biol. 215:1–5.
10. **Cox, D. C., and J. E. Shaw.** 1974. Inhibition of the initiation of cellular DNA synthesis after reovirus infection. J. Virol. 13:760–761.
11. **Debiasi, R. L., M. K. Squler, B. Pike, M. Wynes, T. S. Dermody, J. J. Cohen, and K. L. Tyler.** 1999. Reovirus-induced apoptosis is preceded by increased cellular calpain activity and is blocked by calpain inhibitors. J. Virol. 73:695–701.

12. **Dermody, T. S., M. L. Nibert, R. Bassel-Duby, and B. N. Fields.** 1990. Sequence diversity in S1 genes and S1 translation products of 11 serotype 3 reovirus strains. J. Virol. **64**:4842–4850.
13. **Draetta, G., and D. Beach.** 1988. Activation of cdc2 protein kinase during mitosis in human cells: cell cycle-dependent phosphorylation and subunit rearrangement. Cell **54**:17–26.
14. **Draetta, G., and J. Eckstein.** 1997. Cdc25 protein phosphatases in cell proliferation. Biochim. Biophys. Acta **1332**:M53–M63.
15. **Draetta, G., H. Piwnica-Worms, D. Morrison, B. Druker, T. Roberts, and D. Beach.** 1988. Human cdc2 protein kinase is a major cell-cycle regulated tyrosine kinase substrate. Nature **336**:738–744.
16. **Duke, R. C., and J. J. Cohen.** 1992. Morphological and biochemical assays of apoptosis, p. 3.17.1–3.17.16. *In* J. E. Coligan (ed.), Current protocols in immunology. Wiley, New York, N.Y.
17. **Duncan, M. R., S. M. Stanish, and D. C. Cox.** 1978. Differential sensitivity of normal and transformed human cells to reovirus infection. J. Virol. **28**:444–449.
18. **Ensminger, W. D., and I. Tamm.** 1969. Cellular DNA and protein synthesis in reovirus-infected L cells. Virology **39**:357–360.
19. **Ensminger, W. D., and I. Tamm.** 1969. The step in cellular DNA synthesis blocked by reovirus infection. Virology **39**:935–938.
20. **Ernst, H., and A. J. Shatkin.** 1985. Reovirus hemagglutinin mRNA codes for two polypeptides in overlapping reading frames. Proc. Natl. Acad. Sci. USA **82**:48–52.
21. **Fajardo, E., and A. J. Shatkin.** 1990. Expression of the two reovirus S1 gene products in transfected mammalian cells. Virology **178**:223–231.
22. **Fajardo, J. E., and A. J. Shatkin.** 1990. Translation of bicistronic viral mRNA in transfected cells: regulation at the level of elongation. Proc. Natl. Acad. Sci. USA **87**:328–332.
23. **Fournier, N., K. Raj, P. Saudan, S. Utzig, R. Sahli, V. Simanis, and P. Beard.** 1999. Expression of human papillomavirus 16 E2 protein in *Schizosaccharomyces pombe* delays the initiation of mitosis. Oncogene **18**:4015–4021.
24. **Gaulton, G. N., and M. I. Greene.** 1989. Inhibition of cellular DNA synthesis by reovirus occurs through a receptor-linked signaling pathway that is mimicked by antiidiotypic, antireceptor antibody. J. Exp. Med. **169**:197–211.
25. **Gomatos, P., and I. Tamm.** 1963. Macromolecular synthesis in reovirus-infected L cells. Biochim. Biophys. Acta **72**:651–653.
26. **Hand, R., W. D. Ensminger, and I. Tamm.** 1971. Cellular DNA replication in infections with cytocidal RNA viruses. Virology **44**:527–536.
27. **Hand, R., and I. Tamm.** 1974. Initiation of DNA replication in mammalian cells and its inhibition by reovirus infection. J. Mol. Biol. **82**:175–183.
28. **He, J., S. Choe, R. Walker, P. Di Marzio, D. O. Morgan, and N. R. Landau.** 1995. Human immunodeficiency virus type 1 viral protein R (Vpr) arrests cells in the G_2 phase of the cell cycle by inhibiting p34cdc2 activity. J. Virol. **69**:6705–6711.
29. **Hobbs, W. E., and N. A. DeLuca.** 1999. Perturbation of cell cycle progression and cellular gene expression as a function of herpes simplex virus ICP0. J. Virol. **73**:8245–8255.
30. **Jacobs, B. L., and C. E. Samuel.** 1985. Biosynthesis of reovirus-specified polypeptides: the reovirus s1 mRNA encodes two primary translation products. Virology **143**:63–74.
31. **Jowett, J. B., V. Planelles, B. Poon, N. P. Shah, M. L. Chen, and I. S. Chen.** 1995. The human immunodeficiency virus type 1 vpr gene arrests infected T cells in the G_2 + M phase of the cell cycle. J. Virol. **69**:6304–6313.
32. **King, R. W., P. K. Jackson, and M. W. Kirschner.** 1994. Mitosis in transition. Cell **79**:563–571.
33. **Krishan, A.** 1975. Rapid flow cytofluorometric analysis of mammalian cell cycle by propidium iodide staining. J. Cell Biol. **66**:188–193.
34. **Morla, A. O., G. Draetta, D. Beach, and J. Y. Wang.** 1989. Reversible tyrosine phosphorylation of cdc2: dephosphorylation accompanies activation during entry into mitosis. Cell **58**:193–203.
35. **Re, F., D. Braaten, E. K. Franke, and J. Luban.** 1995. Human immunodeficiency virus type 1 Vpr arrests the cell cycle in G_2 by inhibiting the activation of p34cdc2-cyclin B. J. Virol. **69**:6859–6864.
36. **Rodgers, S. E., E. S. Barton, S. M. Oberhaus, B. Pike, C. A. Gibson, K. L. Tyler, and T. S. Dermody.** 1997. Reovirus-induced apoptosis of MDCK cells is not linked to viral yield and is blocked by Bcl-2. J. Virol. **71**:2540–2546.
37. **Rodgers, S. E., J. L. Connolly, J. D. Chappell, and T. S. Dermody.** 1998. Reovirus growth in cell culture does not require the full complement of viral proteins: identification of a σ1s-null mutant. J. Virol. **72**:8597–8604.
38. **Roner, M. R., and D. C. Cox.** 1985. Cellular integrity is required for inhibition of initiation of cellular DNA synthesis by reovirus type 3. J. Virol. **53**:350–359.
39. **Sarkar, G., J. Pelletier, R. Bassel-Duby, A. Jayasuriya, B. N. Fields, and N. Sonenberg.** 1985. Identification of a new polypeptide coded by reovirus gene S1. J. Virol. **54**:720–725.
40. **Sharpe, A. H., and B. N. Fields.** 1981. Reovirus inhibition of cellular DNA synthesis: role of the S1 gene. J. Virol. **38**:389–392.
41. **Shaw, J. E., and D. C. Cox.** 1973. Early inhibition of cellular DNA synthesis by high multiplicities of infectious and UV-inactivated reovirus. J. Virol. **12**:704–710.
42. **Stewart, S. A., B. Poon, J. B. Jowett, and I. S. Chen.** 1997. Human immunodeficiency virus type 1 Vpr induces apoptosis following cell cycle arrest. J. Virol. **71**:5579–5592.
43. **Tyler, K. L., R. T. Bronson, K. B. Byers, and B. Fields.** 1985. Molecular basis of viral neurotropism: experimental reovirus infection. Neurology **35**:88–92.
44. **Tyler, K. L., M. K. Squler, A. L. Brown, B. Pike, D. Willis, S. M. Oberhaus, T. S. Dermody, and J. J. Cohen.** 1996. Linkage between reovirus-induced apoptosis and inhibition of cellular DNA synthesis: role of the S1 and M2 genes. J. Virol. **70**:7984–7991.
45. **Tyler, K. L., M. K. Squler, S. E. Rodgers, B. E. Schneider, S. M. Oberhaus, T. A. Grdina, J. J. Cohen, and T. S. Dermody.** 1995. Differences in the capacity of reovirus strains to induce apoptosis are determined by the viral attachment protein sigma 1. J. Virol. **69**:6972–6979.

JOURNAL OF VIROLOGY, Sept. 2000, p. 8135–8139
0022-538X/00/$04.00+0

Vol. 74, No. 17

Reovirus-Induced Apoptosis Is Mediated by TRAIL

PENNY CLARKE,[1] SUZANNE M. MEINTZER,[1] SPENCER GIBSON,[2,3] CHRISTIAN WIDMANN,[2,3] TIMOTHY P. GARRINGTON,[2,3] GARY L. JOHNSON,[2,3,4] AND KENNETH L. TYLER[1,5,6]*

Departments of Neurology,[1] Pharmacology,[4] and Medicine, Microbiology and Immunology,[5] University of Colorado Health Sciences Center, and Denver Veteran's Affairs Medical Center,[6] Denver, Colorado 80262, and Program in Molecular Signal Transduction[2] and Division of Basic Sciences,[3] National Jewish Center for Immunology and Respiratory Medicine, Denver, Colorado 80206

Received 13 April 2000/Accepted 9 June 2000

Members of the tumor necrosis factor (TNF) receptor superfamily and their activating ligands transmit apoptotic signals in a variety of systems. We now show that the binding of TNF-related, apoptosis-inducing ligand (TRAIL) to its cellular receptors DR5 (TRAILR2) and DR4 (TRAILR1) mediates reovirus-induced apoptosis. Anti-TRAIL antibody and soluble TRAIL receptors block reovirus-induced apoptosis by preventing TRAIL-receptor binding. In addition, reovirus induces both TRAIL release and an increase in the expression of DR5 and DR4 in infected cells. Reovirus-induced apoptosis is also blocked following inhibition of the death receptor-associated, apoptosis-inducing molecules FADD (for FAS-associated death domain) and caspase 8. We propose that reovirus infection promotes apoptosis via the expression of DR5 and the release of TRAIL from infected cells. Virus-induced regulation of the TRAIL apoptotic pathway defines a novel mechanism for virus-induced apoptosis.

Studies using mammalian reoviruses have provided fundamental insights into the molecular and genetic basis of viral pathogenesis and virus-induced cell death. Reovirus infection induces apoptosis in cultured cells in vitro (13, 15, 26) and in target tissues in vivo, including the central nervous system, heart, and liver (12, 13). Reovirus induces apoptosis by a p53-independent mechanism that involves cellular proteases including calpains (4), is dependent on reovirus-induced NF-κB activation (3), and is inhibited by overexpression of Bcl-2 (15). Strain-specific differences in the capacity of reoviruses to induce apoptosis are determined by the viral S1 gene (26) and require viral binding to cell surface receptors but not completion of the full viral replication cycle (15). Reovirus-induced apoptosis correlates with pathology in vivo and is a critical mechanism by which disease is triggered in the host (12). Inhibition of apoptosis in vivo reduces the extent of tissue injury (R. L. Debiasi et al., Am. Soc. Virol. Sci. Program Abstr., abstr. W52-1, 1999), emphasizing the importance of apoptosis in reovirus pathogenesis. We have thus used reovirus infection to study mechanisms of virus-induced apoptosis.

Cellular death receptors (DRs) transmit apoptosis-inducing signals initiated by specific death ligands, most of which are primarily expressed as biologically active type II membrane proteins that are cleaved into soluble forms. Fas ligand (FasL) activates Fas/CD95/Apo1, tumor necrosis factor (TNF) activates TNFR1 (TNF receptor 1), Apo 3L/TWEAK activates DR3, and TRAIL (for TNF-related apoptosis-inducing ligand; also called Apo2L) activates DR4 (TRAILR1) and DR5 (TRAILR2/TRICK2). Ligand-mediated activation triggers a cascade of events that begins with DR oligomerization and the close association of their cytoplasmic death domains (DDs). This is followed by DD-associated interaction with adapter molecules and cellular proteases critical to DR-induced apoptosis (reviewed in reference 1). In this paper we describe a novel mechanism for virus-induced cell death involving the upregulation of DR5, the release of TRAIL from infected cells, and subsequent TRAIL-mediated apoptosis.

* Corresponding author. Mailing address: Department of Neurology (127), Denver VA Medical Center, 1066 Clermont St., Denver, CO 80220. Phone: (303) 393-2874. Fax: (303) 393-4686. E-mail: Ken.Tyler@uchsc.edu.

† Present address: Institute de Biologie Cellulaire et de Morphologie, Lausanne, Switzerland.

MATERIALS AND METHODS

Cells, virus, and inhibitors. HEK293 cells (ATCC CRL1573) were grown in Dulbecco's modified Eagle's medium supplemented with 100 U each of penicillin and streptomycin per ml and containing 10% fetal bovine serum. HeLa cells (ATCC CCL2) were grown in Eagle's minimal essential medium supplemented with 2.4 mM L-glutamine, nonessential amino acids, 60 U each of penicillin and streptomycin per ml, and containing 10% fetal bovine serum (Gibco BRL, Gaithersburg, Md.). FADD-DN cells express amino acids 80 to 208 of the Fas-associated DD (FADD) cDNA (with the addition of an AU1 epitope tag at the N terminus), from the cytomegalovirus promoter from pcDNA3 (Invitrogen, Carlsbad, Calif.). Reovirus (type 3 Abney [T3A]) is a laboratory stock which has been plaque purified and passaged (twice) in L929 (ATCC CCL1) cells to generate working stocks (27). Virus growth was determined by plaque assay as previously described (25).

Western blot analysis and antibodies. Twenty-four hours following infection with reovirus, cells were pelleted by centrifugation, washed twice with ice-cold phosphate-buffered saline, and lysed by sonication in 200 μl of a buffer containing 15 mM Tris (pH 7.5), 2 mM EDTA, 10 mM EGTA, 20% glycerol, 0.1% NP-40, 50 mM β-mercaptoethanol, 100 μg of leupeptin and 2 μg of aprotinin per ml, 40 μM Z-D-DCB, and 1 mM phenylmethylsulfonyl fluoride. The lysates were then cleared by centrifugation at 16,000 × *g* for 5 min, normalized for protein amount, mixed 1:1 with sodium dodecyl sulfate (SDS) sample buffer (100 mM Tris [pH 6.8], 2% SDS, 300 mM β-mercaptoethanol, 30% glycerol, 5% pyronine Y), boiled for 5 min, and stored at −70°C. Proteins were electrophoresed by SDS–10% polyacrylamide gels and probed with polyclonal antibodies directed against DR4 (366891N [PharMingen, San Diego, Calif.] and sc-6823 [Santa Cruz Biotechnology, Santa Cruz, Calif.]), DR5 (210-730-C100 [Alexis Corporation, Pittsburgh, Pa.] and sc-7191 [Santa Cruz Biotechnology]), DCR-2 (33060-100; Biovision, Palo Alto, Calif.), Fas (sc-714-G; Santa Cruz Biotechnology), and actin (CP01; Oncogene, Cambridge, Mass.). Additional antibodies directed against FasL (sc-834-G; Santa Cruz Biotechnology) and TRAIL (3210-732-R100 [Alexis Corporation] and antibody from Affinity Bioreagents, Golden, Color.) were used for antibody blocking experiments. Autoradiographs were quantitated by densitometric analysis using ImageQuant (Amersham Pharmacia Biotech, Inc., Piscataway, N.J.).

Apoptosis assays and reagents. Forty-eight hours after infection with reovirus, cells were harvested and stained with acridine orange, for determination of nuclear morphology, and ethidium bromide, to distinguish cell viability, at a final concentration of 1 μg/ml each (5). Following staining, cells were examined by epifluorescence microscopy (Nikon Labophot-2; B-2A filter; excitation, 450 to 490 nm; barrier, 520 nm; dichroic mirror, 505 nm). The percentage of cells containing condensed nuclei and/or marginated chromatin in a population of 100 cells was recorded. The specificity of this assay has been previously established in

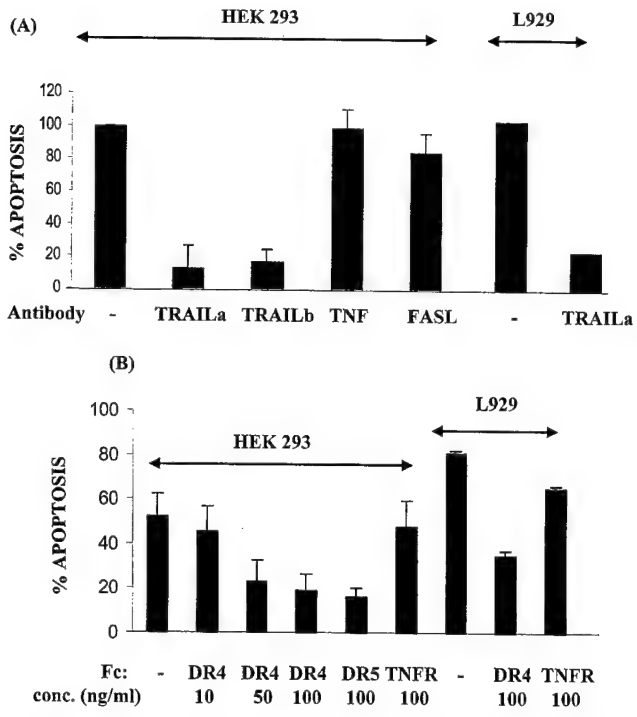

FIG. 1. TRAIL mediates reovirus-induced apoptosis. Anti-TRAIL antibodies and soluble TRAIL receptors (Fc:DR4 and Fc:DR5) specifically inhibit reovirus-induced apoptosis. HEK293 and L929 cells were pretreated for 1 h with two different anti-TRAIL (TRAILa and TRAILb) antibodies (A) or increasing concentrations of soluble TRAIL receptors (B) before being infected with reovirus (MOIs of 10 and 50, respectively, for antibody and receptor experiments). After infection cells were incubated in media containing antibody or receptor for 48 h before cells were harvested and the percentage of apoptotic cells was determined. The graphs show percent apoptosis compared to untreated cells in reovirus-infected minus mock-infected cells (A) and the actual percent apoptosis in reovirus-infected minus mock-infected cells (B). Error bars represent standard error of the mean. Antibodies directed against TNF and FasL were used as controls in the antibody blocking experiments. Soluble TNFR (Fc:TNFR) was used as a control in the receptor experiments.

reovirus-infected cells using DNA laddering techniques and electron microscopy (26). Soluble TRAIL was obtained from Upstate Biotechnology, Lake Placid, N.Y. Soluble DRs Fc:DR4, Fc:DR5, and Fc:TNFR were obtained from Alexis Corporation. Z-IETD-FMK (granzyme B inhibitor III), a specific inhibitor of caspase 8 activity, was obtained from Clontech, Palo Alto, Calif.

RESULTS

Reovirus-induced apoptosis is mediated by TRAIL. We investigated the role of ligand-mediated apoptosis in reovirus-induced cell death using two separate polyclonal antibodies directed against TRAIL and antibodies directed against FasL and TNF to block ligand binding during reovirus infection. HEK293 cells were pretreated with antiligand antibodies (30 μg/ml) for 1 h before viral infection (multiplicity of infection [MOI] of 10) and were maintained in antibody-containing media following infection with reovirus. Antibody was not present during viral infection. The percentage of apoptotic cells was determined at 48 h postinfection. Anti-TRAIL antibodies, but not antibodies directed against FasL (TRAIL versus FasL, $P = 0.008$) or TNF (TRAIL versus TNF, $P = 0.003$) significantly inhibit reovirus-induced apoptosis (Fig. 1A). Thus, anti-TRAIL antibodies specifically inhibit reovirus-induced apoptosis. Anti-TRAIL antibody also inhibits reovirus-induced apoptosis in L929 cells (Fig. 1A), indicating that TRAIL-mediated apoptosis is likely to be a general feature of reovirus-induced apoptosis. Both anti-TRAIL antibodies bound soluble ligand in Western blot analysis (results not shown).

TRAIL binding was further shown to be essential for reovirus-induced apoptosis using the soluble TRAIL receptors Fc:DR4 and Fc:DR5 (Fig. 1B). These molecules contain the extracellular domain of DR4 or DR5 fused to the Fc portion of human immunoglobulin G and inhibit TRAIL-induced apoptosis by preventing TRAIL binding to DR4 and DR5 present on the cell surface (7). Cells were pretreated with soluble receptor for 1 h before virus infection (MOI of 50) and were maintained in receptor-containing media following infection. Soluble receptor was not present during viral infection. Treatment of cells with Fc:DR4 or Fc:DR5 (not shown) produces a dose-dependent inhibitory effect on reovirus-induced apoptosis (Fig. 1B). Thus, Fc:DR4 and Fc:DR5 appear to be similar in potency for TRAIL binding. Fc:DR4 (100 ng/ml) and Fc:DR5 (100 ng/ml) reduced reovirus-induced apoptosis by 65% (from 54% to 19%, $P = 0.048$) and by 70% (from 54% to 16%), respectively. Soluble TNFR (Fc:TNFR; 100 ng/ml) does not significantly inhibit reovirus-induced apoptosis, indicating that the inhibition is specific for the TRAIL-associated receptors DR4 and DR5. In L929 cells, Fc:DR4, but not Fc:TNFR, also significantly inhibited reovirus-induced apoptosis by 57% (from 81% to 35% [Fig. 1B]), again indicating that TRAIL-mediated apoptosis is likely to be a general feature of reovirus-induced apoptosis. To confirm that antibody or soluble receptor-mediated inhibition of apoptosis was not due to any effect of these reagents on viral replication, we measured viral yield in anti-TRAIL and soluble receptor-treated cells and found no significant difference compared with untreated cells (results not shown).

TRAIL is released from cells following infection with reovirus. Having shown that TRAIL is required for reovirus-induced apoptosis, we next wanted to determine whether cleaved, soluble TRAIL is released from in reovirus-infected cells.

Following infection of HEK293 cells with reovirus (MOI of 100), the supernatant was collected and transferred onto HeLa cells, which are sensitive to TRAIL-induced apoptosis (Fig. 2). Supernatants collected from virus-infected HEK293 cells 24, 36, and 48 h postinfection induce apoptosis (18, 30, and 68%, respectively) when transferred onto HeLa cells. Apoptotic

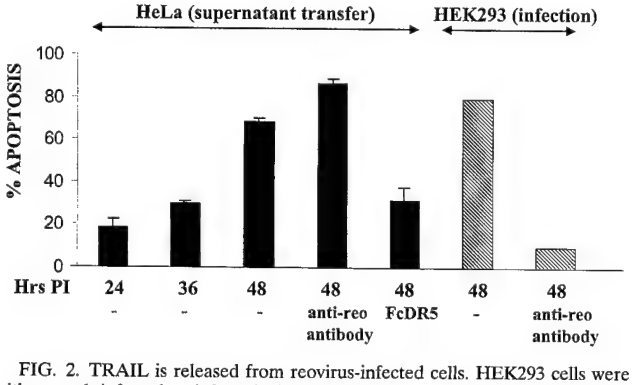

FIG. 2. TRAIL is released from reovirus-infected cells. HEK293 cells were either mock infected or infected with reovirus (MOI of 100). At various times postinfection (PI), supernatant from infected HEK293 cells was transferred onto TRAIL-sensitive HeLa cells. Apoptosis was assayed in HeLa cells 24 h following supernatant transfer. The graph shows the percent increase of apoptotic nuclei in HeLa cells following treatment with supernatants taken from reovirus-infected, compared to mock-infected, HEK293 cells. Error bars represent standard errors of the mean. Soluble DR5 (Fc:DR5) and an antireovirus (anti-reo) antibody were used as TRAIL specificity controls. The shaded bars demonstrate that reovirus-induced (MOI of 100) apoptosis is blocked by the antireovirus antibody in HEK293 cells.

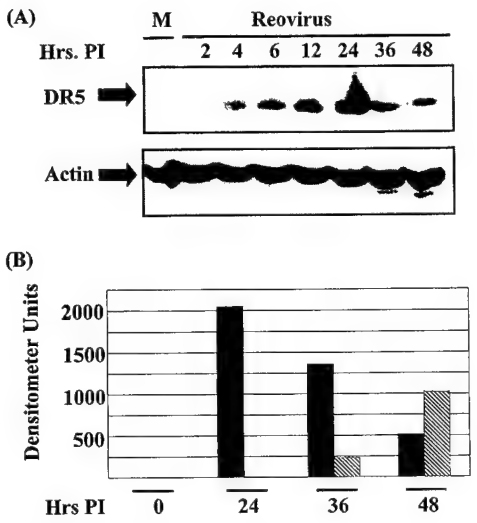

FIG. 3. DR5 is up-regulated during reovirus-induced apoptosis. Cell lysates were prepared and examined by Western blotting using antibodies directed against DR5 and actin (A). Following autoradiography, densitometric analysis was performed (B). The graph shows the increase in signal observed in reovirus-infected compared to mock-infected cells for DR5 (black columns) and DR4 (shaded columns). M, mock infection; PI, postinfection.

HeLa nuclei were assayed 24 h following treatment with supernatant from reovirus-infected HEK293 cells. Supernatant-induced apoptosis of HeLa cells is inhibited 64% (from 68% to 31%, $P = 0.001$) by soluble DR5 (Fc:DR5; 100 ng/ml [Fig. 2]) and by soluble DR4 (Fc:DR4; 100 ng/ml [results not shown]), indicating that the apoptosis seen in the HeLa cells following supernatant transfer is TRAIL specific. TRAIL is thus released from reovirus-infected cells and induces apoptosis in HeLa cells. The apoptotic effects of infected cell supernatants are not due to the presence of infectious virus in the transferred supernatant since addition of a neutralizing polyclonal antireovirus antiserum that blocks apoptosis induced by infectious virus (26) does not block apoptosis induced in HeLa cells by supernatant transfer (Fig. 2). This antibody inhibits reovirus (MOI of 100)-induced apoptosis in HEK293 cells (Fig. 2).

Expression of DR5 is up-regulated following infection with reovirus. Reovirus-induced apoptosis thus requires TRAIL binding, and TRAIL is released from reovirus-infected cells. We next investigated the expression of TRAIL receptors in reovirus-infected cells. HEK293 cells were infected with reovirus (MOI of 100), harvested at various times postinfection, and examined by Western blot analysis. DR5 is detected in lysates extracted from reovirus-infected but not mock-infected HEK293 cells. DR5 expression is first detected at 4 h postinfection. Expression peaks at 24 h postinfection and then declines (Fig. 3). The expression of DR4 also increases in reovirus-infected cells, but with much less magnitude and only at late times after infection (Fig. 3B). DR5 thus appears to be the TRAIL receptor that is predominantly up-regulated following reovirus infection.

Decoy receptor 1 (DcR-1; also called TRAILR3/TRID/LIT) and DcR-2 (TRAILR4) compete with DR4 and DR5 for TRAIL binding. These decoy receptors do not contain active intracellular DDs do not transduse apoptotic signals, and have antiapoptotic effects (6, 17). Neither DcR-1 nor DcR-2 expression is significantly altered in reovirus-infected cells (results not shown).

Reovirus infection sensitizes cells to TRAIL-induced apoptosis. TRAIL-induced apoptosis is enhanced in cells demonstrating an increase in the surface expression of DR4 and DR5 (7). Having shown that reovirus infection results in increased expression of DR5 and to a lesser extent DR4, we next wished to determine whether these increases occur at the cell surface by demonstrating that reovirus sensitizes cells to TRAIL-induced apoptosis. Cells were infected with reovirus (MOI of 10), treated with TRAIL (200 ng/ml) at various times postinfection and assayed for apoptosis 24 h later. Mock-infected HEK293 cells do not undergo apoptosis when treated with TRAIL. However, following infection with reovirus, HEK293 cells become sensitive to TRAIL-induced apoptosis (Fig. 4), and the percentage of apoptotic nuclei in TRAIL-treated, reovirus-infected cells is greater than that in cells treated with reovirus alone (Fig. 4). At 12, 24, 30, and 48 h after infection with reovirus, TRAIL-treated cells demonstrated 2.4-, 3.7-, 3.3-, and 1.8-fold increases in apoptosis, respectively, compared to TRAIL-treated mock-infected cells. Since TRAIL-induced apoptosis is apparent 12 h following infection with

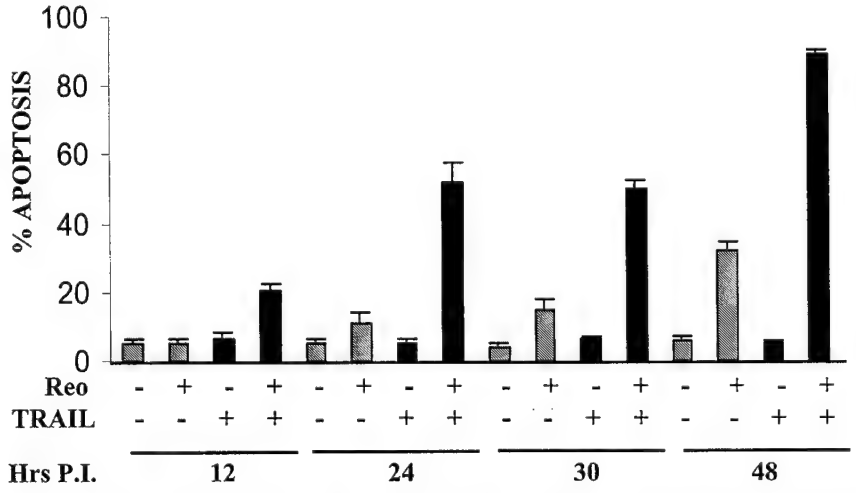

FIG. 4. Reovirus infection sensitizes cells to TRAIL-induced apoptosis. The effectiveness of TRAIL (200 ng/ml)-induced apoptosis was assayed in mock (−)- or reovirus (+; MOI of 10)-infected cells. Cells were treated with TRAIL (black bars) or left untreated (shaded bars). At various times postinfection (P.I.), cells were assayed for the presence of apoptotic nuclei. The graph shows the mean percentage of apoptotic nuclei. Error bars represent standard errors of the mean.

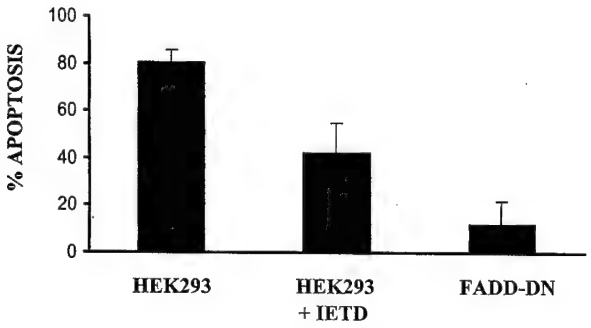

FIG. 5. Reovirus-induced apoptosis involves FADD and caspase 8 activity. HEK293 cells expressing FADD-DN or HEK293 cells treated with a specific inhibitor of caspase 8 (IETD) were infected with reovirus (MOI of 50). Apoptosis was assayed 48 h postinfection. The graph shows the mean percentage of apoptotic nuclei. Error bars represent standard errors of the mean.

reovirus and since the up-regulation of DR4 is not seen until 24 h postinfection, this again suggests that it is the increased expression of DR5 rather than DR4 that is the primary TRAIL receptor involved in reovirus-induced apoptosis.

FADD and caspase 8 are involved in reovirus-induced apoptosis. DRs mediate apoptosis through receptor-associated DD containing adapter proteins, exemplified by FADD (also called Mort 1). These adapter molecules contain their own DDs that bind to the clustered receptor DDs, resulting from receptor-ligand binding (reviewed in reference 1). Studies with dominant negative (DN) mutants of FADD (28) and cells derived from FADD gene knockout mice (31) indicate that FADD is necessary for apoptosis mediated by Fas, TNFR1, and DR3 (1, 9, 28). Apoptotic signals induced by DR4 and DR5 also appear to be mediated either by FADD or a FADD-like adapter molecule (1, 29). We constructed a HEK293 cell line expressing DN FADD (FADD-DN) in order to inhibit FADD and therefore DR-mediated apoptosis. Reovirus-induced apoptosis in HEK293 cells (and in HEK293 cells expressing vector alone [not shown]) is reduced by 85% (from 80.3% to 12%, $P = 0.0012$) in reovirus-infected HEK293 cells expressing FADD-DN (Fig. 5). These results confirm our findings that reovirus-induced apoptosis involves cellular DRs.

DR-induced, FADD-mediated apoptosis requires the activity of caspase 8. Activation of caspase 8 requires association of its death effector domains with those of FADD. Activated caspase 8 then activates the downstream effector caspases, including caspase 3 (reviewed in references 16 and 23). To further support the role of the TRAIL/DR pathway in reovirus-induced apoptosis, we demonstrate that IETD-fmk (50 μM), a specific inhibitor of caspase 8, reduces reovirus-induced apoptosis by 48% (from 80.3% to 42%, $P = 0.372$), indicating that caspase 8 is involved in reovirus-induced apoptosis (Fig. 5).

DISCUSSION

We have shown that reovirus-induced apoptosis requires TRAIL binding to its apoptosis-inducing receptors DR5 and/or DR4. However, exogenous TRAIL (200 ng/ml) does not induce apoptosis in uninfected HEK293 cells since these cells do not express sufficient cell surface DR4 or DR5. To induce apoptosis, reovirus must therefore up-regulate both TRAIL and a death-associated TRAIL receptor. We therefore determined that there is both an increase in the release of TRAIL and an increase in the expression of DR5, and to a lesser extent DR4, in reovirus-infected cells. It seems unlikely that the up-regulation of both DR4 and DR5 is required for TRAIL-mediated expression in reovirus-infected cells. The quicker and more dramatic increase in DR5 expression compared to DR4 expression suggests that DR5 is the major receptor involved in triggering apoptosis. Furthermore, the increased sensitivity of reovirus-infected HEK293 cells to TRAIL-induced apoptosis is detectable 12 h following infection, whereas the alteration in expression of DR4 does not occur until 24 h postinfection. These results suggest that the contribution of DR4 to reovirus-induced apoptosis may be a secondary event and that its up-regulation in reovirus-infected cells may function to amplify the effects of TRAIL/DR5 regulation.

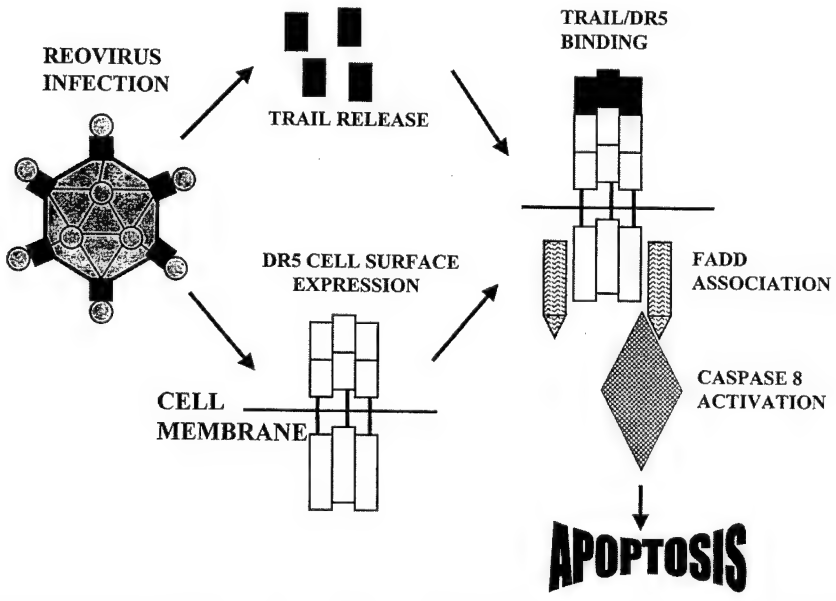

FIG. 6. Reovirus induces the TRAIL apoptotic pathway in infected cells by inducing the release of TRAIL and the up-regulation of DR5. The consequent binding of TRAIL to DR5 then promotes FADD association and the activation of caspase 8.

We propose a model in which reovirus infection results in the up-regulation of DR5 and the release of TRAIL, thereby activating the TRAIL pathway of cell death (Fig. 6). Similar to other DR-mediated apoptotic pathways, reovirus-induced apoptosis requires the participation of an adapter molecule (FADD) and the activation of the caspase cascade since it is reduced in the presence of inhibitors of FADD or caspase 8 activity. We have recently shown that reovirus-induced apoptosis requires the transcription factor NF-κB (3). Future studies will be directed at examining the role of NF-κB in the up-regulation of TRAIL and DR5 in reovirus-infected cells.

Our results demonstrate the involvement of the TRAIL apoptotic pathway in reovirus-induced cell death and provide the first direct evidence for the involvement of this pathway in virus-induced apoptosis. Additional support for the potential role of DR4 and DR5 in virus-induced apoptosis comes from studies suggesting that human immunodeficiency virus (HIV) infection increases the expression of TRAIL and sensitizes T cells to TRAIL-mediated apoptosis (10). Previous studies have suggested that other members of the TNFR DR superfamily may also be involved in apoptosis induced in cells infected with a variety of viruses. Alteration of the cell surface expression of Fas may be involved in virus-induced, or viral regulation of, apoptosis in cells infected with influenza virus (21, 22), herpes simplex virus type 2 (19), bovine herpesvirus 4 (30), adenovirus (24), and HIV type 1 (2, 11). Similarly, apoptosis induced by hepatitis B virus (20), HIV type 1 (8), bovine herpesvirus 4 (30), and parvovirus H-1 (14) may involve the TNFR signaling pathway. TRAIL and TRAIL receptor expression have been shown to mediate gamma interferon-induced antiviral activity (18), although the mechanism by which this occurs is unknown.

We propose that the regulation of TRAIL and its death-promoting receptors is a primary mediator of apoptosis that is induced not only following viral infection but also as a component of apoptosis-inducing stress responses, including chemotherapy (7).

ACKNOWLEDGMENTS

This work was supported by Public Health Service grants 1RO1AG14071 and GM30324 from the National Institutes of Health, Merit and REAP grants from the Department of Veterans Affairs, and U.S. Army Medical Research and Material Command grant USAMRMC98293015 (K.L.T.) S.G. is a Leukemia Society fellow. The University of Colorado Cancer Center provided core tissue culture and media facilities.

We thank Terrence S. Dermody and Jodi L. Connelly for helpful advice during the development of this project.

REFERENCES

1. **Ashkenazi, A., and V. M. Dixit.** 1998. Death receptors: signaling and modulation. Science **281:**1305–1308.
2. **Conaldi, P. G., L. Biancone, A. Bottelli, A. Wade-Evans, L. C. Racusen, M. Boccellino, V. Orlandi, C. Serra, G. Camussi, and A. Toniolo.** 1998. HIV-1 kills renal tubular epithelial cells in vitro by triggering an apoptotic pathway involving caspase activation and Fas up regulation. J. Clin. Investig. **102:** 2041–2049.
3. **Connolly, J. L., S. E. Rodgers, P. Clarke, D. W. Ballard, L. D. Kerr, K. L. Tyler, and T. S. Dermody.** 2000. Reovirus-induced apoptosis requires activation of transcription factor NF-κB. J. Virol. **74:**2981–2989.
4. **Debiasi, R. L., M. K. T. Squier, B. Pike, M. Wynes, T. S. Dermody, J. J. Cohen, and K. L. Tyler.** 1999. Reovirus-induced apoptosis is preceded by increased cellular calpain activity and is blocked by calpain inhibitors. J. Virol. **73:**695–701.
5. **Duke, R. C., and J. J. Cohen.** 1992. Morphological and biochemical assays of apoptosis, p. 3.17.1–3.17.16. *In* J. E. Coligan et al. (ed.), Current protocols in immunology. John Wiley & Sons, New York, N.Y.
6. **French, L. E., and J. Tschopp.** 1999. The TRAIL to selective tumor death. Nat. Med. **5:**146–147.
7. **Gibson, S. B., R. Oyer, A. C. Spalding, S. M. Anderson, and G. L. Johnson.** 2000. Increased expression of death receptors 4 and 5 synergizes the apoptosis response to combined treatment with etopiside and TRAIL. Mol. Cell. Biol. **20:**205–212.
8. **Herbein, G., U. Mahlknecht, F. Batliwalla, P. Gregerson, T. Pappas, J. Butler, W. A. O'Brian, and E. Verdin.** 1999. Apoptosis of CD8+ T cells is mediated by macrophages through interaction of gp120 with chemokine receptor CXCR4. Nature **395:**189–194.
9. **Hu, S., C. Vincenz, M. Buller, and V. M. Dixit.** 1997. A novel family member of viral death effector domain-containing molecules that inhibit both CD-95- and tumor necrosis factor receptor-1-induced apoptosis. J. Biol. Chem. **272:** 9621–9624.
10. **Jeremias, I., I. Herr, T. Boehler, and K.-M. Debatin.** 1998. TRAIL/Apo-2-ligand-induced apoptosis in human T cells. Eur. J. Immunol. **28:**143–152.
11. **Kaplan, D., and S. Sieg.** 1998. Role of the Fas/Fas ligand apoptotic pathway in human immunodeficiency virus type 1 disease. J. Virol. **72:**6279–6282.
12. **Oberhaus, S. M., R. L. Smith, G. H. Clayton, T. S. Dermody, and K. L. Tyler.** 1997. Reovirus infection and tissue injury in mouse central nervous system are associated with apoptosis. J. Virol. **71:**2100–2106.
13. **Oberhaus, S. M., T. S. Dermody, and K. L. Tyler.** 1998. Apoptosis and the cytopathic effects of reovirus. Curr. Top. Microbiol. Immunol. **233:**23–49.
14. **Rayet, B., J.-A. Lopez-Guerrero, J. Rommelaere, and C. Dinsart.** 1998. Induction of programmed cell death by parvovirus H-1 in U937 cells: connection with the tumor necrosis factor alpha-signaling pathway. J. Virol. **72:**8893–8903.
15. **Rodgers, S. E., E. S. Barton, S. M. Oberhaus, B. Pike, C. A. Gibson, K. L. Tyler, and T. S. Dermody.** 1997. Reovirus-induced apoptosis of MDCK cells is not linked to viral yield and is blocked by Bcl-2. J. Virol. **71:**2540–2546.
16. **Salvesen, G., and V. M. Dixit.** 1997. Caspases: intracellular signaling by proteolysis. Cell **91:**443–446.
17. **Schneider, P., J. L. Bodmer, M. Thome, K. Hofmann, T. Kataoka, N. Holler, and J. Tschopp.** 1997. Characterization of two receptors for TRAIL. FEBS Lett. **416:**329–334.
18. **Sedger, L. M., D. M. Shows, R. A. Blanton, J. J. Peschon, R. G. Goodwin, D. Cosman, and S. R. Wiley.** 1999. IFN-γ mediates a novel antiviral activity through dynamic expression of TRAIL and TRAIL receptor expression. J. Immunol. **163:**920–926.
19. **Sieg, S., Z. Yildirim, D. Smith, N. Kayagaki, H. Yagita, Y. Huang, and D. Kaplan.** 1996. Herpes simplex virus type 2 inhibition of Fas ligand expression. J. Virol. **70:**8747–8751.
20. **Su, F., and R. J. Schneider.** 1997. Hepatitis B virus HBx protein sensitizes cells to apoptotic killing by tumor necrosis factor α. Proc. Natl. Acad. Sci. USA **94:**8744–8749.
21. **Takizawa, T., S. Matsukawa, Y. Higuchi, S. Nakamura, Y. Nakanishi, and R. Fukuda.** 1993. Induction of programmed cell death (apoptosis) by influenza virus infection in tissue culture cells. J. Gen. Virol. **74:**2347–2355.
22. **Takizawa, T., R. Fukuda, T. Miyawaki, K. Ohashi, and Y. Nakanishi.** 1995. Activation of the apoptotic Fas antigen-encoding gene upon influenza virus infection involving spontaneously produced beta-interferon. Virology **209:** 288–296.
23. **Thornberry, N. A., and Y. Lazebnik.** 1998. Caspases: enemies within. Science **281:**1312–1316.
24. **Tollefson, A. E., T. W. Hermiston, D. L. Lichtenstein, C. F. Colle, R. A. Tripp, T. Dimitrov, K. Toth, C. E. Wells, P. C. Doherty, and W. S. Wold.** 1998. Forced degradation of Fas inhibits apoptosis in adenovirus-infected cells. Nature **392:**726–730.
25. **Tyler, K. L., R. T. Bronson, K. B. Byers, and B. N. Fields.** 1985. Molecular basis of viral neurotropism: experimental reovirus infection. Neurology **35:** 88–92.
26. **Tyler, K. L., M. K. T. Squier, S. E. Rodgers, B. E. Schneider, S. M. Oberhaus, T. A. Grdina, J. J. Cohen, and T. S. Dermody.** 1995. Differences in the capacity of reovirus strains to induce apoptosis are determined by the viral attachment protein sigma 1. J. Virol. **69:**6972–6979.
27. **Tyler, K. L., M. K. T. Squier, A. L. Brown, B. Pike, D. Willis, S. M. Oberhaus, T. S. Dermody, and J. J. Cohen.** 1996. Linkage between reovirus-induced apoptosis and inhibition of cellular DNA synthesis: role of the S1 and M2 genes. J. Virol. **70:**7984–7991.
28. **Wajant, H., F. J. Johannes, E. Haas, K. Siemienski, R. Schwenzer, G. Schubert, T. Weiss, M. Grell, and P. Scheurich.** 1998. Dominant-negative FADD inhibits TNFR60-, Fas/Apo-1- and TRAIL-R/Apo2-mediated cell death but not gene induction. Curr. Biol. **8:**113–116.
29. **Walczak, H., M. A. Degli-Esposti, R. S. Johnson, P. J. Smolak, J. Y. Waugh, N. Boiani, M. S. Timour, M. J. Gerhart, K. A. Schooley, C. A. Smith, R. G. Goodwin, and C. T. Rauch.** 1997. TRAIL-R2: a novel apoptosis-mediating receptor for TRAIL. EMBO J. **16:**5386–5397.
30. **Wang, G. H., J. Bertin, Y. Wang, D. A. Martin, J. Wang, K. J. Tomaselli, R. C. Armstrong, and J. I. Cohen.** 1997. Bovine herpesvirus 4 BORFE2 protein inhibits Fas- and tumor necrosis factor receptor 1-induced apoptosis and contains death effector domains shared with other gamma-2-herpesviruses. J. Virol. **71:**8928–8932.
31. **Zhang, J., D. Cado, A. Chen, N. H. Kabra, and A. Winoto.** 1998. Fas-mediated apoptosis and activation-induced T-cell proliferation are defective in mice lacking FADD/Mort1. Nature **392:**296–299.

REV.
Journal of Virology (In Press), 2000 JVI961-00

Calpain Inhibition Protects Against Virus-Induced Apoptotic Myocardial Injury

Roberta L DeBiasi [1,2,7], Charles L. Edelstein[3], Barbara Sherry[4], and Kenneth L. Tyler [2,3,5,6,7*]

Departments of Pediatric Infectious Diseases[1], Neurology[2], Medicine[3], Microbiology[5], and Immunology[6], University of Colorado Health Sciences Center, and Denver Veterans Affairs Medical Center[7], Denver, Colorado 80262, and Department of Microbiology[4], College of Veterinary Medicine, North Carolina State University, Raleigh NC 27606

*Corresponding author. Mailing address: Department of Neurology (B-182), University of Colorado Health Sciences Center, 4200 E. 9th Ave., Denver, CO 80262. Phone (303) 393-2874. Fax: (303) 393-4686. E-mail: Ken.Tyler@UCHSC.edu

ABSTRACT

Viral myocarditis is an important cause of human morbidity and mortality for which reliable and effective therapy is lacking. Using reovirus strain 8B infection of neonatal mice, a well characterized experimental model of direct virus-induced myocarditis, we now demonstrate that myocardial injury results from apoptosis. Proteases play a critical role as effectors of apoptosis. The activity of the cysteine protease calpain increases in reovirus-infected myocardiocytes, and can be inhibited by the dipeptide alpha-ketoamide calpain inhibitor CX295. Treatment of reovirus-infected neonatal mice with CX295 protects them against reovirus myocarditis as documented by: (1) a dramatic reduction in histopathologic evidence of myocardial injury, (2) complete inhibition of apoptotic myocardial cell death as identified by TUNEL staining, (3) reduction in serum creatine phosphokinase, and (4) improved weight gain. These findings are the first evidence for the importance of a calpain-associated pathway of apoptotic cell death in viral disease. Inhibition of apoptotic signaling pathways may be an effective strategy for the treatment of viral disease in general and viral myocarditis in particular.

INTRODUCTION

The mechanisms by which viruses produce cytopathic effects in their host cells are not well understood. Such knowledge is essential to an understanding of viral pathogenesis and development of novel antiviral therapies. Apoptosis is a mechanism of active cell death distinct from necrosis, characterized by DNA fragmentation, cell shrinkage, and membrane blebbing without rupture (27). Apoptosis plays a critical role in many physiologic (29, 75), as well as infectious and non-infectious pathologic conditions (73). Viruses may either promote or inhibit apoptosis as strategies to maximize pathogenicity in their hosts (39, 55, 68). Several viruses, including adenovirus, poxviruses, herpes viruses, and HPV proliferate and evade host immune responses by interfering with programmed cell death (1, 20, 32, 69). Many other viruses, such as HIV, HTLV, influenza, measles, rubella, poliovirus, HHV-6. Sindbis virus and reoviruses, cause cytopathic effect by induction of apoptosis in their target cells (11, 15, 22-24, 35, 41, 43, 51, 71).

We have used reovirus-induced apoptosis as an experimental model system to study the viral and cellular mechanisms involved in apoptotic cell death (41). Reoviruses are non-enveloped viruses that contain a genome of segmented, double stranded RNA. Infection of cultured fibroblasts and epithelial cells with reoviruses induces apoptosis. Reoviral strains differ in the efficiency with which they induce this cellular response, and these differences are determined by the viral S1 gene (45, 70). Apoptosis also occurs following reovirus infection *in vivo* and colocalizes with areas of pathologic injury (40,41). This suggests that apoptosis is an important mechanism of tissue damage in reoviral infection.

Reovirus strain 8B is a reassortant reovirus that efficiently produces myocarditis in infected neonatal mice (56, 59). Damage has been shown to be a direct effect of viral infection of myocardiocytes (61). This differs from several other models of viral myocarditis (such as coxsackievirus and murine CMV), in which secondary inflammatory responses, or lymphocyte recognition of viral or self antigens on myocardial cells may be the predominant cause of cardiac damage (12, 18, 21, 31, 47). SCID mice infected with reovirus 8B develop myocarditis and passive transfer of reovirus-specific immune cells is protective, rather than harmful, to 8B-infected mice (59, 61). This indicates that immune mechanisms

contribute to amelioration rather than induction of reovirus-induced viral injury (61). However, the mechanism by which direct myocardial injury occurs is not well characterized. Since tissue damage occurs by apoptosis in other *in vivo* models of reoviral infection (40), and apoptosis has been suggested in some models of viral myocarditis (6, 26), we wished to determine if reoviral myocarditis occurs as a result of apoptotic cell injury, and if so, whether manipulation of known signaling pathways preceding apoptosis would be protective.

Protease cascades appear to play critical roles as effectors of apoptosis, including the cysteine proteases, caspases and calpain (10, 33, 42, 63, 80). Caspases are the most extensively investigated members of this class of protease and have been implicated in a wide variety of apoptotic models. However, the role of calpain in apoptosis has been recognized more recently. Calpain is a calcium-dependent neutral cysteine protease that is ubiquitous throughout the cytosols of many cell types (36, 64). Calpains have recently been implicated in several models of apoptosis, including dexamethasone-induced thymocyte apoptosis (66), neuronal cell apoptosis (37), neutrophil apoptosis (65), ischemia-induced rat liver apoptosis (28, 62), myonuclear apoptosis in limb-girdle dystropy (3) and chemical hypoxia-induced apoptosis of rat myocytes (8). We have recently shown that reovirus-induced apoptosis *in vitro* is preceded by increased cellular calpain activity and is inhibited by two classes of calpain inhibitors (14).

We now show that reovirus 8B-induced myocarditis occurs by apoptosis. Calpain activity increases in cardiomyocytes following infection with reovirus 8B and calpain inhibition reduces myocardial injury and morbidity in infected mice. This is evidence that interference with apoptotic signaling pathways may prove of benefit as a therapeutic strategy in the treatment of viral infection in general and viral myocarditis in particular.

MATERIALS AND METHODS

VIRUS: Reovirus 8B is an efficiently myocarditic reovirus that has been previously characterized (59). 8B stocks were triply plaqued, and passaged twice in mouse L cells prior to use.

MICE: Swiss-Webster (Taconic) mouse litters were housed in individual filter-topped cages in an AALAC accredited animal facility. All animal procedures were performed under protocols approved by the appropriate institutional committees.

MOUSE INOCULATIONS: 2 day-old Swiss-Webster (Taconic) mice were intramuscularly inoculated with 1000 pfu 8B reovirus in the left hindlimb (20 μl volume). Mock-infected mice received gel saline vehicle inoculation (equal volume) (137 mM NaCl, 0.2 mM $CaCl_2$, 0.8 mM $MgCl_2$, 19 mM H_3BO_3, 0.1 mM $Na_2B_4O_7$, 0.3% gelatin).

HISTOLOGIC ANALYSIS: At 7 days post-infection, mice were sacrificed and hearts were immediately immersed in 10% buffered formalin solution. After mounting as transverse sections, hearts were embedded in paraffin and section to 6 μm thickness. For quantification of degree of myocardial injury, hematoxylin- and eosin-stained midcardiac sections (at least 6 per heart) were examined at 125X magnification by light microscopy and scored blindly. Scoring was performed using a previously validated system (59) with scores ranging from 0-4 (0 = no lesions, 1 = one or a few small lesions, 2 = many small or a few large lesions, 3 = multiple small and large lesions, and 4 = massive lesions). 23-24 mice were scored from each group.

DNA FRAGMENTATION: The presence of internucleosomal DNA cleavage in myocardial tissue was investigated by phenol/choloroform extraction of DNA from 8B-infected and mock-infected hearts and precipitation in 95% ETOH. The DNA was then end-labeled with 5 micro-Ci 32P-dGTP using 10 units terminal transferase (#M187, Promega Corporation), resolved by electrophoresis on a 2% agarose gel, fixed in 5% acetic acid/5%methanol, dried, and scanned on a Packard Instant Imager (Packard Instrument Company).

TUNEL STAIN (Terminal deoxynucleotidyl transferase-mediated dUTP nick-end labeling): Evaluation of fragmented DNA was performed by TUNEL, as previously described (40). Paraffin-embedded cardiac midsections were prepared by removing paraffin with xylene, then rehydrating in 100%, 95%, then 70% ethanol solutions. After digestion in proteinase K solution (Boehringer-Mannheim) for 30 minutes at 37°C, slides were pretreated in 0.3% H_2O_2 in PBS for 15 minutes at room temperature and then washed. The terminal deoxynucleotidyl transferase (TdT) labeling reaction was carried out under sialanized cover slips in a humidified chamber for 1 hour at 37° C with TdT and digoxigenen 11-dUTP. (Boehringer-Mannheim). The reaction was stopped with SSC buffer (NaCl, sodium citrate). After blocking in 2% BSA for 10 minutes, sections were probed with Vectastain ABC (avidin DH and biotinylated enzyme, Vector Labs) for one hour at room temperature, then visualized with diaminobenzadine (DAB) peroxidase substrate kit (Vector Labs). Negative and positive controls were used with all reactions.

VIRAL ANTIGEN STAIN: Cardiac midsections were prepared as noted above. Following the hydrogen peroxide incubation, slides were blocked in 2% normal goat serum for 30 minutes at room temperature. Sections were then incubated in rabbit polycolonal anti-Reovirus Type3 Dearing antisera as primary antibody (gift of Terence Dermody, Vanderbilt University) at 1:1000 for 1 hour at 37°C. Biotinylated-goat anti-rabbit antibody was used as the secondary antiserum (1:200 dilution in 2% normal goat serum) for 30 minutes at 37°C. Sections were probed and visualized as noted above.

CALPAIN ACTIVITY IN MYOCYTES: The presence of calpain-specific spectrin (fodrin) breakdown products (150/145 kD doublet) by immunoblot was used as an assay of calpain activity (37). Mouse primary cardiac myocyte cultures were prepared as previously described (5). Cells were plated at 1.6 X 10^6 cells/well in 24 well plates and incubated for 48 hours. Cells were then infected with reovirus strain 8B (MOI 20, in DMEM) or mock-infected (DMEM), then incubated at 37°C. Mock-infected cells were harvested at 48 hours. 8B-infected cells were harvested at 24, 48 and 72 hours post-infection. Cell lysates were prepared by sonication in lysis buffer (15mM Tris pH 7.4, 10mM EDTA, 0.1% NP40, 20% glycerol, 50 mM B-mercaptoethanol, 50 μg/ml pepstatin, 100 μg/ml leupeptin, 1 mM PMSF) and the cytoplasmic fractions were run on a 7.5% polyacrylamide gel. Protein loading for these gels (25 μg/well) was normalized by protein concentration analysis of cell lysates. Following transfer (15 volts overnight),

the nitrocellulose membrane was blocked in 5% non-fat dried milk/TNS for 2 hours, then probed with anti-fodrin mouse monoclonal antibody (ICN) at 1:1000 for 1.5 hours, and then washed. Membranes were then incubated in anti-mouse IgG, horseradish peroxidase-linked whole antibody (Amersham) at 1:1000, as secondary antibody. After washing, ECL Plus was used for detection (Amersham).

In additional experiments, primary cardiac myocytes were infected with 8B reovirus (using the method described above) with and without pretreatment in CX295 (100 uM). Cell lysates were prepared and analyzed for calpain activity by immunoblot as described above.

SPECIFICITY OF CALPAIN INHBITOR CX295: Z-leu-aminobutyric acid-CONH(CH2)3-morpholine (CX295) is a dipeptide alpha-ketoamide compound which inhibits calpain at the active site (kindly provided by Dr. Gary Rogers at Cortex Pharmaceuticals, Inc.). To determine the efficacy of CX295 as a calpain inhibitor, 10 ug purified μ - calpain (Porcine RBC, Calbiochem) was added to the preferred fluorogenic calpain substrate SLY-AMC (Suc-Leu-Tyr-amino-methyl-coumarin) in the presence and absence of CX295 (100 μM), as well as in the presence of the pan-caspase inhibitor Z-D-DCB (100 μM). Calpain assay was performed as previously described (17). Proteolytic hydrolysis of the substrate by purified calpain liberates the highly fluorescent AMC moiety. Fluorescence at 380 nm excitation and 460 nm emission was quantified with a Hitachi F2000 spectrophotometer. An AMC standard curve was determined for each experiment. Calpain activity was expressed in pmol AMC released per minute of incubation time per μg of purified calpain.

To determine the specificity of CX295 as a calpain inhibitor, 10 ng purified caspase 3 (Upstate) was added to the preferred fluorogenic caspase-3 substrate DEVD-AMC in the presence and absence of the pan-caspase inhibitor z-D-DCB (100 μM), as well as CX295 (100 μM). In addition, 57 ng purified caspase-1 (provided by Nancy Thornberry, Merck) was added to the preferred fluorogenic caspase-1 substrate YVAD-AMC in the presence and absence of z-D-DCB, as well as CX295. Caspase activity assay was performed as previously described (17). Caspase activity was expressed as pmol AMC released per minute of incubation time per ng of purified caspase. Experiments were all performed in triplicate.

CALPAIN INHIBITION *IN VIVO*: For calpain inhibition experiments, animals received daily intraperitoneal injections of either active CX295 (70mg/kg in a 50 μL volume) or its inactive saline diluent.

The first dose was given 30 minutes prior to infection with 8B virus. A total of 6 doses were given, at 24 hour intervals. Mice were sacrificed at 7 days post-infection.

VIRAL TITER DETERMINATION: Injected hind limbs and whole hearts were placed in 1 ml gel saline and immediately frozen at –70C. After three freeze (-70° C) thaw (37° C) cycles, the tissues were sonicated approximately 15-30 seconds by using a microtip probe (Heat Systems Model XL2020) until a homogenous solution was obtained. The virus suspensions were serially diluted in 10-fold steps in gel saline and placed in duplicate on L-cell monolayers for plaque assay, as previously described (14). Virus titers were expressed as $\log_{10}$ pfu per ml.

SERUM CREATINE-PHOSPHOKINASE: Following decapitation, whole blood was collected from individual mice into plasma separator tubes with lithium heparin to prevent coagulation (Microtainer, Becton Dickinson). Samples were collected from 8B-infected mice treated with CX295 (N=20), 8B-infected mice treated with the inactive diluent (N= 20), and uninfected age-matched controls (N=9). Serum creatine phosphokinase measurements were performed by the University of Colorado Health Sciences Center Clinical Laboratory and were expressed as U/L.

GROWTH: Mice were infected with 10 pfu 8B reovirus. Infected, drug treated (N=15) and infected, control (N= 15) mice were weighed daily on days 0-14 post-infection. Additional experiments using a higher dose of virus (1000 pfu) were also completed, with daily weighing on days 0-7 post-infection. In these experiments, weights were also compared to normal age-matched uninfected mice.

STATISTICS: The results of all experiments are reported as means ± SEM. Means were compared using parametric two-tailed t-tests (Graph Pad, Prism) and differences were considered significant if p values were < 0.05.

RESULTS

A. Reovirus 8B induces myocardial injury by apoptosis

Mice were inoculated intramuscularly into the hindlimb with either 1000 pfu of strain 8B reovirus or gel saline (mock-infection). At 7 days post-infection, mice were sacrificed and transverse cardiac sections prepared for histologic evaluation. In the 8B-infected hearts, there was marked myocardial disruption and diffuse edema (Figure 1b). Numerous pyknotic nuclei and apoptotic bodies were present (Figures 1b and 4e). Despite the degree of myocardial injury, only rare mononuclear cells (predominantly macrophages) and neutrophils were present. Myocardial disruption and edema were not seen in mock-infected hearts (Figure 1a). Extensive areas of apoptotic TUNEL-positive nuclei were noted in the 8B-infected hearts (Figure 1d), which correlated with the areas of histologic abnormality described above. Mock-infected hearts were TUNEL-negative (Figure 1c). Large regions of reovirus antigen-positive tissue were noted in the 8B-infected hearts (Figure 1f), and occurred in the same distribution as the areas of histologic injury and TUNEL-positive staining cells.

In order to provide further confirmation that the morphological changes seen in virus-infected hearts were indeed due to apoptosis, DNA was extracted from 8B-infected and mock-infected hearts, end-labeled, and analyzed by agarose gel electrophoreses. DNA from infected hearts, but not mock-infected controls, showed fragmentation into oligonucleosomal length ladders, characteristic of apoptosis (Figure 2). Taken together, these findings indicate that reovirus-induced myocardial injury is due to apoptosis.

B. Calpain is activated in 8B infected murine cardiac myocytes

We have previously shown that reovirus infection in L929 cells results in increased calpain activity, which precedes apoptosis (14). We wished to determine whether calpain activity was also increased in myocardial cells following reovirus infection. Proteolysis of spectrin (fodrin), a preferred calpain substrate, was examined as an indication of calpain activation. Intact spectrin (280 kD) is degraded by calpain resulting in a characteristic spectrin breakdown product doublet seen at 150/145 kD. Mouse primary cardiac myocyte cultures were infected with reovirus strain 8B (MOI 20) or mock-infected. Lysates were prepared after harvesting cells at 24, 48 and 72 hours post-infection. Western Blot analysis of these cytoplasmic fractions revealed increased calpain activity following 8B-infection compared to mock-

infection. This increase was first detectable at 24 hours, reached maximal intensity by 48 hours, and was still present at 72 hours post-infection (Figure 3a). Densitometric analysis of calpain specific breakdown products revealed a peak four-fold increase in calpain activity following virus infection (Figure3b). Caspase degradation of spectrin results in breakdown products at 120 kD, which were not observed in this experiment. This data demonstrates that an increase in calpain activity occurs following infection of myocardiocytes with reovirus strain 8B, in a time course that parallels the onset of apoptosis.

C. CX295 is an effective calpain inhibitor and does not appreciably inhibit caspases

Based on our findings that (1) 8B-induced myocarditis is due to apoptosis, (2) calpain is activated in 8B-infected myocardiocytes, and (3) inhibition of calpain activation inhibits reovirus-induced apotosis *in vitro*, we wished to determine if calpain inhibition could prevent 8B-induced myocardial injury *in vivo*. CX295 is a dipeptide alpha-ketoamide compound that inhibits calpain at the active site and is non-toxic and effective *in vivo* (4, 49). To confirm the specificity of the compound, the activity of purified calpain was monitored in the presence and absence of CX295. The inactive diluent of CX295 and the pan-caspase inhibitor Z-D-DCB were used as controls. Purified calpain activity (measured as cleavage of SLY-AMC) was markedly reduced by CX295 (Figure 4a). Calpain activity was decreased from 1255 ± 22 pmol/min/ug to 206 ± 4 pmol/min/ug in the presence of CX295; $p<0.0001$. Neither the diluent or z-D-DCB controls had appreciable effect on calpain activity.

To further confirm that CX295 is a specific calpain inhibitor and does not inhibit caspases, the activity of purified caspase-1 and caspase-3 was monitored in the presence and absence of CX295, as well as in the presence of the known pan-caspase inhibitor Z-D-DCB (positive control). CX295 had minimal inhibitory effect on either caspase-1 or caspase- 3 activity (measured as cleavage of YVAD-AMC and DEVD-AMC, respectively), whereas z-D-DCB inhibited both caspases nearly completely (Figures 4b and 4c). Purified caspase 1 activity decreased from 6829 ± 39 pmol/min/ng to 6496 ± 36 pmol/min/ng in the presence of CX295, compared to 0 pmol/min/ng in the presence of z-D-DCB. Purified caspase-3 activity decreased from 1752 ± 6 pmol/min/ng to 1533 ± 9 pmol/min/ng in the presence of CX95, compared to 118 ± 4 pmol/min/ng in the presence of z-D-DCB.

CX295 also effectively inhibited calpain activity in primary cardiomyocyte culture . Calpain activity was quantified by immunoblot in reovirus-infected myocytes, in the presence and absence of CX295.

Calpain activity (measured by densitometric analysis of 150/145 calpain-specific fodrin breakdown product) increased by 2.4 fold in 8B-infected compared to mock-infected cardiomyocytes.. Calpain activity was significantly reduced in CX295-treated, 8B-infected cells compared to infected, untreated cells ($p= 0.04$) (Figure 4d and 4e).

These experiments confirm that CX295 is both an effective and specific calpain inhibitor.

D. Calpain inhibitor CX295 inhibits 8B-induced myocardial injury

2 day-old Swiss-Webster mice were infected with 1000 pfu 8B virus and received six daily intraperitoneal injections of either active CX295 (70 mg/kg) or its inactive saline diluent as a control (see methods). Mice were sacrificed on day 7 post-infection and myocardial sections were prepared.

Transverse cardiac sections from 8B- infected mice treated with CX295 or its inactive diluent (control) were stained with hematoxylin- and eosin and viewed by light microscopy (Figures 5a-5f). Cardiac tissue from control mice (Figure 5a) showed extensive focal areas of myocardial damage, which were absent in the CX295-treated animals, despite identical viral infection (Figure 5b). Marked disruption of the normal myocardial architecture was evident in hearts of control mice (Figure 5c), compared to drug-treated animals (Figure 5d). Nuclei with apoptotic morphology were easily seen within these areas in the control mice (Figure 5e), including cells with condensed and pyknotic nuclei, as well as apoptotic bodies. These findings were absent in the drug-treated animals (Figure 5f). TUNEL staining of comparable sections from drug treated and diluent-treated (control) infected mice were compared. TUNEL positive staining nuclei were virtually absent in the drug-treated mice (Figure 5h), compared to control infected animals (Figure 5g).

For quantification of the degree of myocardial injury, hematoxylin- and eosin-stained midcardiac sections (at least 6 sections per heart) were scored using a previously validated scoring system (59). 20 infected, CX295 treated animals and 23 control (infected, diluent-treated) mice were evaluated. There was a highly significant reduction in myocardial injury score in animals treated with CX295. The mean score for control animals was 3.0 ± 0.1 (range 2-4), compared to 0.6 ± 0.1 (range 0-1.5) for CX295-treated animals, $p < 0.0001$ (Figure 6).

Creatine Phosphokinase (CPK) is an intracellular enzyme present in cardiac and skeletal muscle that is released upon tissue injury. It can be measured in the serum and used as a quantitative marker of

skeletal and cardiac muscle damage (2). Blood was collected from infected mice treated with CX295 and inactive diluent-treated controls at 7 days post-infection, as well as uninfected age-matched mice. Serum CPK values were significantly elevated in 8B-inoculated mice compared to uninfected mice, indicative of 8B-induced muscle injury. There was a statistically significant reduction in serum CPK level toward normal in CX295-treated mice compared to control mice (Figure 7). Uninfected age-matched mice had a mean CPK of 4521 ± 431 U/L. 8B-infected mice had a mean CPK of 5658 ± 359 U/L, representing an increase of 1137 U/L above normal. Treatment of infected animals with CX295 reduced the mean CPK to 4634 ± 350 U/L, not significantly elevated compared to normals, but significantly reduced compared to infected, non-treated animals ($p < 0.05$).

To determine if reductions in myocardial injury were also associated with reduction in viral titer at primary (hind limb) and secondary (heart) sites of replication, tissues were titered for virus by plaque assay of tissue homogenates. There was a 0.5 $\log_{10}$ reduction in hindlimb viral titer of CX295 -treated animals compared to controls (7.2 ± 0.1 $\log_{10}$ pfu/ml to 6.7 ± 0.2 $\log_{10}$ pfu/ml; p=0.003). Hearts of CX295-treated animals had a 0.7 log reduction in viral titer (6.1 ± 0.2 log10 pfu/ml to 5.4 ± 0.2 log10 pfu/ml; $p< 0.01$) (Figure 8). Although these decrements were statistically significant, they were modest in degree, and substantial viral replication occurred in both the drug treated and control animals (1000-10000 fold).

We wished to determine whether the reduction in myocardial damage caused by CX295 treatment reduced morbidity in mice. We therefore measured growth (weight gain) in infected, drug-treated mice compared to infected, untreated controls. CX295-treated mice had improved growth compared to control mice (4.6 ± 0.4 grams versus 3.6 ± 0.1 grams at 7 days post-infection; $p = 0.008$) and growth was not significantly different from that of uninfected age-matched animals (4.6 ± 0.4 grams versus 4.8 ± 0.1 grams; p= 0.6, NS) (Figure 9).

DISCUSSION

Viral myocarditis remains a serious disease without reliable or effective treatment. The events following viral attachment and replication in myocardial tissue that lead to myocarditis are not clearly understood. A variety of mechanisms from varying models have been suggested, including direct viral injury and persistence (9, 25), autoimmune phenomena (18, 46, 52), cytokine fluxes (19, 34, 53, 60), inflammation (30, 54) and apoptosis (12, 78, 79). A clearer understanding of pathogenic mechanisms is crucial for the development of effective therapeutic strategies, since currently employed antiviral agents have not made significant impact on outcomes from this clinical syndrome. Reoviral myocarditis is an ideal model with which to study these events, since myocardial injury is a direct effect of virus infection and does not involve immune-mediated effects.

Reovirus 8B induces myocarditis by apoptosis. Reovirus 8B induces myocarditis in mice by direct viral injury to myocytes and we now show that this occurs by induction of apoptosis. This is supported by the presence of distinctive morphologic criteria upon microscopic examination of infected heart tissues, TUNEL positive nuclei were found exclusively in regions of viral infection and myocardial injury. The presence of apoptosis was confirmed by the presence of the characteristic intranucleosomal cleavage pattern of extracted DNA. It has been shown previously that multiple viral genes (M1, L1 and L2, S1), encoding core and attachment proteins are determinants of reovirus-induced acute myocarditis (57). Interactions between these proteins determine myocarditic potential. Several of these genes have been associated with reovirus RNA synthesis and reovirus induction of and sensitivity to beta-interferon in cardiac myocyte cultures, which are determinants of reovirus myocarditic potential. In addition, the S1 gene, which codes for the viral attachment protein $\sigma 1$, is the primary determinant of apoptotic potential among strains of reovirus (70). It is most likely therefore, that the extent of reovirus-induced myocardial injury is determined by a combination of host responses, encompassing both the interferon and apoptosis pathways. Indeed, just as inhibition of the interferon pathway was sufficient to enhance reovirus-induced myocarditis (60), we show here that inhibition of the apoptotic pathway is sufficient to abrogate reovirus-induced myocarditis. Thus, apoptosis is an integral component of reovirus-induced myocardial injury.

Calpain activity is increased in reovirus-infected myocardiocytes and calpain inhibition is protective against reovirus-induced myocarditis. Calpain is a calcium-activated cysteine protease that has proven importance with regard to the initiation of apoptosis in the reoviral model, as well as several other unrelated models of apoptosis (see introduction). We first demonstrated that calpain activity is increased in cardiac myocytes *in vitro* following 8B infection, in a time course paralleling induction of apoptosis. We then demonstrated that calpain inhibition resulted in reduction of calpain activity in infected cells, and dramatic reductions in reovirus-induced injury, as well as apoptosis. Clinically significant reduction in myocardial injury was documented by reduced serum CPK levels and improved growth in treated mice.

It is likely that CX295 acted primarily by interfering with crucial signal transduction cascades involving calpain, required for induction of apoptotic cell death. Additionally, it is possible that CX295 provided some portion of its effect by inhibiting viral growth at either the primary (hindlimb) or secondary (heart) sites of replication, since viral titers were slightly lower in drug-treated animals compared to controls. Slight reductions in viral titer do not seem a likely explanation for the majority of drug effect, since in prior experiments involving reovirus-induced myocarditis, yield of virus at early and late times post-infection did not correlate with the degree of myocardial injury (58). In addition, efficiently myocarditic and poorly myocarditic reovirus strains replicate to similar titer in the heart; thus differences in myocarditic potential do not simply reflect viral growth in the heart (57).

One must be cautious in attributing a role for calpain in disease pathogenesis, based solely on data derived from calpain inhibition. Currently available calpain inhibitors suitable for *in vivo* use have weak, but measurable inhibitory activity against other cysteine proteases. However, the inhibitor employed in our experiments, CX295, is 500-900 fold more active against calpains than cathepsins (Ki for calpain = 0.027 – 0.042 uM, versus Ki for cathepsin B = 24 uM) and failed to inhibit caspase activity in *vitro*, as described in this paper. We believe that inhibition of calpain, rather than other cysteine proteases is the essential element of CX295's protective effect against 8B–induced myocardial apoptosis and injury.

It is not clear what constitutes the upstream and downstream components of a signaling cascade within which calpain might fit, either during reovirus infection or in other systems where calpain is involved. The mechanisms by which reovirus triggers increased cellular calpain activity are not known, but

could include initiation of calcium fluxes following viral attachment, as demonstrated with rotavirus, a closely related virus (16), upregulation of growth factors which facilitate calpain activation (38, 67), or upregulation of endogenous calpain activator proteins which have been characterized in several cell types (50). Calpain may play a physiologic role in the regulation of a variety of cellular transcription factors and cell-cycle regulating factors implicated in apoptosis, including Jun, Fos, p53, cyclin D and NF-κB (3, 7, 74). We have recently shown that activation of NF-κB is required for reovirus-induced apoptosis (13), suggesting the possibility that calpain inhibition may act to modulate NF-κB-induced signal transduction. Calpains may also modulate cell death by cleaving Bax, a pro-apoptotic protein located in the cytosol (76). In addition, the caspase and calpain proteolytic cascades may interact. Caspases may play in role in the regulation of calpain by cleavage of calpastatin, the endogenous inhibitor of calpain (44, 72, 77). Reflexively, calpain may be involved in the proteolytic activation of some caspases (48).

Potential therapeutic efficacy of calpain inhibitors. In conclusion, our data suggest that reoviral-induced myocarditis occurs by direct viral induction of apoptotic cell death, and that injury can be markedly reduced with the use of a calpain inhibitor. To our knowledge, this is the first successful demonstration of the use of calpain inhibition *in vivo* to ameliorate myocarditis in particular and viral-induced disease in general. However, future experiments are needed to determine whether calpain inhibition remains effective when administered after the onset of viral infection. Our results demonstrate the utility of apoptosis inhibition as a strategy for protection against viral infection.

ACKNOWLEDGEMENTS

We thank Gary Rogers of Cortex Pharmaceutical for providing calpain inhibitor CX295 and its inactive diluent. The University of Colorado Cancer Center provided core tissue culture and media facilities.

This work was supported by Public Health Service grant 1RO1AG14071 from the National Institute of Aging, Merit and REAP grants from the Department of Veterans Affairs, a US Army Medical Research and Material Command grant (USAMRMC 98293015) [KLT], a Young Investigator Award from the National Kidney Foundation [CLE], Public Health Service grant 1 R01HL57161 and North Carolina State University College of Veterinary Medicine Grant 204743 [BS].

REFERENCES

1. Aubert, M., and J.A. Blaho. 1999. The herpes simplex virus type 1 regulatory protein ICP27 is required for the prevention of apoptosis in human cells. *J. Virol.* 73:2803-2813.
2. Bachmeir, K., J. Mair, F. Offner, C. Pummerer, and N. Neu. 1995. Serum cardiac troponin T and creatine kinase-MB elevations in murine autoimmune myocarditis. *Circulation.* 92:1927-1932.
3. Baghdiguian, S., M. Martin, I. Richard, F. Pons, C. Astier, N. Bourg, R.T. Hay, R. Chemaly, G. Haleby, J. Loiselet, L.V. Anderson, A. Lopez de Muvigin, M. Fardeu, P. Mangeat, J.S. Beckmann, and G. Lefranc. 1999. Calpain 3 deficiency is associated with myonuclear apoptosis and profound perturbation of the IκBα/NF-KB pathway in limb-girdle muscular dystrophy type 2A. *Nature Medicine.* 5:503-511.
4. Bartus, R.T., K.L. Baker, A.D. Heiser, S.D. Sawyer, R.L. Dean, P. J. Elliott, and J.A. Straub. 1994. Postischemic administration of AK275, a calpain inhibitor, provides substantial protection against focal ischemic brain damage. *J. Cerebral Blood Flow and Metab.* 14:537-544.
5. Baty, C.J., and B. Sherry. 1993. Cytopathogenic effect in cardiac myocytes but not in cardiac fibroblasts is correlated with reovirus-induced myocarditis. *J. Virol.* 67:6295-6298.
6. Bowles, N.E., and J.A. Towbin. 1998. Molecular aspects of myocarditis. *Curr. Opin. Cardiol.* 13:179-184.
7. Chen, F.., Y. Lu, D.C. Kuhn, M. Maki, X. Shi, and L.M. Demers. 1997. Calpain contributes to silica-induced IKB- degradation and nuclear factor κB activation. *Arch. Biochem. Biophys.* 34:383-388.
8. Chen, S.J., M.E. Bradley, and T.C. Lee. 1998. Chemical hypoxia triggers apoptosis of cultured neonatal rat cardiac myocytes: Modulation by calcium-regulated proteases and protein kinases. *Mol. Cell. Biochem.* 178:141-149.
9. Chow, L.H., K.W. Beisel, and B.M. McManus. 1992. Enteroviral infection of mice with severe combined immunodeficiency. Evidence for direct viral pathogenesis of myocardial injury. *Lab. Invest.* 66:24-31.
10. Cohen, G.M. 1997. Caspases: the executioners of apoptosis. *Biochem. J.* 326:1-16.
11. Colamussi, M.L., M.R. White, E. Crouch, and K.L. Hartshorn. 1999. Influenza A virus accelerates neutrophil apoptosis and markedly potentiates apoptotic effects of bacteria. *Blood.* 93:2395-2403.

12. Colston, J.T., B. Chandrasakar, and G.L. Freeman. 1998. Expression of apoptosis-related proteins in experimental coxsackie myocarditis. *Cardovasc. Research.* 38:158-168.

13. Connolly, J.L., S.E. Rodgers, B. Pike, P. Clarke, K.L.Tyler and T.S. Dermody. 1998. Reovirus-induced apoptosis requires activation of transcription factor NF-κB. In *Abstracts of the 17th Annual meeting of the American Society for Virology*. 89:Abstract 17-2.

14. DeBiasi, R.L., M.K.T. Squier, B. Pike, M. Wynes, T.S. Dermody, and K.L. Tyler. 1999. Reovirus-induced apoptosis is preceded by increased cellular calpain activity and is blocked by calpain inhibitors. *J. Virol.* 73:695-701.

15. Dockrell, D.H., A.D. Badley, J.S. Villacian, C.J. Heppelman, A. Algeciras, S. Ziesvnar, H. Yagita, D.H. Lynch, P.C. Roche, P.J. Leibson, and C.V. Paya. 1998. The expression of Fas Ligand by macrophages and its upregulation by human immunodeficiency virus infection. *J. Clin. Invest.* 101:2394-2405.

16. Dong, Y., C.Q. Zeng, J.M. Ball, M.K. Estes, and A.P. Morris. 1997. The rotavirus enterotoxin NSP4 mobilizes calcium in human intestinal cells by stimulating phospholipase C-mediated inositol 1,4,5-triphosphate production. *Proc. Natl. Acad. Sci. USA.* 94:3960-3965.

17. Edelstein, C.L., H. Ling, P.E. Gengaro, R.A. Nemenoff, B.A. Bahr, and R.W. Schrier. 1997. Effect of glycine on prelethal and postlethal increases in calpain activity in rat renal proximal tubules. *Kidney International.* 52:1271-1278.

18. Fairweather, D., C.M. Lawson, A.J. Chapman, C.M. Brown, T.W. Booth, J. M. Papadimitriou, and G.R. Snellam. 1998. Wild isolates of murine cytomegalovirus induce myocarditis and antibodies that cross-react with virus and cardiac myosin. *Immunology.* 94:263-270.

19. Freeman, G.L., J.T.Colston, M. Zabalgoitia, and B. Chandrasekar. 1998. Contractile depression and expression of proinflammatory cytokines and iNOS in viral myocarditis. *Am. J. Physiol.* 274:H249-258.

20. Galvan, V., R. Brandimarti, and B. Roizman. 1999. Herpes simplex virus 1 blocks caspase-3-independent and caspase-dependent pathways to cell death. *J. Virol.* 73:3219-3226.

21. Gauntt, C.J. 1997. Roles of the humoral response in coxsackievirus B-induced disease. *Curr. Top. Microbiol. Immunol.* 223:259-282.

22. Girard, S., T. Couderc, J.D. Destombes, J. Thiesson, F. Delpeyroux, and B. Blondel. 1999. Poliovirus induces apoptosis in the mouse central nervous system. *J. Virol.* 73(7):6066-6072.

23. Ichimi, R.T., Jin-o, and M. Ito. 1999. Induction of apoptosis in cord blood lymphocytes by HHV-6. *J. Medical Virol.* 58:63-68

24. Jaworski, A., and S.M. Crowe. 1999. Does HIV cause depletion of CD4+ T cells in vivo by the induction of apoptosis? *Immunology and Cell Biology.* 77:90-98

25. Kanda, T., H. Koike, M. Arai, J.E. Wilson, C.M. Carthy, D. Yang, B.M. McManus, R. Nagai, and I. Kobayashi. 1999. Increased severity of viral myocarditis in mice lacking lymphocyte maturation. *International J. Cardiol.* 68:13-22.

26. Kawai, C. 1999. From myocarditis to cardiomyopathy: mechanisms of inflammation and cell death: learning from the past for the future. *Circulation.* 99:1091-1100

27. Kerr, J.F.R., A.H. Wylie, and A.R. Currie. 1972. Apoptosis: a basic biological phenomenon with wide-ranging implications in tissue kinetics. *Br. J. Cancer.* 26:239-257.

28. Kohli, V., J.F. Madden, R.C. Bentley, and P.A. Clavien. 1999. Calpain mediates ischemic injury of the liver through modulation of apoptosis and necrosis. *Gastroenterology.* 116:168-178.

29. Krammer, P.H., I. Behrmann, P. Daniel, J. Dhein, and K.M. Debatin. 1994. Regulation of apoptosis in the immune system. *Curr. Opin. Immunol.* 6:276-289.

30. Lee, J.K., S.H. Zaidi, P. Liu, F. Dawood, A.Y. Cheah, W.H. Wen, Y. Saiki, and M. Rabinovitch. 1998. A serine elastase inhibitor reduces inflammation and fibrosis and preserves cardiac function after experimentally-induced murine myocarditis. *Nature Medicine.* 4:1383-1391.

31. Liu, P., T. Martino, M.A. Opavsky, and J. Penninger. 1996. Viral myocarditis: balance between viral infection and immune response. *Canadian J. Cardiol.* 12:935-943.

32. Marshall, W.L., C. Yim, E. Gustafson, T. Graf., D.R. Sage, K. Hanify, L. Williams, J. Fingeroth, and R.W. Finberg. 1999. Epstein-Barr virus encodes a novel homolog of the bcl-2 oncogene that inhibits apoptosis and associates with Bax and Bak. *J. Virol.* 73:5181-5185.

33. Martin, S.J., and D.R. Green. 1995. Protease activation during apoptosis: death by a thousand cuts? *Cell.* 82:349-352

34. Matsumori, A. 1996. Cytokines in myocarditis and cardiomyopathies. *Current Opin. Cardiol.* 11:302-309.

35. Megyeri, K., K. Berencsi, T.D. Halazonetis, G.C. Prendergast, G. Gri, S.A. Plotkin, G. Rovera, and E. Gonczol. 1999. Involvement of a p53-dependent pathway in rubella virus-induced apoptosis. *Virology.* 259:74-84.

36. Murachi, T. 1983. Calpain and calpastatin. *Trends Biochem. Sci.* 8:167-169.

37. Nath, R., K.J. Raser, D. Stafford, I. Hajimohammadreza, A. Posner, H. Allen, R.V. Talanian, P. Yuen, R.B. Gilbertsen, and K.K. Wang. 1996. Non-erythroid α-spectrin breakdown by calpain and interleukin 1 B-converting-enzyme-like protease(s) in apoptotic cells: contributory roles of both protease families in neuronal apoptosis. *Biochem. J.* 319:686-690.

38. Neuberger, T., A.K. Chakrabarti, T. Russell, G.H. DeVreis, E.L. Hogan, and N.L. Banik. 1997. Immunolocalization of cytoplamic and myelin mCalpain in transfected Schwann cells. I.Effect of treatment with growth factors. *J. Neurosci. Res.* 47:521-530.

39. O'Brien, V. 1998. Viruses and apoptosis. *J. Gen. Virol.* 79:1833-1834

40. Oberhaus, S.M., R.L. Smith, G.H. Clayton, T.S. Dermody, and K.L. Tyler. 1997. Reovirus infection and tissue injury in the mouse central nervous system are associated with apoptosis. *J. Virol.* 71:2100-2106.

41. Oberhaus, S.M., T.S. Dermody, and K.L.Tyler. 1998. Apoptosis and the cytopathic effects of reovirus. *Curr. Top. Microbiol. Immunol.* 233:23-49.

42. Patel, T., G.J. Gores, and S.H. Kaufmann. 1996. The role of proteases during apoptosis. *FASEB J.* 10:587-597.

43. Pignata, C., M. Fiore, S. deFilippo, M. Cavalcanti, L. Gaetaniello, and I. Scotese. 1998. Apoptosis as a mechanism of peripheral blood mononuclear cell death after measles and varicella-zoster virus infections in children. *Pediatric Research.* 43:77-83.

44. Porn-Ares, M.I., A. Samali, and S. Orenius. 1998. Cleavage of the calpain inhibitor, calpastatin, during apoptosis. *Cell Death and Differentiation.* 5:1028-1033.

45. Rodgers, S.E., E.S. Barton, S.M. Oberhaus, B. Pike, C.A. Gibson, K.L. Tyler, and T.S. Dermody. 1997. Reovirus-induced apoptosis of MDCK cells is not linked to viral yield and is blocked by Bcl-2. *J. Virol.* 71:2540-2546.

46. Rose, N.R., A. Herskowitz, and D.A. Neumann. 1993. Autoimmunity in myocarditis: models and mechanisms. *Clin. Immunol. Immunopath.* 68:95-99.

47. Rose, N.R., and S.L. Hill. 1996. The pathogenesis of postinfectious myocarditis. *Clin.Immunol.and Immunopath.* 80:S92-99.

48. Ruiz-Vela, G. Gonzalez de Buitrago, and Martinez-A, C. 1999. Implication of calpain in caspase activation during B cell clonal deletion. *EMBO.* 18:4988-4998.

49. Saatman, K.E., H. Murai, R.T. Bartus, D.H. Smith, N.J. Hayward, B.R. Perri, and T.K. McIntosh. 1996. Calpain inhibitor AK295 attenuates motor and cognitive deficits following experimental brain injury in the rat. *Proc. Natl. Acad. Sci USA.* 93:3428-3433.

50. Salamino, F., R. DeTullio, P. Mengotti, P.L. Viotti, E. Melloni, and S. Pontremoli. 1993. Site-directed activation of calpain is promoted by a membrane-associated natural activator protein. *Biochem. J.* 290:191-197.

51. Schultz-Cherry, S., and V.S. Hinshaw. 1996. Influenza virus neuraminidase activates latent transforming growth factor beta. *J. Virol.* 70:8624-8629.

52. Schwimmbeck, P.L., S.A. Huber, and H.P. Schultheiss. 1997. Roles of T cells in coxsackie-B induced disease. *Current Top. Microbiol. Immunol.* 223:283-303.

53. Seko, Y., N. Takahashi, H. Yagita, K. Okumura, and Y. Yazaki. 1997. Expression of cytokine mRNA's in murine hearts with acute myocarditis caused by coxsackievirus b3. *J. Pathol.* 183:105-108.

54. Seko, Y., N. Takahashi, M. Azuma, H. Yagita, K. Okumura, and Y. Yazaki. 1998. Expression of costimulatory molecule CD40 in murine heart with acute myocarditis and reduction of inflammation by treatment with anti-CD40L/B7-1 monoclonal antibodies. *Circ.Res.* 83:463-469.

55. Shen, Y., and T.E. Shenk. 1995. Viruses and apoptosis. *Curr. Opin. Genet. Dev.* 5:105-111.

56. Sherry, B. Pathogenesis of reovirus myocarditis. 1998. In *Reoviruses II: Cytopathogenicity and Pathogenesis*. K.L. Tyler and M.B.A. Oldstone, editors. Berlin: Springer-Verlag. 51-66.

57. Sherry, B. and M.A. Blum. 1994. Multiple viral core proteins are determinants of reovirus-induced acute myocarditis. *J. Virol.* 63:8461-8465.

58. Sherry, B., C.J. Baty, and M.A. Blum. 1996. Reovirus-induced acute myocarditis in mice correlates with viral RNA synthesis rather than generation of infectious virus in cardiac myocytes. *J. Virol.* 70:6709-6715.

59. Sherry, B., F.J. Schoen, E. Wenske, and B.N. Fields. 1989. Derivation and characterization of an efficiently myocarditic reovirus variant. *J. Virol.* 63:4840-4849.

60. Sherry, B., J. Torres, and M.A. Blum. 1998. Reovirus induction of and sensitivity to beta interferon in cardiac myocyte cultures correlate with induction of myocarditis and are determined by viral core proteins. *J. Virol.* 72:1314-1323.

61. Sherry, B., X-Y. Li, K.L. Tyler, J.M. Cullen, and H.W. Virgin. 1993. Lymphocytes protect against and are not required for reovirus-induced myocarditis. *J. Virol.* 67:6119-6124.

62. Sindram, D., V. Kohli, J.F. Madden, and P.A. Clavien. 1999. Calpain inhibition prevents sinusoidal endothelial cell apoptosis in the cold ischemic rat liver. *Transplantation.* 68:136-140.

63. Solary, E., B. Eymin, N. Droin, and M. Haugg. 1998. Proteases, proteolysis, and apoptosis. *Cell Biology and Toxicology.* 14:11-32.

64. Sorimachi, H., S. Ishiura, and K. Suzuki. 1997. Structure and physiological function of calpains. *Biochem. J.* 328:721-732.

65. Squier, M.K., A.J. Sehnert, K.S. Sellins, A.M. Malkinson, E. Takanoand J.J. Cohen. 1999. Calpain and calpastatin regulate neutrophil apoptosis. *J. Cell. Physiol.* 178:311-319.

66. Squier, M.K.T, and J.J. Cohen. 1997. Calpain, an upstream regulator of thymocyte apotosis. *J. Immunol.* 158:3690-3697.

67. Strong, J.E., D. Tang, and P.W.K. Lee. 1993. Evidence that the epidermal growth factor receptor on host cells confers reovirus infection efficiency. *Virology.* 197:405-411.

68. Teodoro J.G., and P.E. Branton. 1997. Regulation of apoptosis by viral gene products. *J. Virol.* 71:1739-1746.

69. Thomas, M., and L. Banks. 1999. Human papillomavirus (HPV) E6 interactions with Bak are conserved amongst E6 proteins from high and low risk HPV types. *J. Gen. Virol.* 80:1513-1517.

70. Tyler, K.L., M.K.T. Squier, S.E. Rodgers, B.E. Schneider, S.M. Oberhaus, T.A. Grdina, J.J. Cohen, and T.S. Dermody. 1995. Differences in the capacity of reovirus strains to induce apoptosis are determined by viral attachment protein σ1. *J. Virol.* 69:6972-6979.

71. Valentin, H., O. Azocar, B. Horvat, R. Willeims, R. Garrone, A. Evlasher, M.L. Toribio, and C. Rabourdin-Combe. 1999. Measles virus infection induces terminal differentiation of human thymic epithelial cells. *J. Virol.* 73:2212-2221.

72. Wang, K.K., R. Postmantur, R. Nadimpalli, R. Nath, P. Mohan, R.A. Nixon, R.V. Talanian, M. Keegan, L. Herzog, and H. Allen. 1998. Caspase-mediated fragmentation of calpain inhibitor protein calpastatin during apoptosis. *Archives Biochem. Biophys.* 356:187-196.

73. Wang, K.K.W, and P. Yuen. 1994. Calpain inhibition: an overview of its therapeutic potential. *Trends Pharmacol. Sci.* 15:412-419.

74. Watt, F., and P.L. Molloy. 1993. Specific cleavage of transcription factors by the thiol protease, m-calpain. *Nucleic Acids Res.* 21:5092-5100.

75. Weller, M., J.B. Schulz, U. Wullner, P.A. Loschmann, T. Klockgether, and J. Dichgans. 1997. Developmental and genetic regulation of programmed neuronal death. *J. Neural Transm.* 50:115-123.

76. Wood, D.E., A. Thomas, L.A. Devi, Y. Berman, R.C. Beavis, J.C. Reed, and E.W. Newcomb. 1998. Bax cleavage is mediated by calpain during drug-induced apoptosis. *Oncogene.* 17:1069-1078.

77. Wood, D.E., and E.W. Newcomb. 1999. Caspase-dependent activation of calpain during drug-induced apoptosis. *J. Biol. Chem.* 274:8309-8315.

78. Yang, D., J. Yu, Z. Luo, C.M. Carthy, J.E. Wilson, Z. Liu, and B.M. McManus. 1999. Viral myocarditis: identification of five differentially expressed genes in coxsackievirus B3-infected mouse heart. *Circulation Res.* 84:704-712.

79. Yeh, E.T. 1997. Life and death in the cardiovascular system. *Circulation.* 95:782-786.

80. Zhivotovsky, B., D.H. Burgess, D.M. Vanags, and S. Orrenius. 1997. Involvement of cellular proteolytic machinery in apoptosis. *Biochem. Biophys. Res. Commun.* 230:481-488.

FIGURE LEGENDS

Figure 1: Consecutive cardiac midsections from mock-infected (a, c, e) compared to reovirus 8B-infected neonatal mice (b, d, f) 7 days after left hind limb inoculation with 1000 pfu strain 8B reovirus or mock-inoculation. Hematoxylin-and eosin-stained tissue reveals marked disruption of myocardial architecture in the 8B-infected heart (b), compared to the mock-infected animal (a) (25X). Despite the degree of injury, there is minimal inflammatory cell infiltrate. The degree of cellularity seen in both mock-infected and infected hearts is normal for neonatal mice. In situ detection of DNA nick ends by TUNEL revealed positive staining nuclei in the same region of injured 8B-infected heart (d), which is absent in the mock-infected animal (c) (25X). Immunohistochemistry with anti-T3 Dearing reoviral antibody reveals the presence of viral antigen in the areas of myocardial injury in the 8B-infected mouse (f), absent in the mock-infected animal (e) (25X).

Figure 2: DNA laddering in 8B-infected neonatal mice hearts. DNA was extracted from Reovirus 8B-infected and mock-infected hearts and detected by end-labeling analysis. DNA from the heart of a representative 8B-infected mouse (lane 2) is fragmented into oligonucleosomal length pieces. These fragments result from internucleosomal DNA cleavage, a hallmark of apoptosis. (Arrows indicate DNA fragments, ranging in length from 200 – 1000 base pairs). Fragmentation is absent in the mock –infected animal (lane 1).

Figure 3: Calpain activity in reovirus infected primary cardiac myocyte culture. (a) Activity was measured by monitoring proteolysis of spectrin (280kD), a preferred calpain substrate, to its calpain-specific breakdown products (150/145 kD doublet) by immunoblot assay. Lysates of 8B-infected cardiomyocytes (MOI 20) were prepared at 24, 48, and 72 hours post-infection and compared to lysates of mock-infected cells at 48 hours post-infection (all conditions performed in duplicate). Compared to mock-infection, 8B-infected mice had increased calpain activity (150/145 kD doublet) beginning at 24 hours post-infection, which was markedly increased at 48 hours post-infection, and still present, but decreasing at 72 hours post-infection. No change was detectable in the intact (280 kD) spectrin band following infection.

(b) Densitometric analysis of calpain specific spectrin breakdown products (150/145 doublet) reveals a peak four-fold increase in calpain activity following infection with 8B reovirus.

Figure 4: Efficacy and specificity of calpain inhibitor CX295. The effect of calpain inhibitor CX295 on purified calpain (a), caspase-3 (b), and caspase-1 (c) activity were evaluated using a fluorogenic substrate assay, in which SLY-AMC, DEVD-AMC, and YVAD-AMC, respectively, served as substrates. Activities are expressed as purified calpain or caspase activity per minute, per μmole or pmole of substrate. 100 uM CX295 significantly inhibited calpain activity *$p<0.0001$ (a), but had minimal effect on caspase-3 or caspase-1 activity. z-D-DCB, a pan-caspase inhibitor, was used as a control. Z-D-DCB had no effect on calpain activity, but nearly completely inhibited caspase-3 and 1 activities (b, c). CX295 also effectively inhibited calpain activity in 8B-infected cardiomyocytes in *vitro*. (Figure 4d and 4e). Calpain activity (measured by densitometric analysis of 150/145 calpain-specific fodrin degradation product) increased by 2.4 fold in 8B-infected compared to mock-infected cardiomyocytes. Calpain activity was significantly reduced in CX295 treated, 8B-infected cells compared to infected, untreated cells ($p=0.04$). (The 150/145 kD doublet appears as a single large band due to the gel conditions).

Figure 5: Cardiac midsections from Reovirus 8B-infected neonatal mice treated with calpain inhibitor CX295 (b, d, f, h) compared to inactive diluent control (a, c, e, g) 7 days following intramuscular inoculation with 1000 pfu reovirus 8B. Hematoxylin- and eosin-stained sections at 25X reveal extensive focal areas of myocardial injury (arrows) in the control animal (a), which is absent in the CX295-treated animal, (b) despite identical viral infection. Views at 50X demonstrate minimal inflammatory cell infiltrate in the affected area (c), but myocardial architecture is dramatically disrupted, compared to CX295 treated mouse (d). At 100 X power, nuclei with apoptotic morphology are easily seen in the control animal (e), including cells with condensed and pyknotic nuclei (long arrow) as well as apoptotic bodies (shorter arrows). These findings are absent in the drug treated mouse (f). TUNEL analysis of the control animal reveals extensive areas of positive staining cells in the same regions of injury (g), whereas, there are no TUNEL positive areas noted in the drug-treated mouse (h).

Figure 6: Reduction in myocardial injury score. Myocardial injury of 8B-infected animals quantified by blindly scoring hematoxylin- and eosin-stained midcardiac sections of drug-treated and control (inactive diluent treated) animals by light microscopy. At least 6 sections per heart were scored from 20-23 animals in each group. A highly significant reduction in myocardial injury score was noted in drug-treated animals: Mean lesion score 3.0 ± 0.1 (range 2-4) for controls, compared to 0.6 ± 0.1 (range 0-1.5) for CX295-treated animals, $*p<0.0001$.

Figure 7: Reduction in Serum Creatine Phosphokinase (CPK). CPK was measured as a marker of myocardial damage in 8B-infected animals treated with CX295, and compared to control (inactive diluent-treated) infected animals, as well as age-matched uninfected controls. There was a significant reduction in serum CPK toward normal in CX295-treated infected mice compared to infected control animals, $p<0.05$.

Figure 8: Tissue-specific viral titers. Titers were measured by plaque assay at 7 days post-infection from homogenates of limbs (site of primary replication) and hearts (site of secondary replication) of 8B-infected mice. A slight reduction in peak viral titers was seen in the CX295-treated group. Both CX295-treated and control animals showed > 3 $\log_{10}$ of viral replication over the input inoculum (10^3 pfu/mouse).

Figure 9: Growth of infected mice. Growth, as measured by weight gain, was assessed in 8B-infected mice treated with CX295 and inactive diluent (control). Improved growth was noted in infected, CX295-treated animals at 7 days post-infection compared to infected controls ($*p = 0.008$). Weights of infected, treated animals were not significantly different from uninfected, age matched controls.

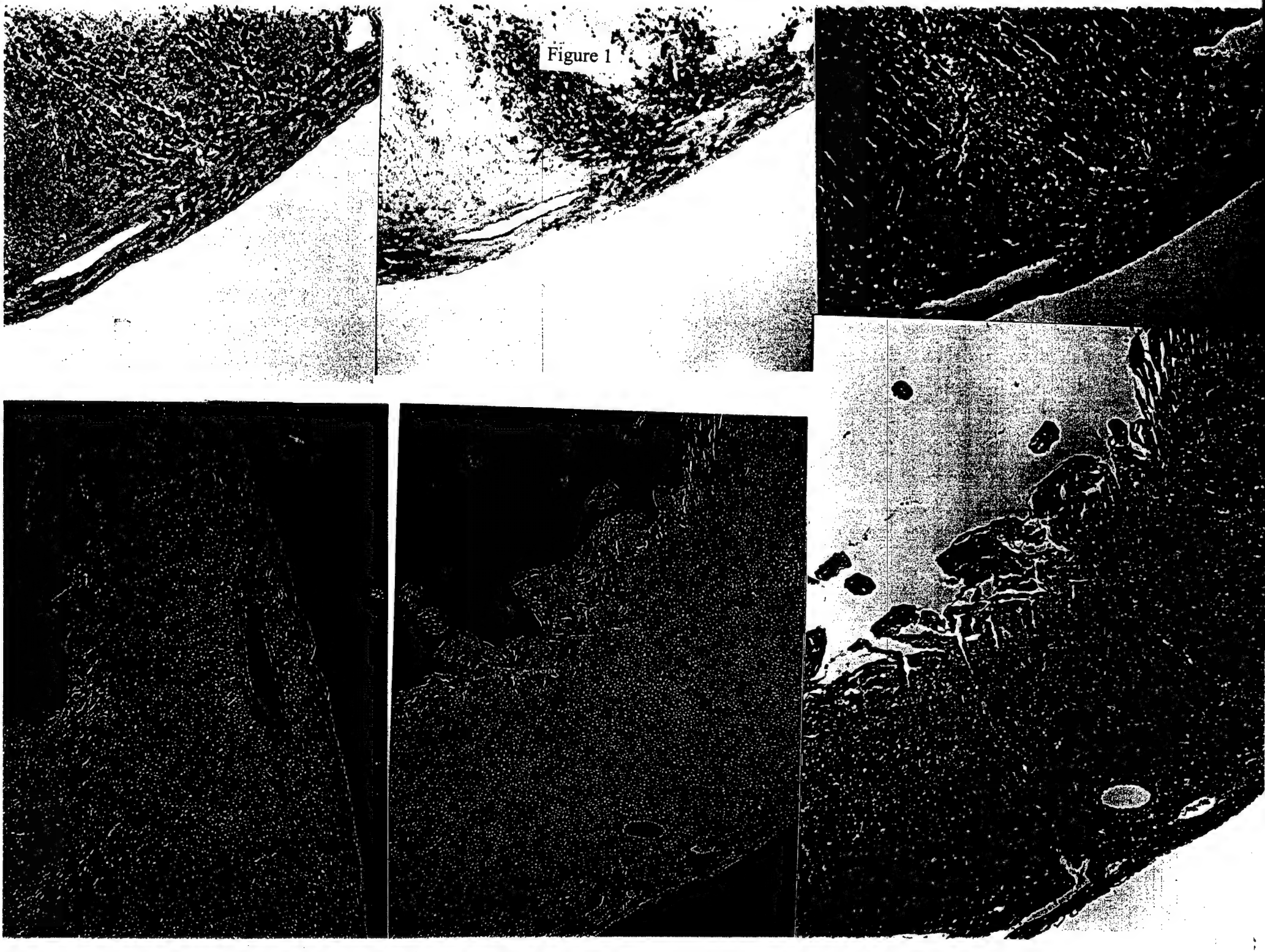

Figure 1

Figure 2

3a
b

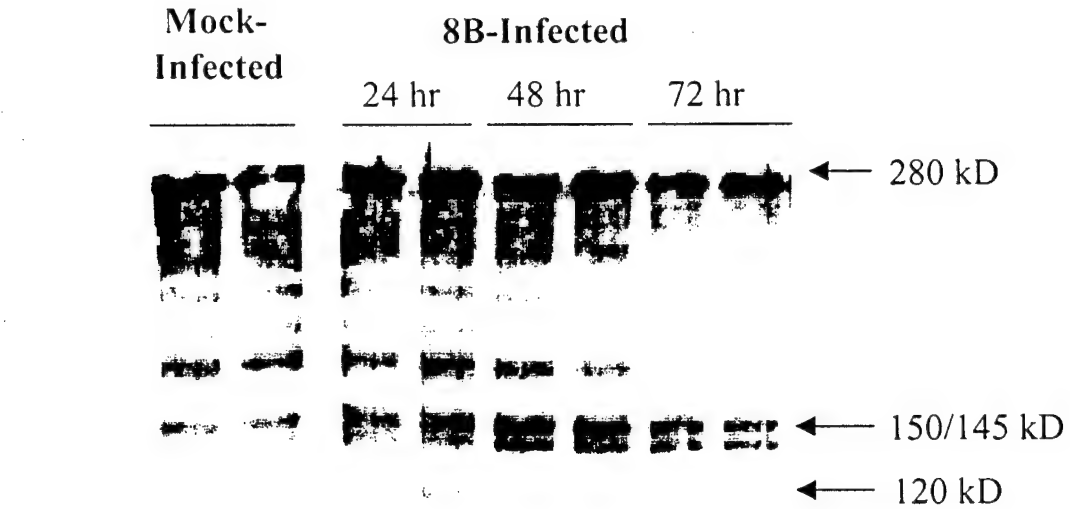
Mock-Infected
8B-Infected
24 hr
48 hr
72 hr
280 kD
150/145 kD
120 kD

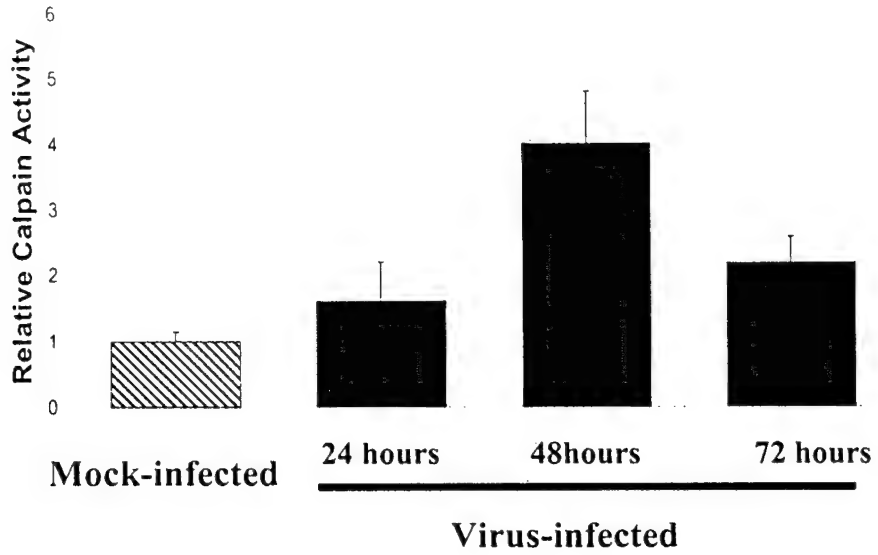
Relative Calpain Activity
0
1
2
3
4
5
6
Mock-infected
24 hours
48hours
72 hours
Virus-infected

Figure 3

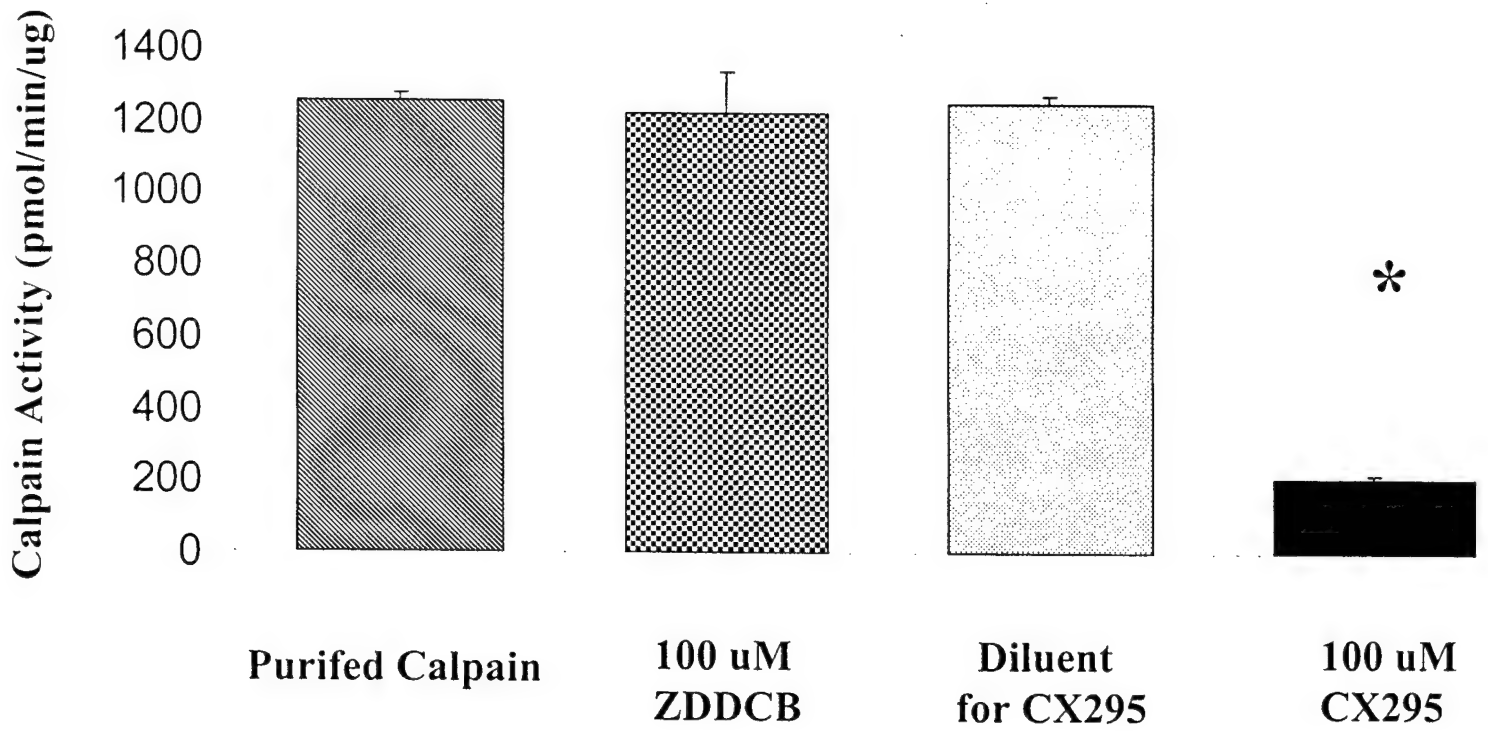
Calpain Activity (pmol/min/ug)
1400
1200
1000
800
600
400
200
0
*
Purifed Calpain
100 uM ZDDCB
Diluent for CX295
100 uM CX295

Figure 4A

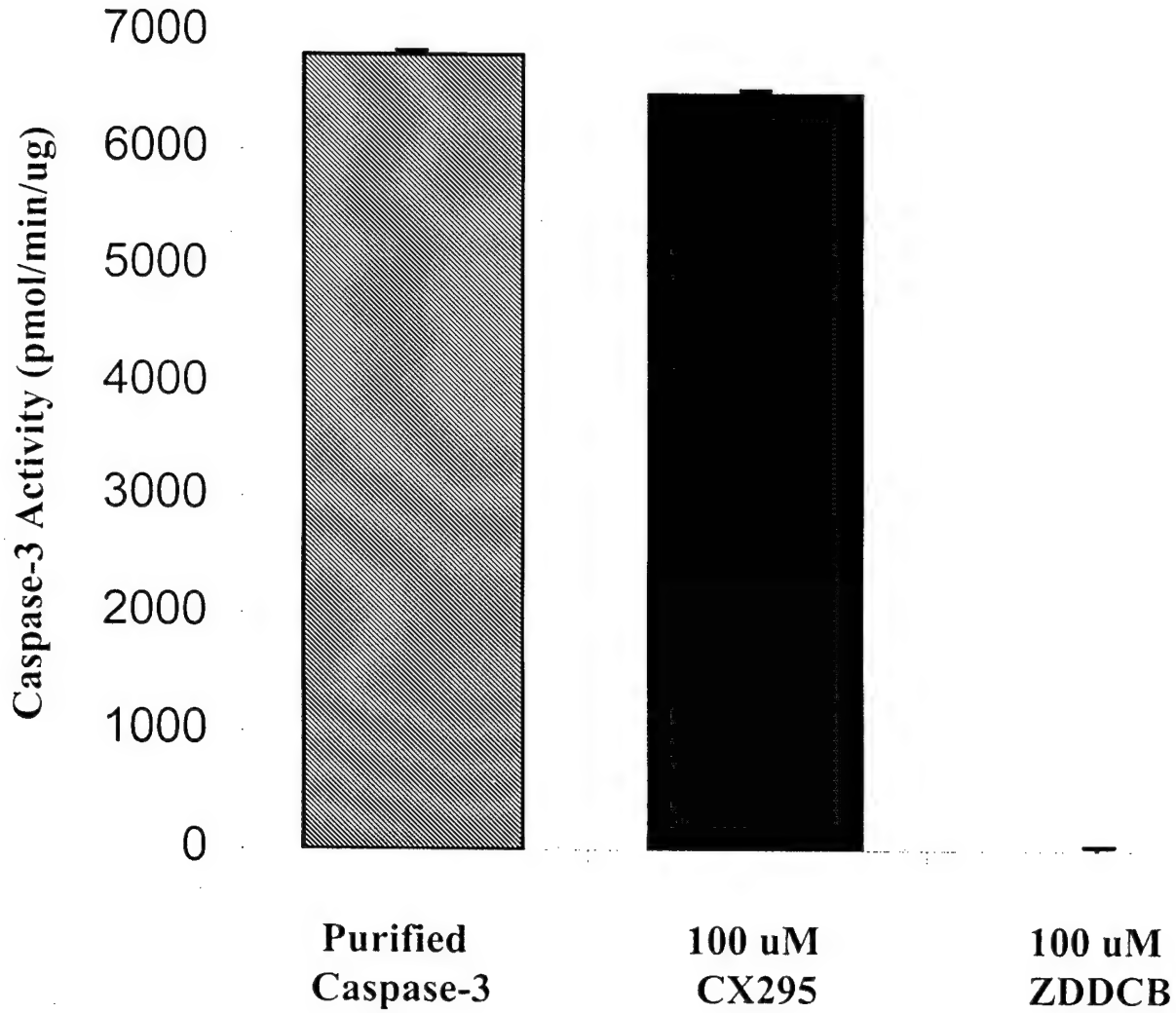
Caspase-3 Activity (pmol/min/ug)
7000
6000
5000
4000
3000
2000
1000
0
Purified Caspase-3
100 uM CX295
100 uM ZDDCB

Figure 4B

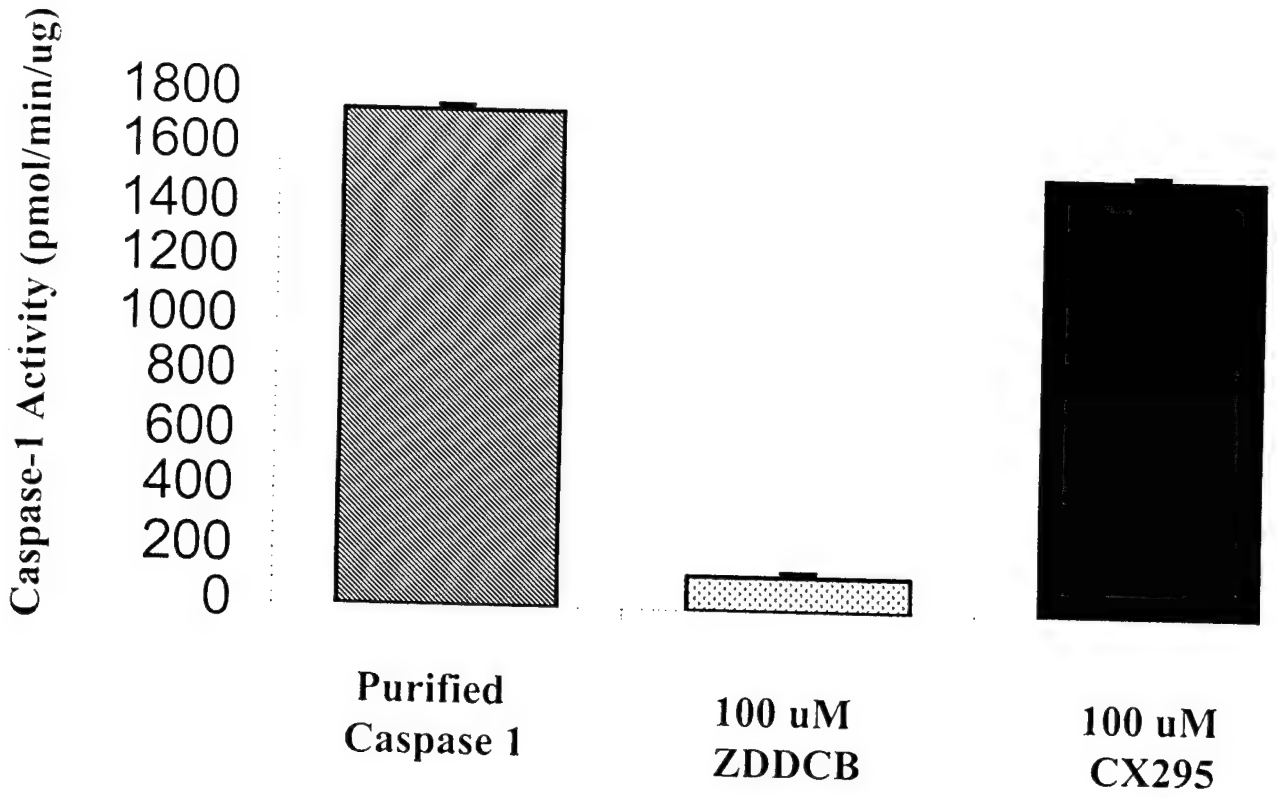
Caspase-1 Activity (pmol/min/ug)
1800
1600
1400
1200
1000
800
600
400
200
0
Purified Caspase 1
100 uM ZDDCB
100 uM CX295

Figure 4C

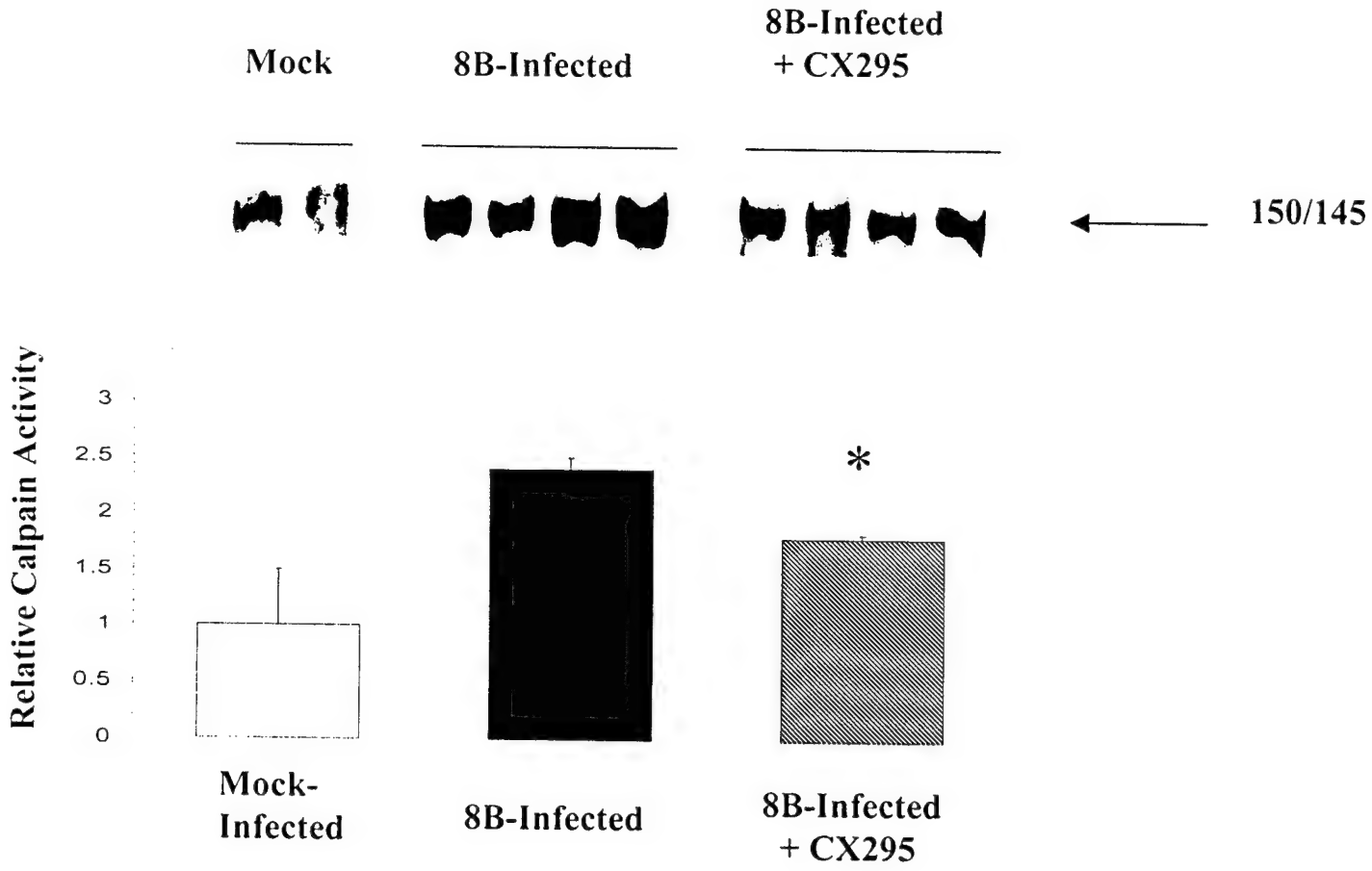
Mock
8B-Infected
8B-Infected
+ CX295
150/145
Relative Calpain Activity
3
2.5
2
1.5
1
0.5
0
*
Mock-
Infected
8B-Infected
8B-Infected
+ CX295

Figure 4D, E

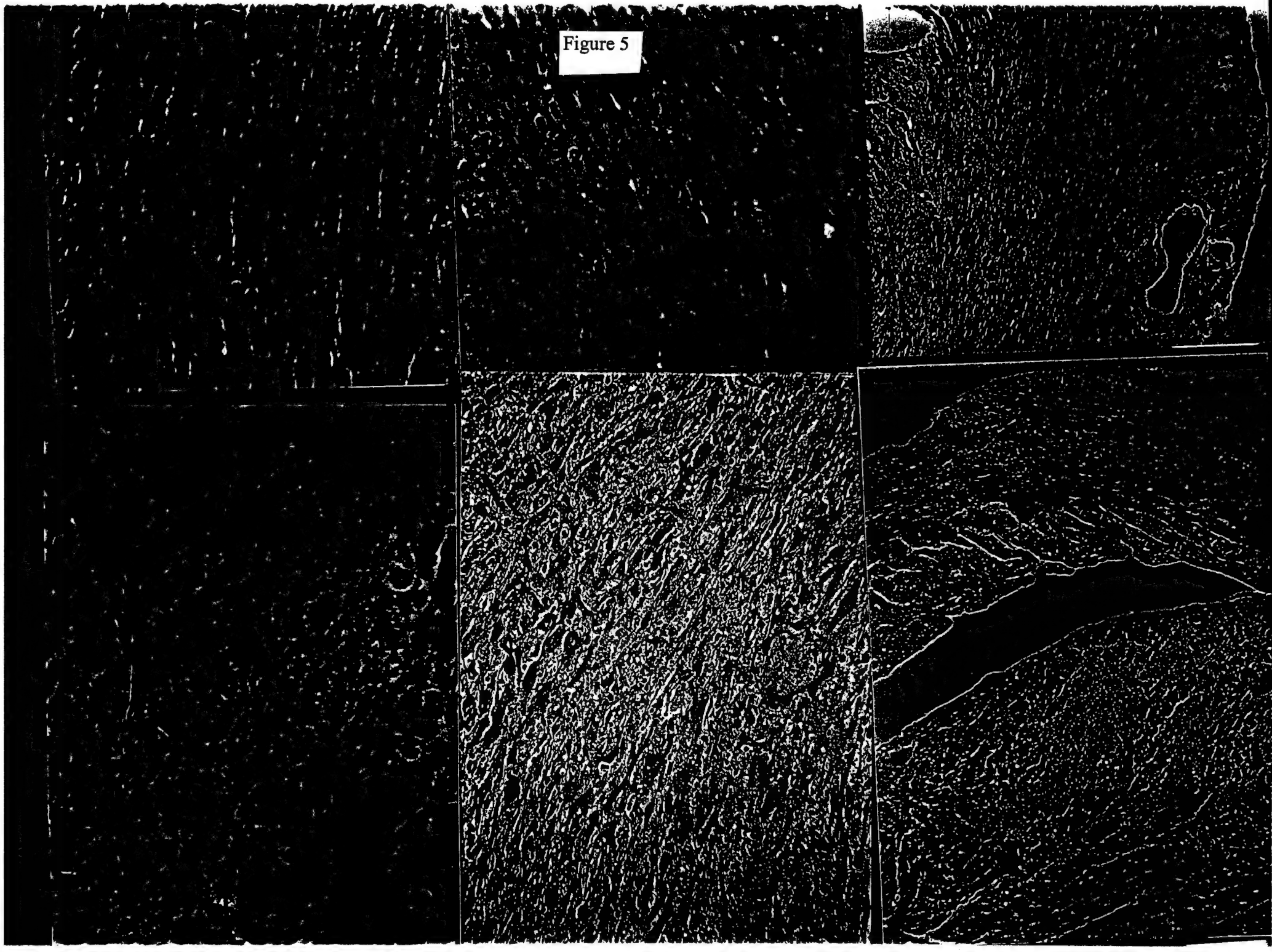
Figure 5

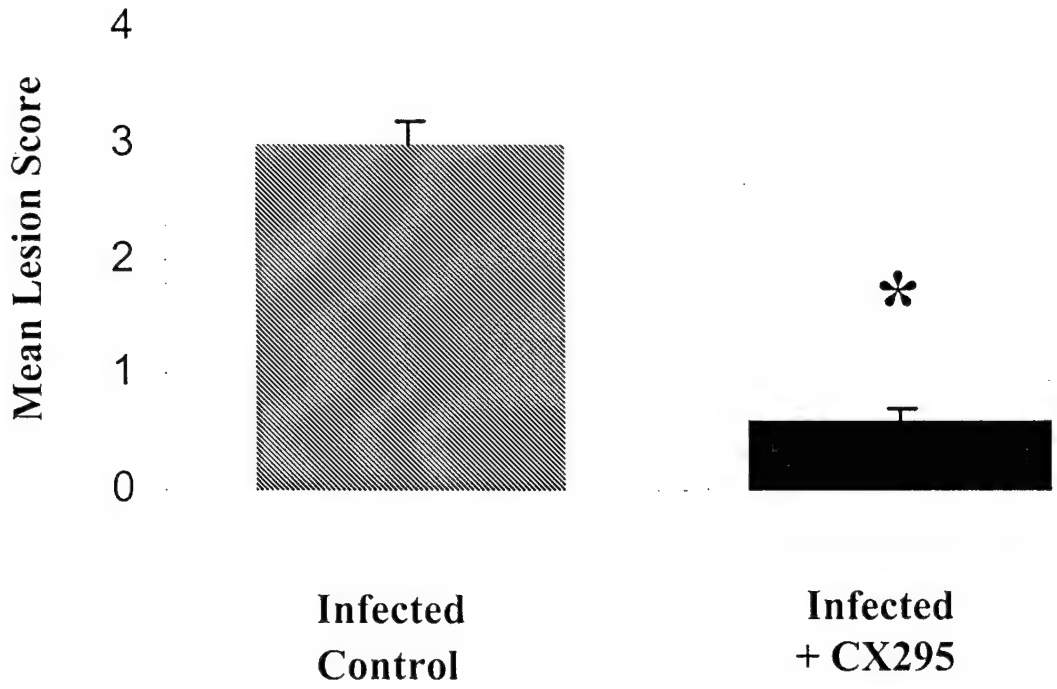

Heart Lesion Scoring

0 = no lesions
1 = one or a few small
2 = many small or a few large
3 = multiple small and large
4 = massive

Figure 6

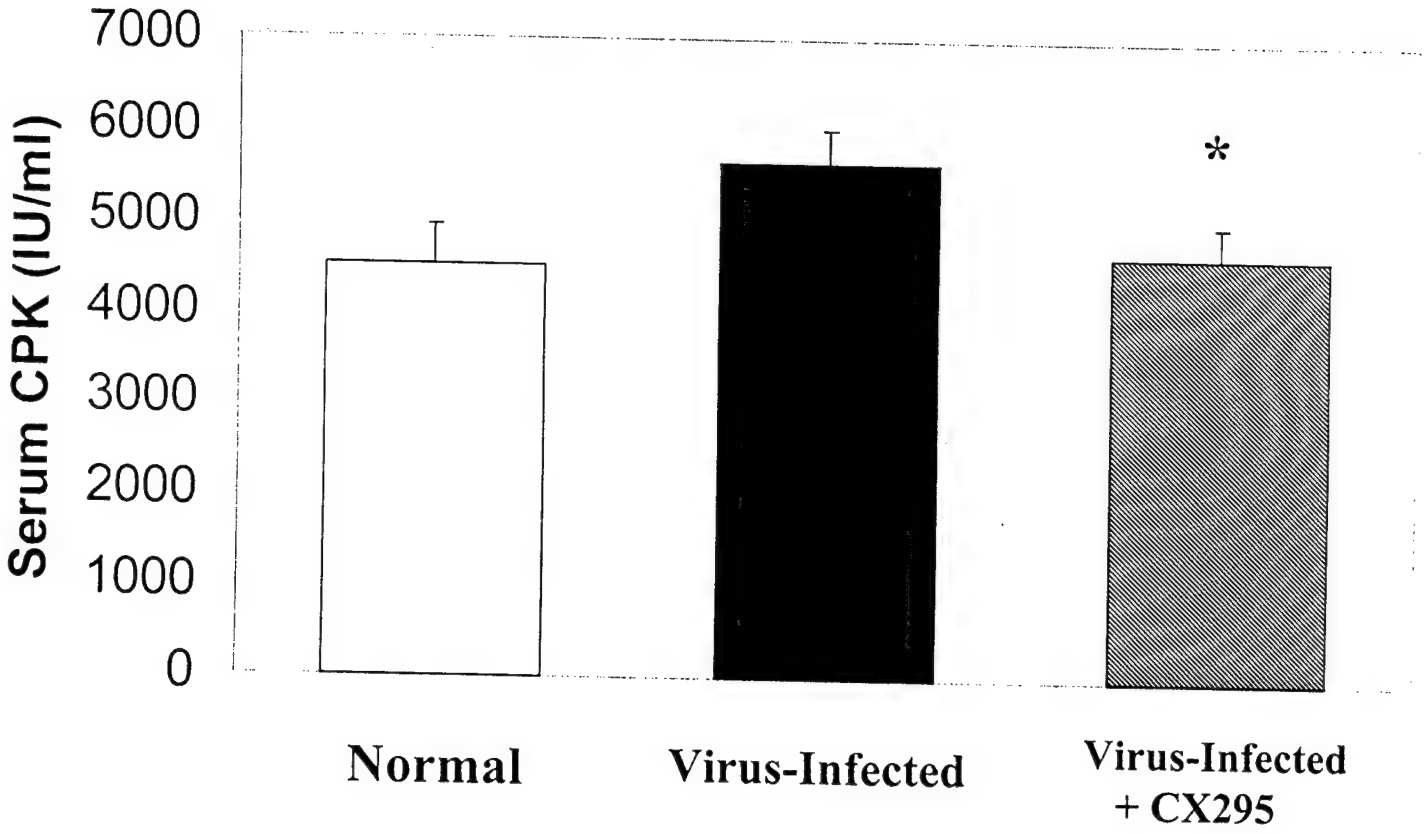
Serum CPK (IU/ml)
7000
6000
5000
4000
3000
2000
1000
0
*
Normal
Virus-Infected
Virus-Infected
+ CX295

Figure 7

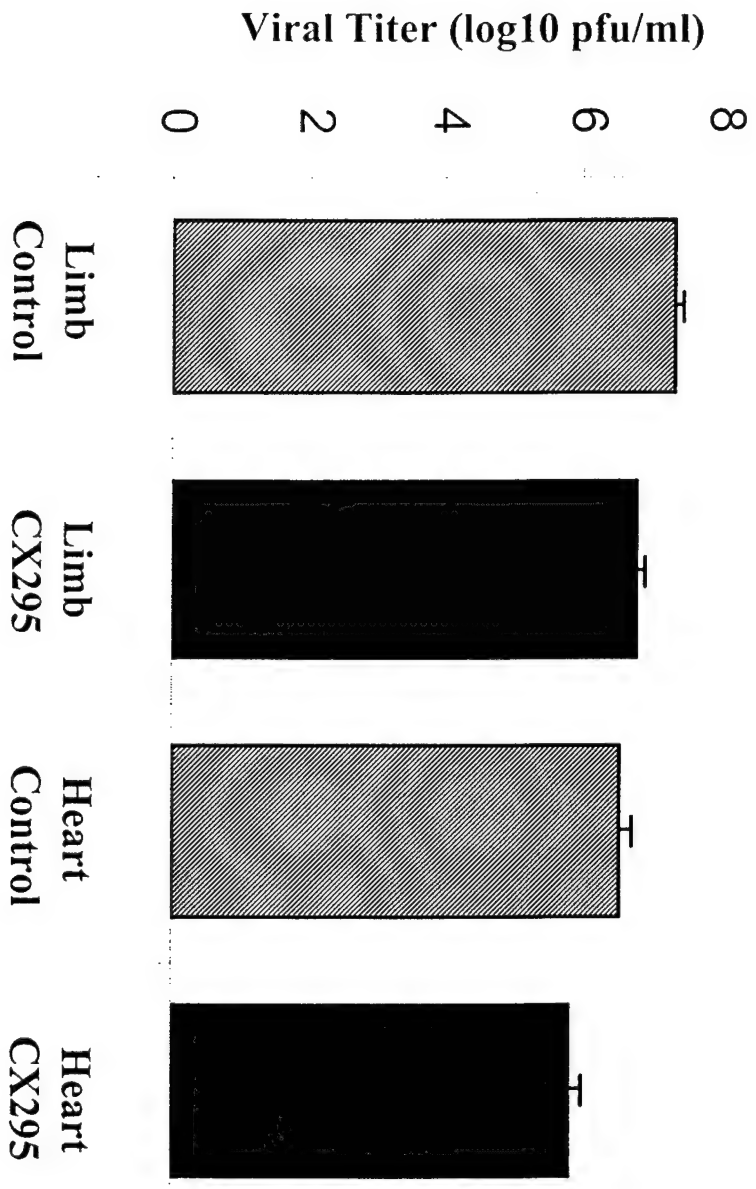
Viral Titer (log10 pfu/ml)
0
2
4
6
8
Limb Control
Limb CX295
Heart Control
Heart CX295

Figure 8

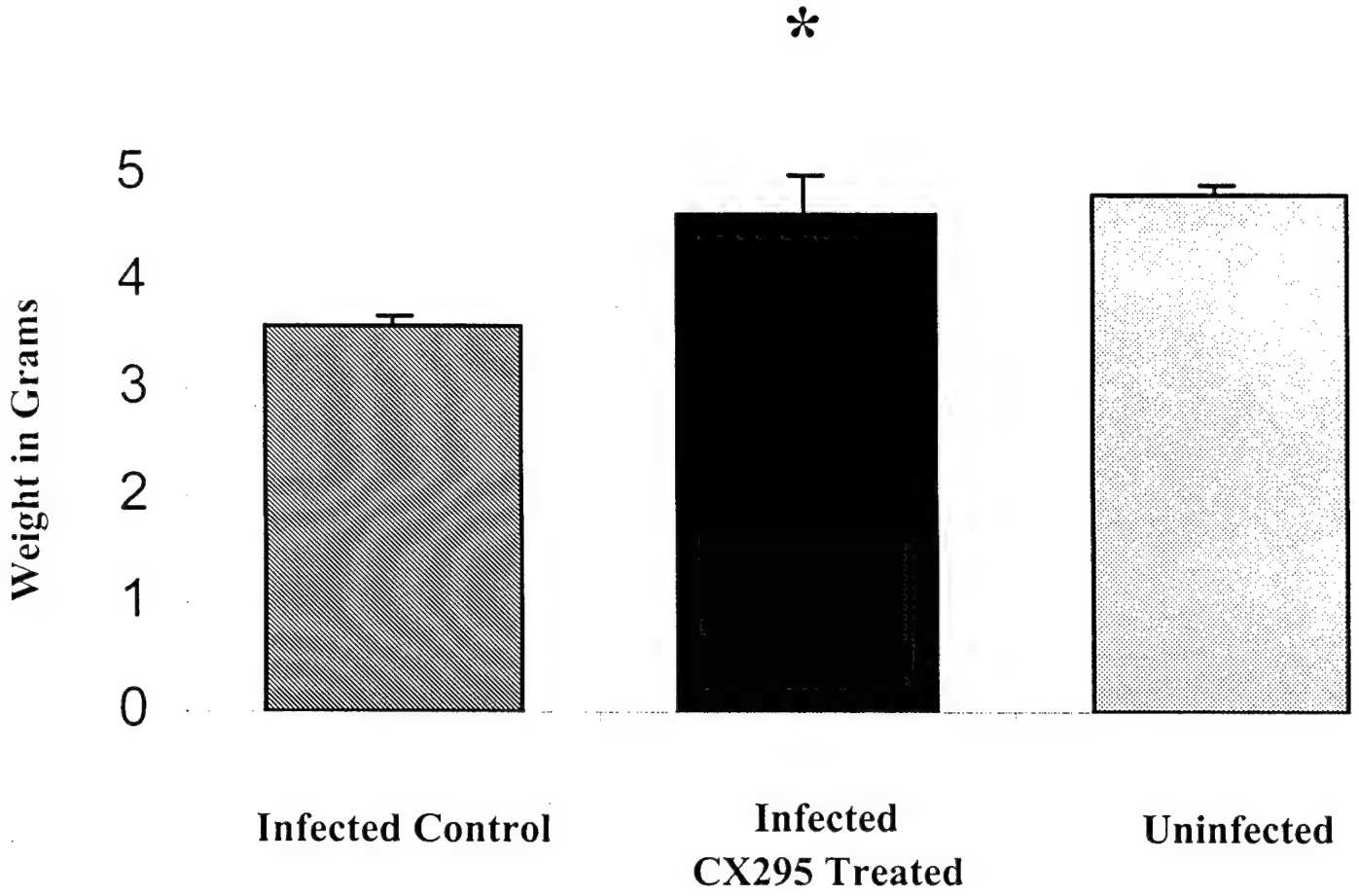
*
Weight in Grams
5
4
3
2
1
0
Infected Control
Infected
CX295 Treated
Uninfected

Figure 9

Journal of Virology (submitted)

Reovirus-Induced Apoptosis Involves both Death Receptor- and Mitochondrial-Mediated Caspase-dependent Pathways of Cell Death

Running title: Reovirus-Induced Caspase Activation

DOUGLAS J. KOMINSKY[1], RYAN J. BICKEL[1], SUZANNE M. MEINTZER[1], PENNY CLARKE[1], AND KENNETH L. TYLER[1,2,3*]

Departments of Neurology[1], Medicine, Microbiology, and Immunology[2], University of Colorado Health Science Center, and Denver Veteran's Affairs Medical Center[3], Denver, Colorado 80262

*Corresponding author. Mailing address: Department of Neurology (127), Denver VA Medical Center, 1066 Clermont St., Denver, CO 80220. Phone: (303) 393-2874. Fax: (303) 393-4686. E-mail: Ken.Tyler@uchsc.edu.

Abstract

Apoptosis induction or its inhibition play an important role in the pathogenesis of many viral infections. Apoptotic cell death can be triggered by death receptor activation, mitochondrial insult, or stress within the endoplasmic reticulum or Golgi. Virtually all apoptotic pathways described to date involve the sequential activation of a family of cysteine proteases known as caspases. Delivery of an apoptotic stimulus to the cell triggers the autocatalytic activation of initiator caspases, which subsequently induce the activation of effector caspases. We have recently shown that reovirus-induced apoptosis involves the DR4/DR5/TRAIL cell death receptor system. We now demonstrate that reovirus infection of HEK293 cells results in the activation of the effector caspase, caspase-3, as demonstrated by fluorogenic substrate assay and western blot analysis. Inhibition of caspase-3 activation reduces reovirus-induced apoptosis. Because a number of initiator caspases can activate caspase-3, we next analyzed the initiator caspases involved in caspase-3 activation. Western blot analysis and synthetic peptide inhibitor data revealed that caspase-8 is activated and involved in caspase-3 activation. Reovirus infection also induces the release of cytochrome *c* from the mitochondria, leading to the activation of caspase-9. Inhibition of either caspase-8 or caspase-9 inhibits caspase-3 activation and reovirus-induced apoptosis. These results show that reovirus-induced apoptosis involves the activation of both death receptor-associated and mitochondrial pathways of cell death.

Introduction

Apoptosis is a particular type of cell death that is characterized by distinctive changes in cellular morphology including cell shrinkage, zeiosis, nuclear condensation, chromatin margination and subsequent degradation that are associated with inter-nucleosomal DNA fragmentation. Apoptosis may be initiated by a wide variety of cellular insults including death receptor stimulation, γ-radiation, and cytotoxic compounds. Induction or inhibition of apoptosis is an important feature of many types of viral infection both *in vitro* and *in vivo*.

Mammalian reoviruses are capable of inducing apoptosis in cultured cells *in vitro* (19, 22, 28) as well as in organs *in vivo* including the central nervous system (CNS) and heart (19, 20, DeBiasi et al, submitted for publication). In vivo there is an excellent correlation between the distribution of reovirus antigen, apoptotic cell death, and areas of tissue injury, suggesting that apoptosis plays an important role in reovirus pathogenesis (19, DeBiasi et al, submitted for publication). This is supported by recent evidence showing that inhibition of apoptosis reduces tissue injury *in vivo* (DeBiasi et al, submitted for publication).

Differences in the capacity of reovirus strains to induce apoptosis are determined by the viral S1 gene (28). The S1 gene is bicistronic, encoding two non-homologous proteins (σ1, σ1s) from over-lapping but out of sequence reading frames. The σ1 protein appears to be the primary determinant of apoptosis, whereas σ1s is involved on reovirus-induced perturbations in cell cycle regulation (Poggioli et al, in press). Reovirus-induced apoptosis does not require replication (22), but is dependent upon the activation of the cellular transcription factor NFκB (9) and is associated with the activation of calpains

(10). Apoptosis involves the tumor necrosis factor (TNF) superfamily of cell surface death receptors, specifically DR4, DR5 and their ligand, TNF-related apoptosis-inducing ligand (TRAIL) (6), and can be inhibited by anti-TRAIL antibodies or soluble forms of DR4 or DR5 which inhibit interaction of TRAIL with DR4 and DR5 (6).

Virtually all apoptotic pathways described to date involve a family of cysteine proteases known as the caspases. Delivery of an apoptotic stimulus to the cell triggers the initial activation through autocatalytic mechanisms of initiator caspases, which subsequently induce the activation of a cascade of effector caspases. These caspases are responsible for triggering the morphological changes characteristic of apoptotic cell death. Induction of apoptosis by different types of stimuli activates different initiator caspases. Stimulation of death receptors leads to the activation of caspase-8 and caspase-10 (reviewed in 1). A second pathway, requiring the release of cytochrome *c* from the mitochondria, leads to the activation of caspase-9 (16, 31). Similarly, recent evidence has shown that endoplasmic reticulum (ER) or Golgi complex "stress" leads to the activation respectively of caspase-12 or caspase-2 (17, 18).

Little is known about the exact nature of the apoptotic pathways triggered during viral infection. Different viruses may utilize different apoptotic pathways. For example, some viruses including reovirus, HIV, avian leukosis viruses, Measles virus, and Influenza virus may directly or indirectly induce apoptosis through death receptor-associated pathways (4, 9, 11, 25, 29), whereas others may activate the mitochondrial-dependent pathway (14). In addition, it has recently been shown that accumulation of increased quantities of viral proteins within the ER can trigger ER-related "stress" responses including alterations in transcriptional factors and ER-resident kinases, although there is

still no direct evidence that the ER or Golgi pathways are involved in virus-induced apoptosis.

Reovirus-induced apoptosis has been shown to involve the death receptors DR4 and DR5 and their ligand TRAIL (6). Additionally, reovirus-induced apoptosis is inhibited in a cell line expressing a dominant negative form of the Fas-associated death domain adaptor protein (FADD-DN) or in cells treated with a caspase-8 specific inhibitor, suggesting that both of these molecules are involved in the apoptotic pathway (6). We have previously shown that over-expression of bcl-2 can inhibit reovirus-induced apoptosis (22). Bcl-2 may act by inhibiting the release of cytochrome *c* from the mitochondria, suggesting a potential role for the mitochondrial pathway of apoptosis induction. Finally, recent studies have suggested that rotaviruses, members of the family *Reoviridae*, may activate NF-κB through ER stress related pathways, suggesting that ER or Golgi stress may also lead to caspase activation following infection.

In this paper we describe the nature of caspase cascade activation following reovirus infection. We now show that caspase-8, caspase-9, and caspase-3 are all activated and necessary for reovirus-induced apoptosis. Additionally, GADD-153/CHOP, a transcription factor involved in activation of ER stress pathways (12, 21), is up regulated in reovirus-infected cells.

Materials and Methods

Reagents

Anti-cytochrome *c* (7H8.2C12), anti-PARP (C2-10), anti-caspase-3, anti-caspase-6 (B93-4), anti-caspase-7 (B94-1), anti-caspase-8 (B9-2), anti-caspase-9, and anti-caspase-10

antibodies were purchased from Pharmingen (San Diego, California). Anti-actin antibodies (JLA20) were from Calbiochem (Darmstadt, Germany). Anti-human cytochrome *c* oxidase (subunit II) antibodies (12C4-F12) were from Molecular Probes (Eugene, Oregon). Anti-Fas antibody (CH-11) was from Upstate Biotechnology (Lake Placid, New York). Caspase synthetic peptide inhibitors used were DEVD-CHO (Clontech, Palo Alto, California), Z-IETD-FMK [Z-Ile-Glu(OMe)-Thr-Asp(OMe)-CH_2F], and Z-LEHD-FMK [Z-Leu-Glu(OMe)-His-Asp(OMe)-CH_2F] (Calbiochem, Darmstadt, Germany). ApoAlert caspase-3 fluorometric assay kit was purchased from Clontech (Palo Alto, California).

Cells, Virus, and DNA Constructs

HEK293 cells (ATCC CRL1573) were grown in Dulbecco's modified Eagle's medium (DMEM) supplemented with 100 U/ml each of penicillin and streptomycin and containing 10% fetal bovine serum. Jurkat cells were a gift of Dr. John Cohen and were grown in RPMI supplemented with 100U/ml each of penicillin and streptomycin and containing 10% fetal bovine serum. FADD-DN cells express amino acids 80-208 of the FADD cDNA (with the addition of an AU1 epitope tag at the N-terminus) from the CMV promoter of pcDNA3 (Invitrogen, Calsbad, California). Generation of stable transfectants was done using LipofectAmine Reagent (Life Technologies, Gaithersburg, Maryland). Reovirus (Type 3 Abney, T3A) is a laboratory stock, which has been plaque purified and passaged (twice) in L929 cells (ATCC CCL1) to generate working stocks (27). All experiments were performed using an M.O.I. of 100.

Western Blot Analysis

At the indicated time points following reovirus infection cells were harvested and pelleted by centrifugation, washed with ice-cold phosphate-buffered saline, and lysed by sonication in 150 μl of buffer containing 1% NP40, 0.15 M NaCl, 5.0 mM EDTA, 0.01 M Tris (pH 8.0), 1.0 mM PMSF, 0.02 mg/ml leupeptin, and 0.02 mg/ml trypsin inhibitor. Lysates were cleared by centrifugation at 20,000 g for 2 min, mixed 1:1 with SDS sample buffer, boiled for 5 min, and stored at −70°C. Mitochondrial-free extracts were prepared by pelleting cells, washing twice in ice-cold PBS, and incubated on ice for 30 min in buffer containing 220 mM mannitol, 68 mM sucrose, 50 mM PIPES-KOH (pH 7.4), 50 mM KCl, 5 mM EGTA, 2 mM $MgCl_2$, 1 mM DTT, and protease inhibitors (complete cocktail, Boehringer Mannheim, Indianapolis, Indiana). Cells were lysed using 40 strokes in a Dounce homogenizer (B pestle). Lysates were centrifuged at 14,000 g for 15 min at 4°C to remove debris. Supernatants and mitochondrial pellets were prepared for electrophoresis as above. Proteins were separated by SDS-PAGE electrophoresis and transferred to Hybond-c extra nitrocellulose membrane (Amersham, Buckinghamshire, England) for immunobloting. Blots were probed with anti-cytochrome *c* antibodies (1:2000), anti-cytochrome *c* oxidase (subunit II) antibodies (1:1000), anti-caspase-3 antibodies (1:2000), anti-caspase-6 antibodies (1:3000), anti-caspase-7 antibodies (1:3000), anti-caspase-8 antibodies (1:3000), anti-caspase-9 antibodies (1:2000), anti-PARP antibodies (1:3000), and anti-actin antibodies (1:5000). Proteins were visualized using the ECL detection system (Amersham, Buckinghamshire, England). Densitometric analysis was performed using a FluorS MultiImager system and Quantity One software (Bio-Rad, Hercules, California).

Caspase 3 Activation Assays

Caspase 3 activation assays were performed using a kit obtained from Clontech (Palo Alto, California). Experiments were performed using 1 x 10^6 cells/ time point. Cells were centrifuged at 200 g, supernatants were removed, and the cell pellets were frozen at –70°C until all the time points were collected. Assays were performed in 96-well plates and analyzed using a fluorescent plate reader (CytoFluor 4000, PerSeptive Biosystems, Framingham, Massachusettes). Cleavage of DEVD-AFC, a synthetic caspase-3 substrate, was used to determine if caspase-3 is activated in reovirus-infected HEK293 cells. Cleavage after the second Asp residue produces free AFC that can be detected using a fluorescent plate reader. Therefore, the amount of fluorescence detected is directly proportional to amount of caspase-3 activity. Because all of the fluorogenic substrate assay experiments were performed at the same time, both the mock and reovirus-induced caspase-3 activation profiles are the same in all of these experiments and are included in each figure for ease of comparison. Results of all experiments are reported as means $\pm$ SEM. Means were compared using parametric two-tailed t-tests (Graph Pad, Prism) and differences were considered significant if p values were < 0.05.

Apoptosis Assays

48 hours after infection with reovirus cells were harvested and stained with acridine orange, for determination of nuclear morphology, and ethidium bromide, to distinguish cell viability, at a final concentration of 1 μg/ml each (8). Following staining, cells were examined by epifluorescence microscopy (Nikon Labophot-2: B-2A filter, excitation, 450-490 nm; barrier, 520 nm; dichroic mirror, 505 nm). The percentage of cells containing condensed nuclei and/or marginated chromatin in a population of 100 cells

was recorded. The specificity of this assay has been previously established in reovirus-infected cells using DNA laddering techniques and electron microscopy (28). Statistical analysis was performed as described above.

Results

Reovirus infection is associated with activation of caspase-3. Caspases have been shown to be critical for the execution of virtually all known apoptotic pathways, although the pattern(s) of caspase activation vary for different types of apoptotic stimuli (reviewed in 3, 7, 26). We began by examining the activation state of caspase-3, an important effector caspase that forms part of the final common pathway for death receptor, mitochondrial, and ER/Golgi apoptotic pathways. Caspase-3 activation was evaluated using fluorogenic substrate assays, analysis of the activation associated cleavage of caspase-3, and the cleavage of the caspase-3 substrate poly (ADP-ribose) polymerase (PARP). In fluorogenic substrate assays, caspase-3 activation could be detected at 12 hours post-infection, peaking at approximately 18 hr post-infection with a 1.6 fold induction compared to mock-infected cells (Fig. 1A). Caspase-3 activation is blocked by pretreatment for 1 hr prior to infection with DEVD-CHO (25 μM), a synthetic peptide inhibitor of caspase-3 (Fig. 1A). We next examined the activation of caspase-3 using western blot analysis. Activation of caspase-3 is associated with the appearance of specific cleavage products at 20 kD and 17 kD. As shown in Fig. 1B and 1C, these fragments appear beginning at ~12 hrs post-infection in reovirus infected cells, but not in the mock infected controls. In addition, cleavage of an early caspase-3 substrate, PARP,

to an 85 kD inactive fragment is seen in reovirus-infected but not mock-infected cells, with cleavage first detectable at ~14 hr post-infection (Fig. 1D and 1E).

Having shown that caspase-3 is activated using three different assay systems beginning at approximately 12-14 hr post infection, we wanted to determine if this activation is necessary for reovirus-induced apoptosis. The percentage of apoptosis induced by reovirus was examined at 48 hr post-infection. Apoptosis was reduced by pretreatment for 1 hr with DEVD-CHO (50 μM) by ~ 47% (Fig. 2). Because there are other caspases that act at the level of caspase-3, we also looked at the activation state of two other effector caspases, caspase-6 and caspase-7. Western blot analysis provided evidence indicating that neither of these caspases was activated following reovirus infection (data not shown). These results indicate that specific activation of the effector caspase, caspase-3, plays an important role in reovirus-induced apoptosis. A number of apoptotic pathways lead to the activation of caspase-3. Therefore, we next wanted to examine the initiator caspase(s) that are responsible for the activation of caspase-3.

Caspase-8 activation is required for caspase-3 activation. Recent evidence from our laboratory has shown that reovirus-induced apoptosis involves the death receptors DR4 and DR5 and their cognate ligand TRAIL (6). Apoptosis initiated via TNF receptor superfamily cell death receptors involve the adaptor molecule FADD and subsequent activation of caspases, starting the initiator caspase, caspase-8 (13, 30, 2, 5, 15, 23). We have shown that apoptosis is inhibited in HEK293 cells expressing dominant-negative FADD (FADD-DN) or cells treated with a synthetic peptide inhibitor of caspase-8 (6). We looked for direct evidence of activation of caspase-8 using western blot analysis. As shown in Fig. 3A and 3B, reovirus infection induces the activation of caspase-8 as

evidenced by the disappearance of the full-length proenzyme (seen as a 55/54 kD doublet). Densitometric analysis showed that the proenzyme form of caspase-8 was reduced by greater than 50% at 12 hr post infection (data not shown). In order to determine whether caspase-3 activation was dependent on activation of caspase-8, we examined caspase-3 activity in cells pretreated a synthetic peptide inhibitor of caspase-8 (Z-IETD-FMK), and in cells expressing FADD-DN. HEK293 cells were incubated with the Z-IETD-FMK (25 μM) for 1 hr prior to infection and cells were harvested at the indicated time points following infection. The caspase-8-specific inhibitor abrogated caspase-3 activation (Fig. 4). Cells expressing FADD-DN infected with reovirus also display reduced caspase-3 activation (Fig. 4). These results indicate that reovirus-induced activation of caspase-3 is dependent, at least in part, on the activity of caspase-8.

Reovirus infection is associated with release of mitochondrial cytochrome *c* and activation of caspase-9. Caspase-9 is an initiator caspase, involved in both the activation of effector caspases but also in the activation of caspase-8 (24). Activation of caspase-9 requires the release of cytochrome *c*, a mitochondrial intermembrane space protein, into the cytosol. Cytosolic cytochrome *c*, Apaf-1, and dATP/ATP form a complex with procaspase-9, leading to its activation (16). We examined the cellular localization of the mitochondrial protein cytochrome *c* in reovirus-infected cells. Mitochondria-free lysates were prepared from both mock- and reovirus-infected cells at the indicated time points and analyzed by western blot for the presence of cytosolic cytochrome *c*. Additionally, blots were probed with antisera directed against the mitochondrial integral membrane protein cytochrome *c* oxidase (subunit II) to demonstrate the lack of mitochondrial contamination of the samples. Cytosolic

cytochrome *c* is detected only in reovirus-infected cells at ~ 6 hr post-infection (Fig. 5). Having shown that cytochrome c was released from mitochondria in reovirus-infected cells, we next wished to determine whether this was associated with the activation of caspase-9. Activation of caspase-9 involves the cleavage of the 46 kD pro-enzyme and the appearance of a 37 kD large subunit of the active enzyme. The 37 kD fragment appears only in reovirus-infected cells, with the fragment being first detectable at ~10 hr (Fig. 6A and 6B). We then performed caspase-3 assays to determine if caspase-9 activation plays a role in the activation of caspase-3. Cells were pre-incubated for 1 hr with a synthetic peptide inhibitor of caspase-9 (Z-LEHD-FMK, 25 μM), prior to infection with reovirus. As shown in Fig. 7, pre-treatment with Z-LEHD-FMK abrogates caspase-3 activation. These results indicate that in addition to caspase-8, caspase-9 activation is a prerequisite for caspase-3 activation.

Having shown that caspase-9 activation is necessary for caspase-3 activation following reovirus infection, we wanted to determine the consequence of inhibition of caspase-9 on reovirus-induced apoptosis. Apoptosis was reduced by ~ 49% following pretreatment of HEK 293 cells for 1 hr with Z-LEHD-FMK (50 μM) (Fig. 8).

Discussion

Understanding the mechanisms of virus-induced apoptosis may provide insights into how viral infections lead to disease. Mammalian reoviruses induce apoptosis in several cell lines *in vitro* (19, 22, 28) as well as in a number of target tissues *in vivo* (19, 20). Previous results from our lab indicate that reovirus sensitizes cells to TRAIL, the ligand of the death receptors DR4 and DR5, and that this is at least one mechanism responsible

for reovirus-induced apoptosis (6). Additionally, this process requires the activation of NFκB (9) and is inhibited in a cell line expressing FADD-DN (6).

In the present study we examine the caspases that are responsible for executing the apoptotic program following reovirus infection. We used multiple experimental approaches to show that the effector caspase, caspase-3 is activated starting at ~12-14 hrs post infection and peaking at ~18 hr post infection. Inhibition of caspase-3 activation reduces reovirus-induced apoptosis. We were unable to detect activation of other effector caspases. These results implicate caspase-3 as the primary effector of the reovirus-induced apoptotic program.

We next investigated the activation of initiator caspases in order to determine those that contribute to caspase-3 activation. Previous results showed that inhibition of caspase-8 inhibited reovirus-induced apoptosis (6). In this study we found that caspase-8 was activated at ~10 hr post infection and that caspase-8 activation was inhibited in a cell line expressing FADD-DN. Cleavage of PARP was also inhibited in a FADD-DN expressing cell line (data not shown). This result indicates that caspase-3 activation is dependent, at least in part, on caspase-8 activation. To confirm this we treated cells with a caspase-8 specific synthetic peptide inhibitor prior to reovirus infection and examined the effect on caspase-3 activation. We found that caspase-3 activity was abrogated in cells treated with Z-IETD-FMK, again suggesting that caspase-8 activation is a prerequisite for caspase-3 activation.

Our lab had shown previously that over-expression of the anti-apoptotic protein Bcl-2 inhibited reovirus-induced apoptosis in MDCK cells (27). Bcl-2 has been shown to inhibit cytochrome *c* release from the mitochondria, a required step in the activation of

caspase-9. We therefore looked at the activation of caspase-9 using western blot analysis. Caspase-9 is activated at ~10 hr post infection. Moreover, we detected cytochrome *c* release from the mitochondria beginning between 6-12 hr post infection. Pre-treating cells with Z-LEHD-FMK, a caspase-9 synthetic peptide inhibitor, reduced reovirus induced apoptosis by ~40%. Finally, caspase-3 activity was reduced in cells pre-treated with Z-LEHD-FMK. These results indicate that like caspase-8, caspase-9 activity is necessary for caspase-3 activation and reovirus-induced apoptosis.

The data described here suggest two possible pathways for caspase activation following reovirus infection. In the first cascade, analogous to the Fas/FasL death receptor pathway, caspase-8 is activated through interaction with FADD and the death receptors DR4 and DR5. Activated caspase-8 mediates cytochrome *c* release from the mitochondria, perhaps through cleavage and activation of pro-apoptotic Bcl-2 protein family members such as Bid, leading to the activation of caspase-9. Caspase-9 then acts as the primary activator of the effector caspase, caspase-3. This pathway best explains the caspase-3 fluorogenic substrate assay data showing that inhibition of either caspase-8 or caspase-9 abrogates caspase-3 activation, suggesting a linear caspase activation cascade.

A second mechanism for caspase activation is that cytochrome *c* release and caspase-9 activation occur through stimulus initiated following reovirus infection but separate from the activation of caspase-8. In this model, both caspase-8 and caspase-9 would both act to activate caspase-3, and might act to amplify the activation of each other. This model is consistent with our AO staining data indicating that neither inhibition of caspase-8 nor of caspase-9 completely abrogated reovirus-induced apoptosis, suggesting that they may not

be acting in a linear pathway. In this model reovirus infection would lead to the simultaneous activation of multiple apoptotic pathways.

Acknowledgements

This work was supported by Public Health Service grant 1RO1AG14071 from the National Institute of Aging, Merit and REAP grants from the Department of Veterans Affairs, and a U.S. Army Medical Research and Material Command grant (USAMRMC98293015).

References

1. **Ashkenazi, A. and V. M. Dixit**. 1998. Death receptors: signaling and modulation. Science **281**:1305-1308.

2. **Bodmer, J. L., N. Holler, S. Reynard, P. Vinciguerra, P. Schneider, P. Juo, J. Blenis, and J. Tschopp**. 2000. TRAIL receptor-2 signals apoptosis through FADD and caspase-8. Nat. Cell Biol. **2**:241-243.

3. **Bratton, S. B., M. MacFarlane, K. Cain, and G. M. Cohen**. 2000. Protein complexes activate distinct caspase cascades in death receptor and stress-induced apoptosis. Exp. Cell Res. **256**:27-33.

4. **Brojatsch, J., J. Naughton, M. M. Rolls, K. Zingler, and J. A. Young**. 1996. CAR1, a TNFR-related protein, is a cellular receptor for cytopathic avian leukosis-sarcoma viruses and mediates apoptosis. Cell **87**:845-855.

5. **Chaudhary, P. M., M. Eby, A. Jasmin, A. Bookwalter, J. Murray, and L. Hood**. 1997. Death receptor 5, a new member of the TNFR family, and DR4 induce FADD- dependent apoptosis and activate the NF-kappaB pathway. Immunity. **7**:821-830.

6. **Clarke, P., S. M. Meintzer, S. Gibson, C. Widmann, T. P. Garrington, G. L. Johnson, and K. L. Tyler**. 2000. Reovirus-Induced Apoptosis Is Mediated by TRAIL. J. Virol. **74**:8135-8139.

7. **Cohen, G. M.** 1997. Caspases: the executioners of apoptosis. Biochem. J. **326 (Pt 1)**:1-16.

8. **Cohen, J. J., R. C. Duke, V. A. Fadok, and K. S. Sellins**. 1992. Apoptosis and programmed cell death in immunity. Annu. Rev. Immunol. **10**:267-293.

9. **Connolly, J. L., S. E. Rodgers, P. Clarke, D. W. Ballard, L. D. Kerr, K. L. Tyler, and T. S. Dermody**. 2000. Reovirus-induced apoptosis requires activation of transcription factor NF-kappaB. J. Virol. **74**:2981-2989.

10. **DeBiasi, R. L., M. K. Squier, B. Pike, M. Wynes, T. S. Dermody, J. J. Cohen, and K. L. Tyler**. 1999. Reovirus-induced apoptosis is preceded by increased cellular calpain activity and is blocked by calpain inhibitors. J. Virol. **73**:695-701.

11. **Fujimoto, I., T. Takizawa, Y. Ohba, and Y. Nakanishi**. 1998. Co-expression of Fas and Fas-ligand on the surface of influenza virus- infected cells. Cell Death. Differ. **5**:426-431.

12. **Halleck, M. M., N. J. Holbrook, J. Skinner, H. Liu, and J. L. Stevens**. 1997. The molecular response to reductive stress in LLC-PK1 renal epithelial cells: coordinate transcriptional regulation of gadd153 and grp78 genes by thiols. Cell Stress. Chaperones. **2**:31-40.

13. **Hu, S., C. Vincenz, M. Buller, and V. M. Dixit**. 1997. A novel family of viral death effector domain-containing molecules that inhibit both CD-95- and tumor necrosis factor receptor-1-induced apoptosis. J. Biol. Chem. **272**:9621-9624.

14. **Jan, J. T., S. Chatterjee, and D. E. Griffin**. 2000. Sindbis virus entry into cells triggers apoptosis by activating sphingomyelinase, leading to the release of ceramide [In Process Citation]. J. Virol. **74**:6425-6432.

15. **Kuang, A. A., G. E. Diehl, J. Zhang, and A. Winoto**. 2000. FADD Is Required for DR4- and DR5-mediated Apoptosis. LACK OF TRAIL- INDUCED APOPTOSIS IN FADD-DEFICIENT MOUSE EMBRYONIC FIBROBLASTS. J. Biol. Chem. **275**:25065-25068.

16. **Li, P., D. Nijhawan, I. Budihardjo, S. M. Srinivasula, M. Ahmad, E. S. Alnemri, and X. Wang**. 1997. Cytochrome c and dATP-dependent formation of Apaf-1/caspase-9 complex initiates an apoptotic protease cascade. Cell **91**:479-489.

17. **Mancini, M., C. E. Machamer, S. Roy, D. W. Nicholson, N. A. Thornberry, L. A. Casciola-Rosen, and A. Rosen**. 2000. Caspase-2 is localized at the Golgi complex and cleaves golgin-160 during apoptosis. J. Cell Biol. **149**:603-612.

18. **Nakagawa, T., H. Zhu, N. Morishima, E. Li, J. Xu, B. A. Yankner, and J. Yuan**. 2000. Caspase-12 mediates endoplasmic-reticulum-specific apoptosis and cytotoxicity by amyloid-beta. Nature **403**:98-103.

19. **Oberhaus, S. M., T. S. Dermody, and K. L. Tyler**. 1998. Apoptosis and the cytopathic effects of reovirus. Curr. Top. Microbiol. Immunol. **233 Reovir.ii**:23-49.

20. **Oberhaus, S. M., R. L. Smith, G. H. Clayton, T. S. Dermody, and K. L. Tyler**. 1997. Reovirus infection and tissue injury in the mouse central nervous system are associated with apoptosis. J. Virol. **71**:2100-2106.

21. **Price, B. D. and S. K. Calderwood**. 1992. Gadd45 and Gadd153 messenger RNA levels are increased during hypoxia and after exposure of cells to agents which elevate the levels of the glucose-regulated proteins. Cancer Res. **52**:3814-3817.

22. **Rodgers, S. E., E. S. Barton, S. M. Oberhaus, B. Pike, C. A. Gibson, K. L. Tyler, and T. S. Dermody**. 1997. Reovirus-induced apoptosis of MDCK cells is not linked to viral yield and is blocked by Bcl-2. J. Virol. **71**:2540-2546.

23. **Schneider, P., M. Thome, K. Burns, J. L. Bodmer, K. Hofmann, T. Kataoka, N. Holler, and J. Tschopp**. 1997. TRAIL receptors 1 (DR4) and 2 (DR5) signal FADD-dependent apoptosis and activate NF-kappaB. Immunity. **7**:831-836.

24. **Slee, E. A., M. T. Harte, R. M. Kluck, B. B. Wolf, C. A. Casiano, D. D. Newmeyer, H. G. Wang, J. C. Reed, D. W. Nicholson, E. S. Alnemri, D. R. Green, and S. J. Martin**. 1999. Ordering the cytochrome c-initiated caspase cascade: hierarchical activation of caspases-2, -3, -6, -7, -8, and -10 in a caspase-9-dependent manner. J. Cell Biol. **144**:281-292.

25. **Tateyama, M., N. Oyaizu, T. W. McCloskey, S. Than, and S. Pahwa**. 2000. CD4 T lymphocytes are primed to express Fas ligand by CD4 cross-linking and to contribute to CD8 T-cell apoptosis via Fas/FasL death signaling pathway. Blood **96**:195-202.

26. **Thornberry, N. A. and Y. Lazebnik**. 1998. Caspases: enemies within. Science **281**:1312-1316.

27. **Tyler, K. L., M. K. Squier, A. L. Brown, B. Pike, D. Willis, S. M. Oberhaus, T. S. Dermody, and J. J. Cohen**. 1996. Linkage between reovirus-induced apoptosis and inhibition of cellular DNA synthesis: role of the S1 and M2 genes. J. Virol. **70**:7984-7991.

28. **Tyler, K. L., M. K. Squier, S. E. Rodgers, B. E. Schneider, S. M. Oberhaus, T. A. Grdina, J. J. Cohen, and T. S. Dermody**. 1995. Differences in the capacity of reovirus strains to induce apoptosis are determined by the viral attachment protein sigma 1. J. Virol. **69**:6972-6979.

29. **Vidalain, P. O., O. Azocar, B. Lamouille, A. Astier, C. Rabourdin-Combe, and C. Servet-Delprat**. 2000. Measles virus induces functional TRAIL production by human dendritic cells. J. Virol. **74**:556-559.

30. **Wajant, H., F. J. Johannes, E. Haas, K. Siemienski, R. Schwenzer, G. Schubert, T. Weiss, M. Grell, and P. Scheurich**. 1998. Dominant-negative FADD inhibits TNFR60-, Fas/. Curr. Biol. **8**:113-116.

31. **Zou, H., Y. Li, X. Liu, and X. Wang**. 1999. An APAF-1.cytochrome c multimeric complex is a functional apoptosome that activates procaspase-9. J. Biol. Chem. **274**:11549-11556.

Figure Legends

Fig. 1. **Reovirus infection leads to activation of caspase-3.** HEK 293 cells were mock infected, reovirus infected (T3A, M.O.I. 100), or pretreated with DEVD-CHO (25 μM) prior to reovirus infection (T3A, M.O.I. 100) and caspase-3 activation was determined by fluorgenic substrate assay. Assays were performed in triplicate. Error bars represent standard error of the mean. Fluorescence is expressed as arbitrary units. * Caspase-3 activity was significantly induced in reovirus-infected cells ($p \leq 0.001$) (A). Western blot analysis was performed using HEK 293 lysates harvested at the indicated time points and probed with anti-caspase-3 antibodies (B and C, mock and reovirus infected, respectively) or anti-PARP antibodies (D and E, mock and reovirus infected, respectively).

Fig. 2. **Reovirus-induced apoptosis involves caspase-3.** HEK 293 cells were mock infected, reovirus infected (T3A, M.O.I. 100), or pretreated with the caspase-3 inhibitor DEVD-CHO (50 μM) for 1 hr prior to reovirus infection (T3A, M.O.I. 100). The graph shows mean percentage of apoptotic nuclei at 48 hr post infection. Error bars represent standard error of the mean. * The percentage of apoptotic cells was significantly reduced in DEVD-CHO treated cells ($p=0.002$).

Fig. 3. **Reovirus infection leads to activation of caspase-8.** HEK 293 lysates were prepared at the indicated times points from mock infected (A) or reovirus infected (B) cells and probed with anti-caspase-8 antibodies and anti-actin antibodies. Control lanes

represent lysates prepared from Jurkat cells untreated (-) or treated (+) with anti-Fas antibody and harvested at 8 hr post treatment.

Fig. 4. **Caspase-8 is involved in caspase-3 activation.** HEK 293 cells were mock infected, reovirus infected (T3A, M.O.I. 100), or pretreated with the caspase-8 inhibitor Z-IETD-FMK (25 μM) for 1 hr prior to reovirus infection (T3A, M.O.I. 100). Additionally, HEK 293 cells transfected with FADD-DN were reovirus infected (T3A, M.O.I. 100) and caspase-3 activation was determined by fluorgenic substrate assay. Assays were performed in triplicate. Error bars represent standard error of the mean. Fluorescence is expressed as arbitrary units. * Caspase-3 activity was significantly reduced in FADD-DN expressing cells ($p \leq 0.001$).

Fig. 5. **Cytochrome *c* is present in the cytosol of reovirus-infected cells.** Cell lysates were prepared from mock-infected or reovirus-infected (T3A, M.O.I. 100) HEK 293 cells at the indicated time points as described (see Materials and Methods) and resolved using SDS-PAGE. Western blot analysis was performed using anti-cytochrome *c* antibodies and anti-cytochrome *c* oxidase (subunit II).

Fig. 6. **Caspase-9 is activated in reovirus-infected cells.** HEK 293 cell lysates were prepared from mock (A) or reovirus-infected (B) cells at the indicated time points and resolved by SDS-PAGE. Western blot analysis was performed using anti-caspase-9 antibodies.

Fig. 7. **Caspase-9 is involved in caspase-3 activation.** HEK 293 cells were mock infected, reovirus infected (T3A, M.O.I. 100), or pretreated with the caspase-9 inhibitor Z-LEHD-FMK (25 μM) for 1 hr prior to reovirus infection (T3A, M.O.I. 100). Caspase-3 activation was determined by fluorgenic substrate assay. Assays were performed in

triplicate. Error bars represent standard error of the mean. Fluorescence is expressed as arbitrary units.

Fig. 8. **Reovirus-induced apoptosis involves caspase-9.** HEK 293 cells were mock infected, reovirus infected (T3A, M.O.I. 100), or pretreated with Z-LEHD.FMK (50 μM) for 1 hr prior to reovirus infection (T3A, M.O.I. 100). The graph shows mean percentage of apoptotic nuclei at 48 hr post infection. Error bars represent standard error of the mean. * The percentage of apoptotic cells was significantly reduced in Z-LEHD-FMK treated cells ($p=0.001$).

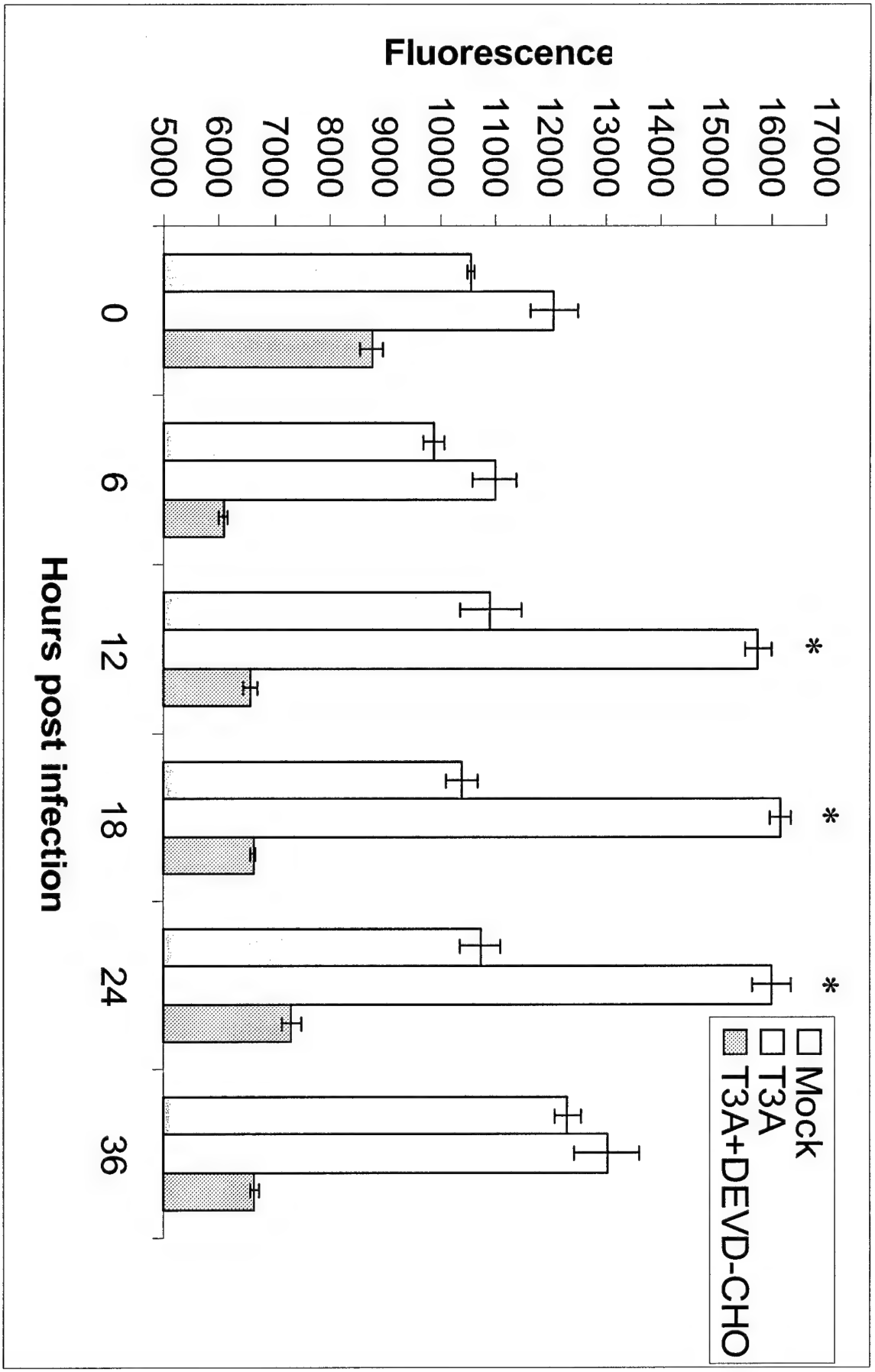
Fluorescence
17000
16000
15000
14000
13000
12000
11000
10000
9000
8000
7000
6000
5000
0
6
12
18
24
36
Hours post infection
*
*
*
Mock
T3A
T3A+DEVD-CHO

Figure 1A

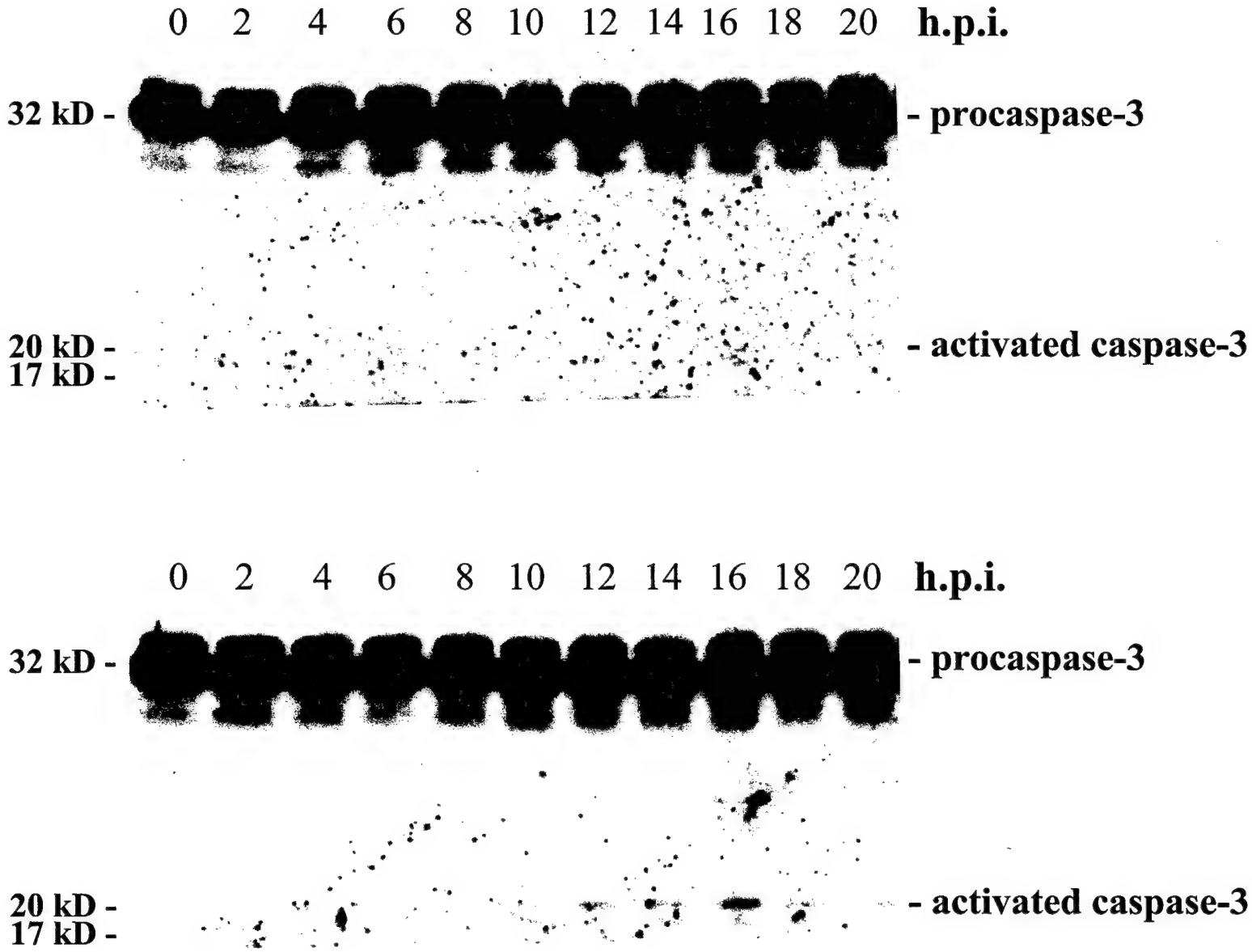
0 2 4 6 8 10 12 14 16 18 20 h.p.i.
32 kD -
- procaspase-3
20 kD -
17 kD -
- activated caspase-3
0 2 4 6 8 10 12 14 16 18 20 h.p.i.
32 kD -
- procaspase-3
20 kD -
17 kD -
- activated caspase-3

Figure 1B

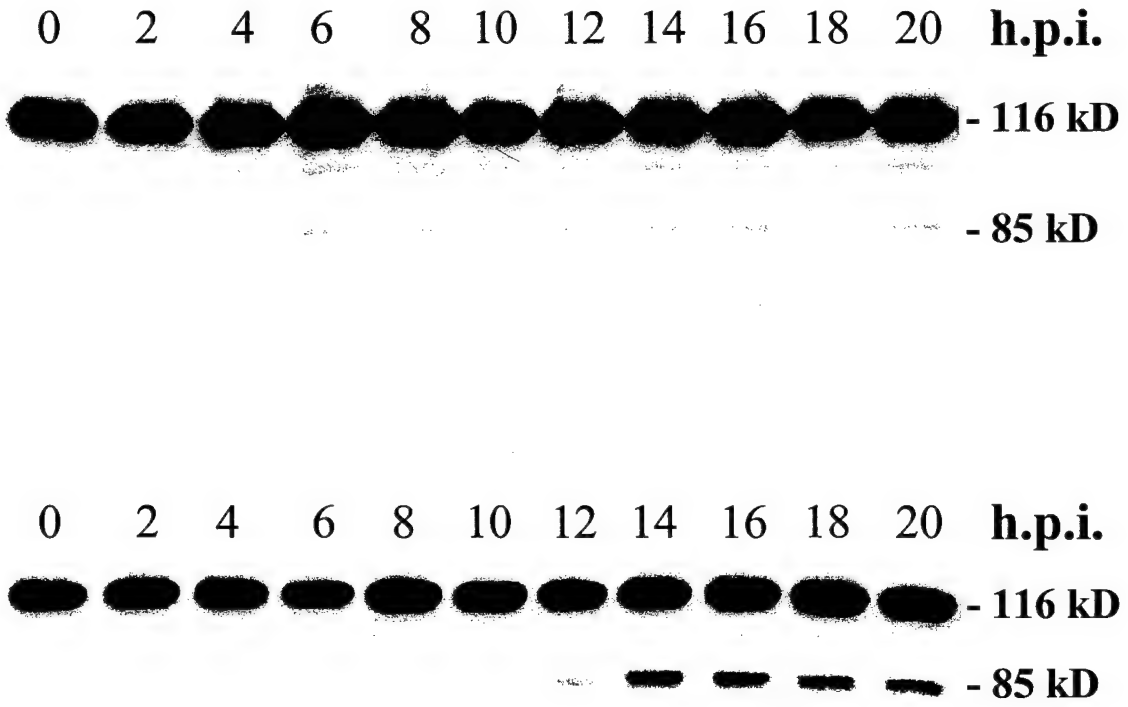
0 2 4 6 8 10 12 14 16 18 20 h.p.i.
- 116 kD
- 85 kD
0 2 4 6 8 10 12 14 16 18 20 h.p.i.
- 116 kD
- 85 kD

Figure 1C

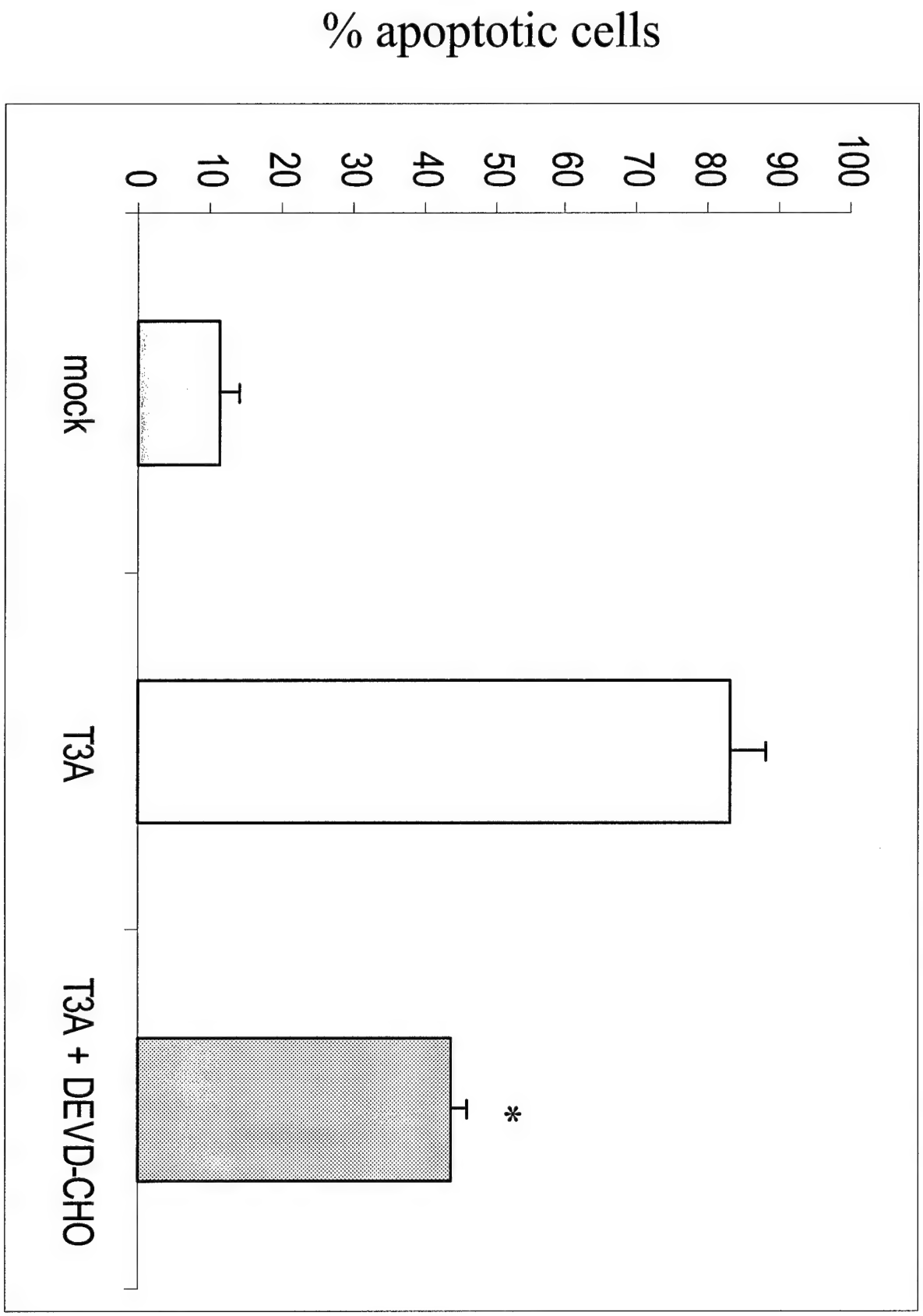
% apoptotic cells
0
10
20
30
40
50
60
70
80
90
100
mock
T3A
T3A + DEVD-CHO
*

Figure 2

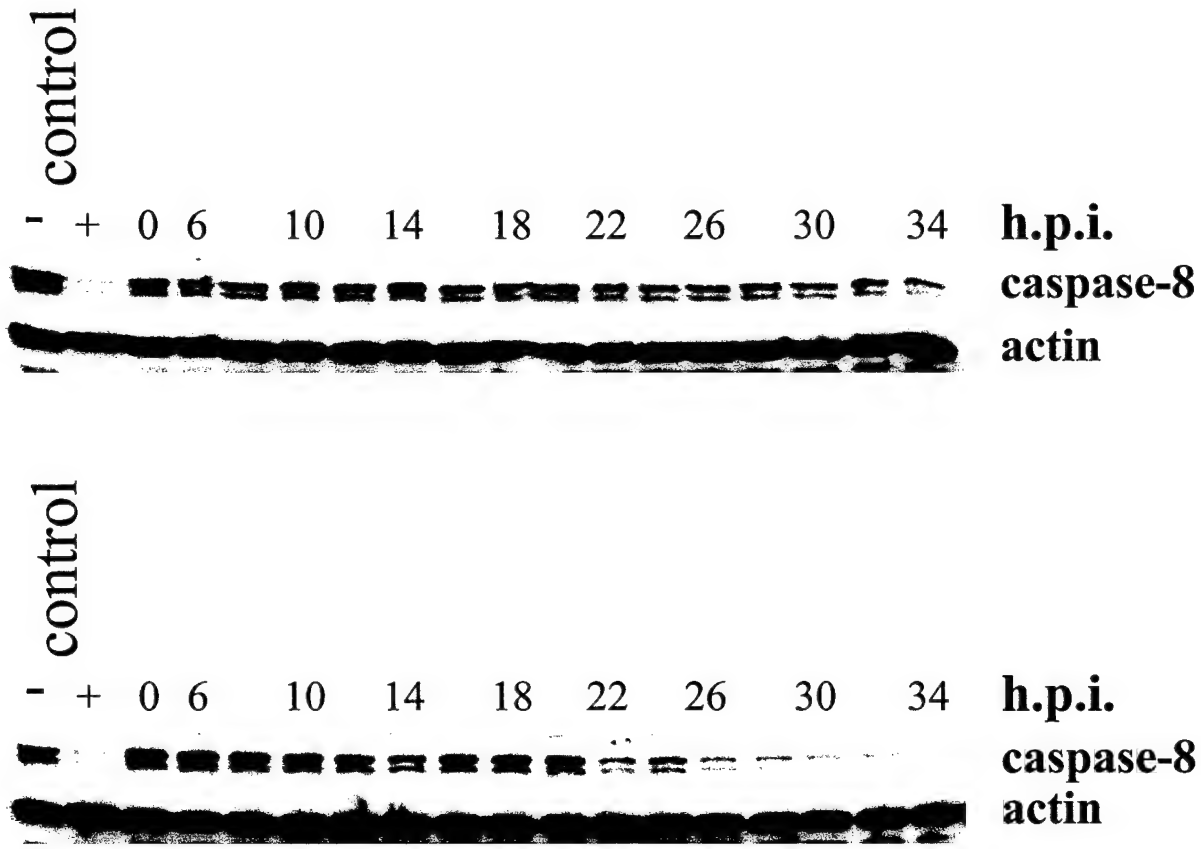
control
- + 0 6 10 14 18 22 26 30 34
h.p.i.
caspase-8
actin
control
- + 0 6 10 14 18 22 26 30 34
h.p.i.
caspase-8
actin

Figure 3

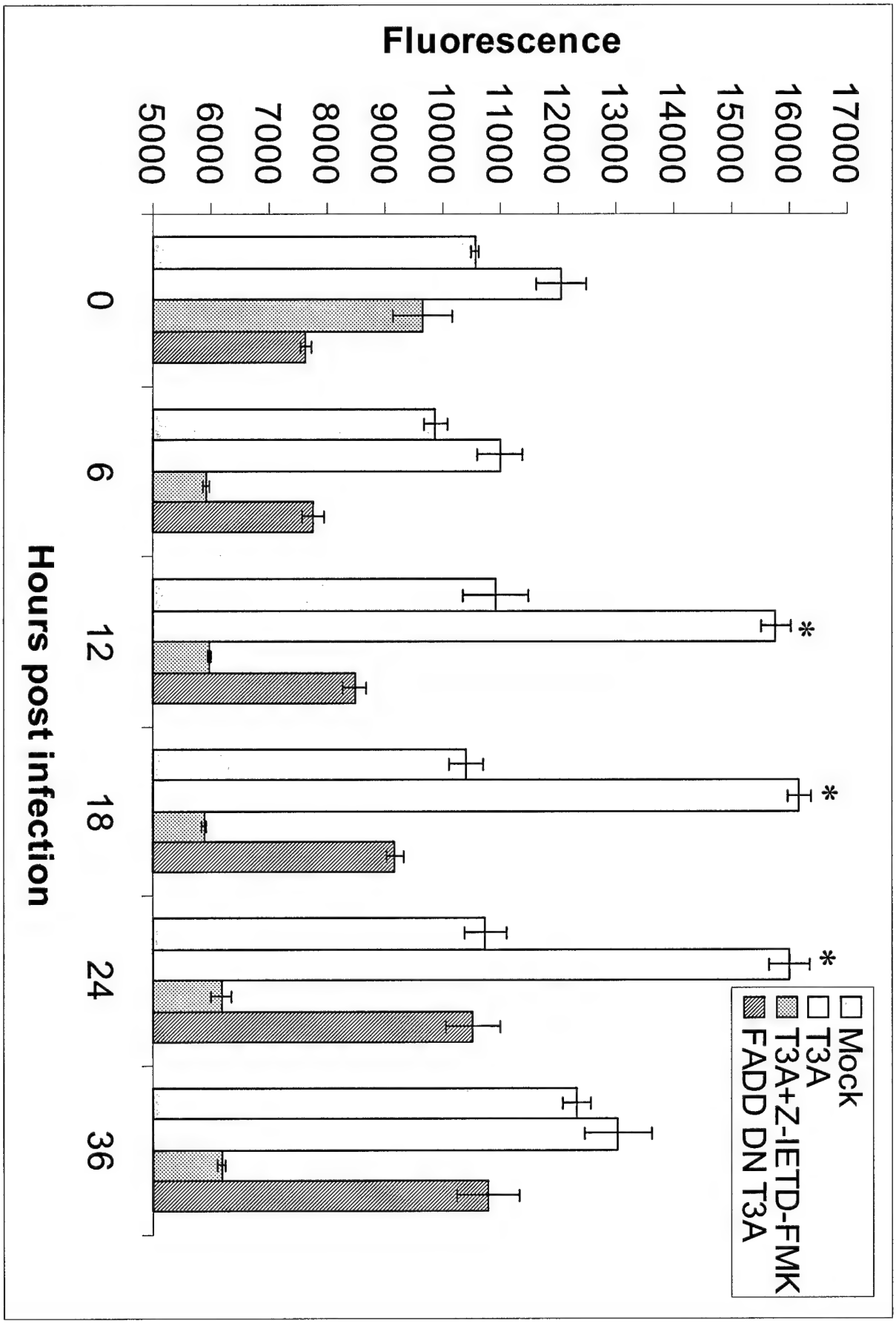
Fluorescence
17000
16000
15000
14000
13000
12000
11000
10000
9000
8000
7000
6000
5000
Hours post infection
0
6
12
18
24
36
*
*
*
Mock
T3A
T3A+Z-IETD-FMK
FADD DN T3A

Figure 4

pellet
supernatant
cytochrome c oxidase
(subunit II) -
cytochrome c -
mock
T3A
0
6
0
6
h.p.i.

Figure 5

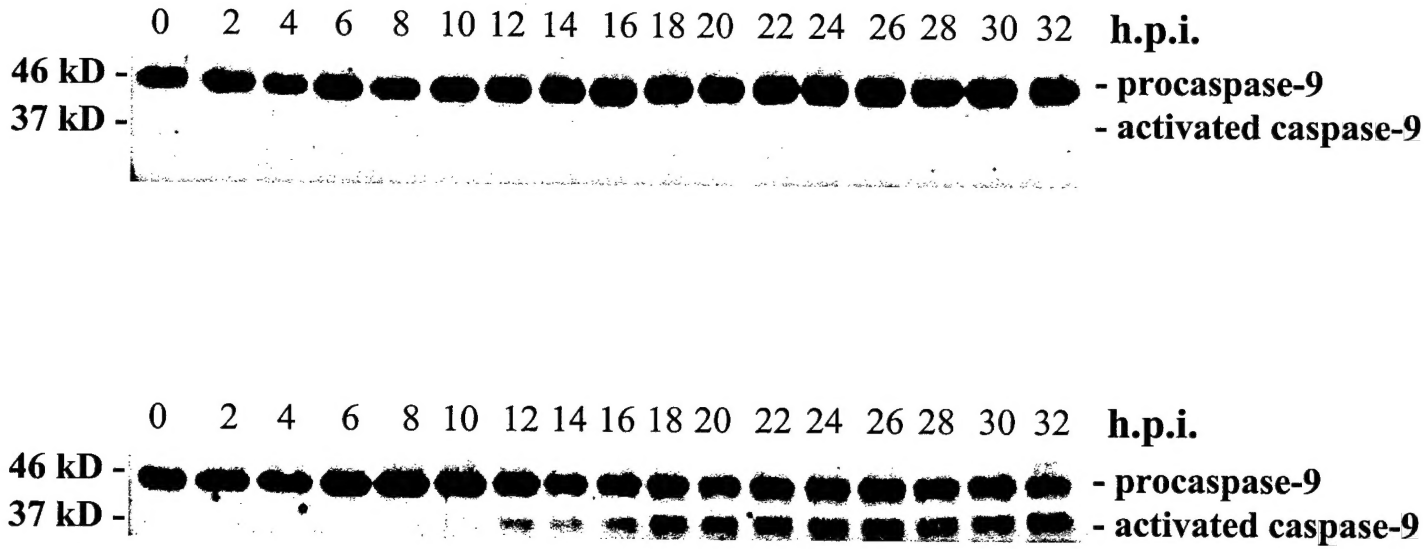
0 2 4 6 8 10 12 14 16 18 20 22 24 26 28 30 32 h.p.i.
46 kD -
37 kD -
- procaspase-9
- activated caspase-9
0 2 4 6 8 10 12 14 16 18 20 22 24 26 28 30 32 h.p.i.
46 kD -
37 kD -
- procaspase-9
- activated caspase-9

Figure 6

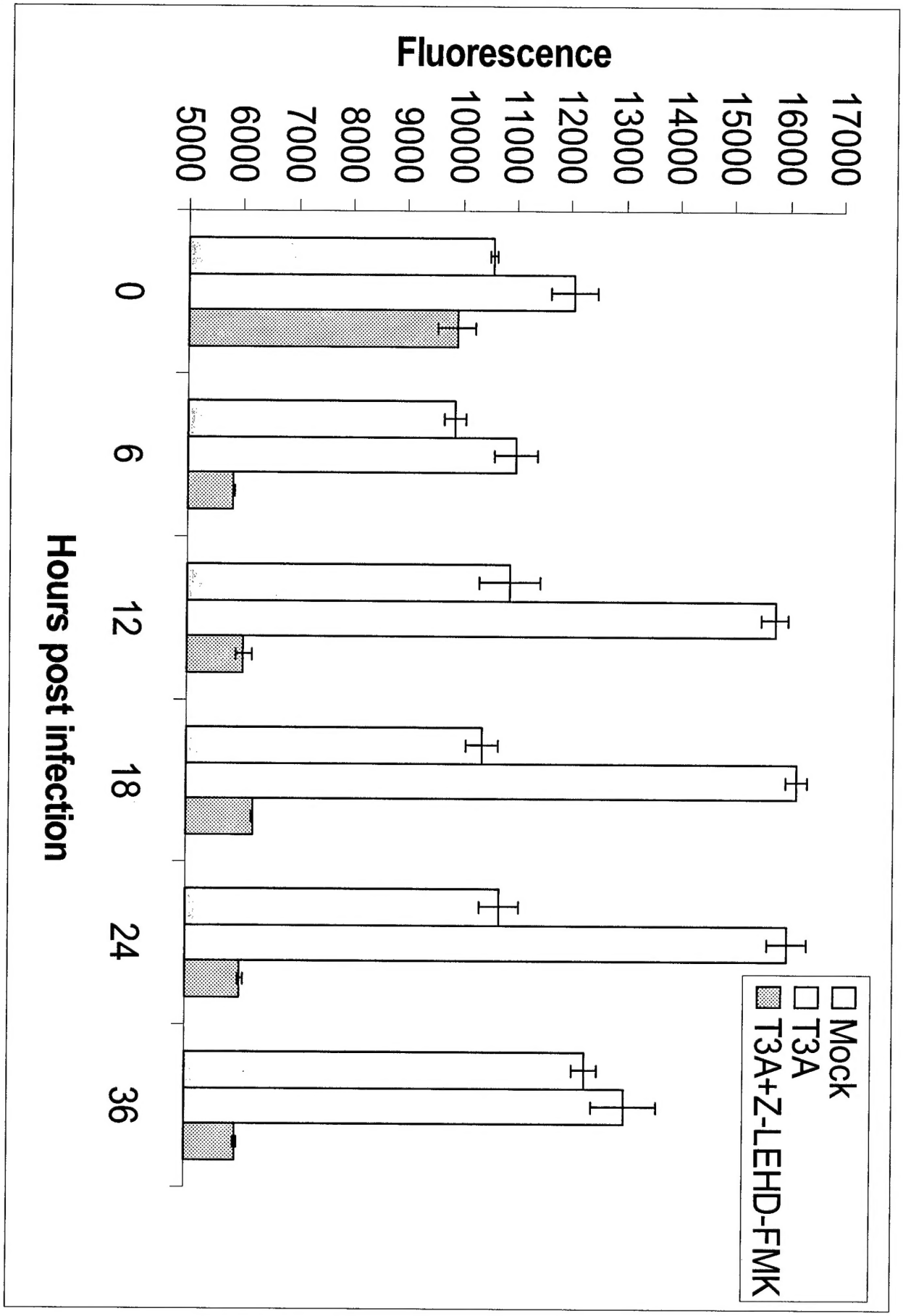
Fluorescence
17000
16000
15000
14000
13000
12000
11000
10000
9000
8000
7000
6000
5000
Hours post infection
0
6
12
18
24
36
Mock
T3A
T3A+Z-LEHD-FMK

Figure 7

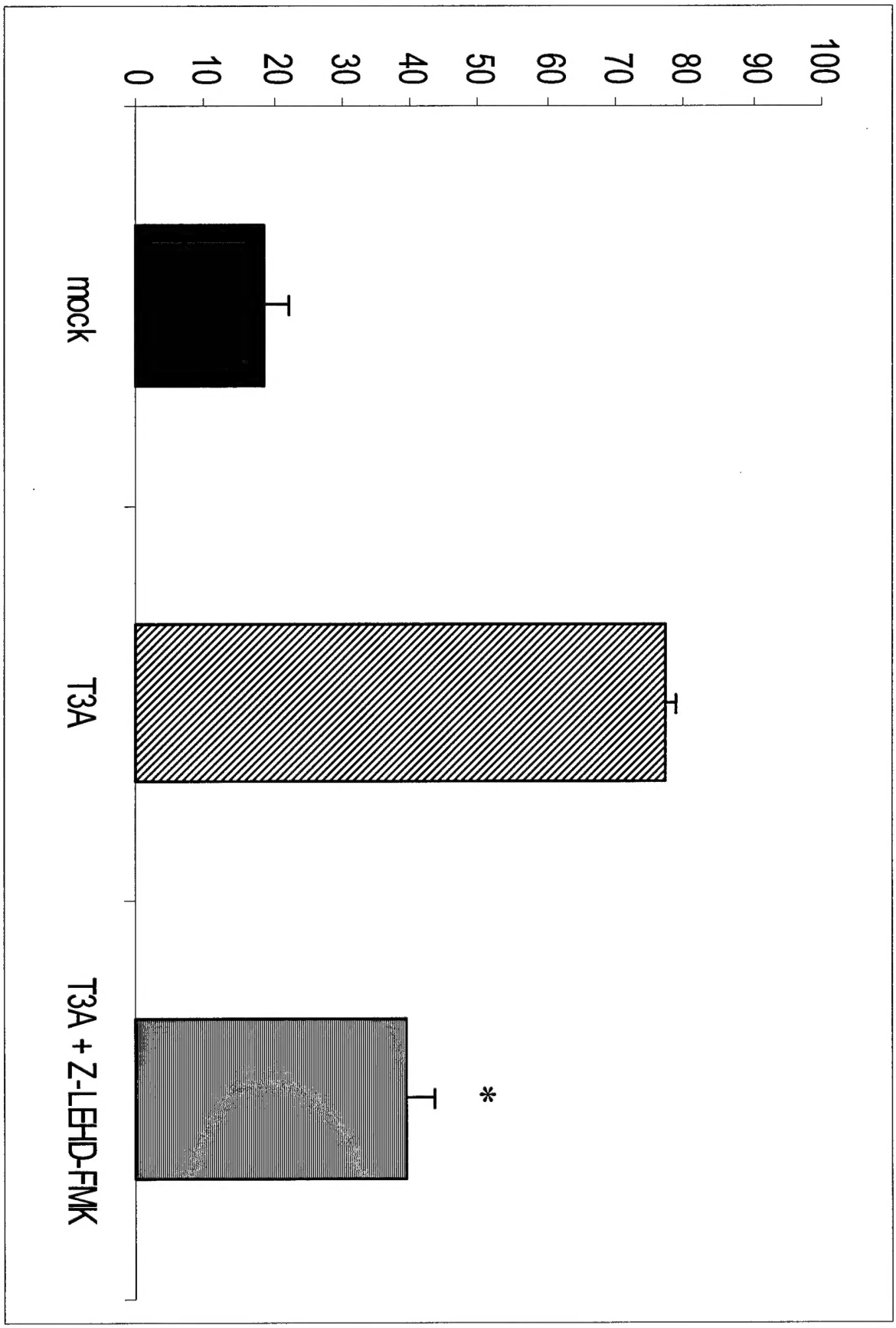
% apoptotic cells
0
10
20
30
40
50
60
70
80
90
100
mock
T3A
T3A + Z-LEHD-FMK
*

Figure 8